1980

The determination of mercury at trace levels by flow-injection analysis with electrochemical detection

Timothy Rhea Lindstrom
Iowa State University

INFORMATION TO USERS

This was produced from a copy of a document sent to us for microfilming. While the most advanced technological means to photograph and reproduce this document have been used, the quality is heavily dependent upon the quality of the material submitted.

The following explanation of techniques is provided to help you understand markings or notations which may appear on this reproduction.

1. The sign or "target" for pages apparently lacking from the document photographed is "Missing Page(s)". If it was possible to obtain the missing page(s) or section, they are spliced into the film along with adjacent pages. This may have necessitated cutting through an image and duplicating adjacent pages to assure you of complete continuity.

2. When an image on the film is obliterated with a round black mark it is an indication that the film inspector noticed either blurred copy because of movement during exposure, or duplicate copy. Unless we meant to delete copyrighted materials that should not have been filmed, you will find a good image of the page in the adjacent frame.

3. When a map, drawing or chart, etc., is part of the material being photographed the photographer has followed a definite method in "sectioning" the material. It is customary to begin filming at the upper left hand corner of a large sheet and to continue from left to right in equal sections with small overlaps. If necessary, sectioning is continued again—beginning below the first row and continuing on until complete.

4. For any illustrations that cannot be reproduced satisfactorily by xerography, photographic prints can be purchased at additional cost and tipped into your xerographic copy. Requests can be made to our Dissertations Customer Services Department.

5. Some pages in any document may have indistinct print. In all cases we have filmed the best available copy.

University
Microfilms
International

300 N. ZEEB ROAD, ANN ARBOR, MI 48106
18 BEDFORD ROW, LONDON WC1R 4EJ, ENGLAND

LINDSTROM, TIMOTHY RHEA

THE DETERMINATION OF MERCURY AT TRACE LEVELS BY FLOW-INJECTION ANALYSIS WITH ELECTROCHEMICAL DETECTION

Iowa State University PH.D. 1980

The determination of mercury at trace levels by flow-injection analysis with electrochemical detection

by

Timothy Rhea Lindstrom

A Dissertation Submitted to the

Graduate Faculty in Partial Fulfillment of the

Requirements for the Degree of

DOCTOR OF PHILOSOPHY

Department: Chemistry
Major: Analytical Chemistry

Approved:

Signature was redacted for privacy.

In Charge of Major Work

Signature was redacted for privacy.

For the Major Department

Signature was redacted for privacy.

For the Graduate College

Iowa State University
Ames, Iowa

1980

TABLE OF CONTENTS

LIST OF FIGURES

LIST OF TABLES

LIST OF ACRONYMS

CFA	Continuous-Flow Analysis
DME	Dropping mercury electrode
DPASV	Differential Pulse Anodic Stripping Voltametry
EC	Electrochemical
FIA	Flow-Injection Analysis
FTD	Flow-through disk
HMDE	Hanging mercury drop electrode
LC	Liquid chromatography
MDE	Mini-disk-electrode
MFE	Mercury-film electrode
NBS	National Bureau of Standards
NDPASV	Normal DPASV
OECD	Organisation (sic) for Economic Co-operation and Development
PAR	Princeton Applied Research
RDE	Rotating disk electrode
RDPASV	Reverse DPASV
RRDE	Rotating ring-disk electrode
SCE	Saturated Calomel Electrode
SRM	Standard Reference Material
SVWC	Stripping voltammetry with collection
TDW	Triply-distilled water
UPD	Underpotential deposition
WIG	Wax-impregnated graphite

PREFACE

When I recall the days of my childhood, some of the events I remember most clearly are those connected to my discovery of an old bottle which was tightly stoppered with a cork and nearly filled with metallic mercury. The discovery was made one day while I rummaged through an old abandoned dump located behind an antiquated house. The children of the neighborhood, myself included, were convinced that the house was haunted; that's another story.

The discoloration of the bottle after weathering for unknown years in the dump, the heaviness of the mysterious silvery liquid, and the rumors associated with the house, all served to enhance the excitement I felt at my discovery. Using the Hg, I could: make a tarnished silver dime shine like new; make a copper penny shine like the silver dime; and change the color of a gold ring to silver. I remember how my curiosity was aroused when some Hg spilled onto the table and I observed for the first time that the Hg broke into little beads that danced over the flat surface. I had quite a time collecting all those tiny beads of Hg and returning them to the bottle.

My parents suggested that I reveal my discovery to my science teacher. I did so, and he said that my bottle of Hg would be quite valuable once the metal had been cleaned. As I recall, the quantity of mercury was about six lb., and on the basis of world prices in 1965, would have been worth $40.00 to $50.00; quite a sum to a small-town boy. However, my teacher not only told me of the value of the metal,

but also warned me that exposure to Hg, i.e., handling of the metal and breathing of the metallic vapors, could be very dangerous to my health. I subsequently released the bottle of Hg into his care for cleaning and safekeeping, but the bottle was stolen from his desk. The theft remains unsolved to this day.

Little did I realize then that my youthful curiosity in the shimmering, liquid metal would ultimately become a significant motivation for my graduate research.

"My decision to publish a frank account of my personal sufferings...is prompted by a keen desire to warn, in the strongest of terms, all who have to deal with metallic mercury of the dangers they face, and to spare them the wretched experiences which have cast a shadow over a great part of my life."

Alfred Stock, 1926

I. INTRODUCTION

The major thrust of this dissertation is the description of the electrochemical (EC) investigations which have been made and the conclusions which have been drawn with respect to the development of a flow-injection, electroanalytical method for the quantitative determination of mercury(II). However, it is appropriate first to present a brief review of the "mercury problem" and then a general discussion of Flow-Injection Analysis (FIA). A more specific discussion of FIA with EC detection will appear in Section IV.A.

A. Mercury

Near the turn of the past decade much public attention was focused on the presence of mercury in various forms in the environment. In the ensuing years a large volume of literature became available which gave broad coverage to the story of mercury. Several books are listed in the bibliography (1-11) which will be used as a broad base of reference for the following discussion. The comprehensive text by Goldwater (1) covering the world literature from ancient times, that by Jones (2) with extensive coverage of industrial aspects in the United States

(USA), and the Russian work by Trakhtenberg (3) are worthy of special mention even though these books have been in print for nearly a decade. More recently, the text edited by McAuliffe (4), and the report by the Panel on Mercury (5), have appeared and are also highly recommended.

1. Historical perspectives of mercury

The most abundant form of mercury present in the earth's crust is cinnabar, a reddish ore containing the sulfide, HgS. Mercury was first used in this form by the Chinese (1, Chap. 5; 12, Chap. 3). As early as 1100 B.C., cinnabar was used in the Far East in the production of a red ink which was used to inscribe "oracle bones" which were left with the dead, especially with royalty. A knowledge of metallic mercury first appears with certainty in the Mediterranean area in about 500 B.C. (12, Chap. 1) and a still for "roasting" of cinnabar ore to release the metal was used in China in about 200 B.C. The heating of cinnabar to distill Hg is to this day the major process for production of the metal (2, Chap. 2).

Hg played a predominant role in alchemy (attempts to make gold and/or silver from base metals) which persisted into the sixteenth century A.D. (12, Chap. 2). However, the importance of Hg in the evolution of chemistry as it is known today is more significant. The discoveries in which Hg or its compounds have played an essential role are discussed by Goldwater (1, Chap. 7) and the major advances are listed here.

1. The discovery of oxygen and study of gases in the eighteenth century.
2. The discovery and isolation of alkali and alkaline earth elements by electrolysis.
3. The initial rejection and then, ultimate acceptance of Avogadro's Hypothesis.
4. The initial advances in organic synthesis in the early nineteenth century.

Nowadays, Hg and its compounds are used extensively worldwide. By far the two largest uses of the metal are in the chloralkali industry (electrolysis of brine to produce chlorine and caustic soda), and in the manufacture of electrical apparatus and scientific instruments, such as thermometers and barometers (6, Chap. 3; 2, Chap. 4; 7, Chap. 3; 13). Inorganic compounds of mercury are applied in the production of felt hats, paints, paper, pulp and pharmaceuticals. The major use of organic formulations with mercury (e.g., methyl, ethyl, phenyl, etc.) has been in agriculture (2, Chap. 4; 14) as fungicidal seed dressings, especially for cereal grains such as wheat, corn, barley, etc. No other group of chemicals provides the broad-spectrum coverage against seed-born diseases at low dosages and low cost as do the mercurials (6, Chap. 1).

The toxicity of mercury, especially the adverse effect resulting from breathing of the metallic vapors, is not a new discovery. Ruska reported that a search of historical writings revealed that the poisonous nature of the metal was probably known as early as the ninth century A.D. (15). It seems likely that such an observation could have been made much earlier, especially in relation to workers who mined the ore and those who operated the crude distillation devices to

obtain the metal. However, despite such knowledge, historical accounts (e.g., 1, Chap. 15) describe the widespread use of mercurial inhalation in medicine for the treatment of syphilis beginning in the sixteenth century A.D., and continuing until about 40 years ago (e.g., 16). Goldwater (1, Chap. 15), after extensive evaluation of the available evidence, holds that the mercurialism "cure" for syphilis was not based upon scientific fact and observation, but upon "the emotional...aura generated by the mercurial vapors." The case against the indiscriminate use of Hg has not been without emotion either. In Germany in the first half of this century, Alfred Stock was a strong advocate of extreme safety precautions in the use and handling of the metal (17-21). Much of his research into the study of the hazards of Hg was prompted by his own experience as indicated in the quotation at the beginning of this section (17; translation taken from 12, Chap. 10). In 1971 the Montagues' book (8) proclaimed afresh the horrors of mercury in the workplace and environment.

2. Environmental concerns about pollution by mercury

About 10 to 15 years ago, public concern about the toxicity of organomercurials was stirred worldwide by the revelation of several accidental poisonings by methylmercury. These incidents, primarily occurring in Japan and the USA, and other discoveries of environmental contamination in Sweden and Canada, as well as the respective governmental regulatory actions taken in response to the crises, are well-documented in the work published by the Organisation (sic) for Economic Co-operation and Development (OECD) in 1974 (6, Part 2).

The predominant disasters cited include: the poisoning of 121 people at Minamata Bay and 49 in Niigata in Japan between 1955 and 1966, of which 60 victims died; and the poisoning of an American family in New Mexico in 1969, of which all four children (one being prenatal during exposure) suffered severe neurological injuries (8). Since 1972, governmental regulations on the use of Hg-based pesticides, fungicides, slimicides, etc., have been increasingly restrictive. Alkylmercurial seed dressings used in agriculture were banned in the USA in 1970 (6, Page 93).

In general, the toxic nature of mercurials follows the pattern given below.

methyl >> alkyl > aryl > inorganic

The toxicological aspects of mercurials are discussed in nearly all books written on the subject of mercury (1-11, 13), whether historical in perspective or specifically written with regard to pollution. Methylmercury is the most insidious problem. The conclusions drawn by the OECD (6, Part 3, Chap. 1) reflect the present understanding of the biological impact of mercury on the environment and man. Some of those conclusions are given below.

1. "Mercury is a chemical element potentially toxic, particularly in the form of methylmercury, to a wide variety of species in the environment.
2. Because of the widespread but as yet incompletely understood possibilities of methylation of inorganic mercury by micro-organisms in the natural environment, any additions to that mercury which is available to circulate

through the web of the ecosystem, must be considered to represent an additional risk to the well-being of some species in the environment, if not man himself.

3. Methylmercury is highly toxic to man (and may other vertebrates), the critical organs being the brain and the nervous system. Unborn children are particularly at risk because of concentration of methylmercury in the foetus" (sic).
4. "Methylmercury has been shown to affect the detoxication system of cells. The possibility must therefore be considered of methylmercury acting synergistically with other foreign substances, and by changing their metabolism, rendering them harmful or increasing their toxicity.
5. Recent findings indicate that a possible functional relationship might exist between mercury and selenium, possibly resulting in protection against the toxic action of methylmercury in the body. This may be important in relation to the high mercury and selenium levels found in marine mammals" (see also 5, Chap. 5).
6. "It is noted that legislative and other controls placed on the use and emission of mercury..., have had a beneficial effect on some environmental mercury levels, both in water and in aquatic and avian species."

The tremendous effort made in the past decade by the scientific community to develop sensitive and accurate analytical methods for the determination of the levels of mercury in environmental samples has been in direct response to findings such as those listed above.

B. Flow-Injection Analysis

The subject of FIA is a relatively new topic in analytical chemistry. The method first appeared in the analytical literature in

1975-1976 (22,23). Since then, articles expanding the scope of application of the method have appeared with increasing frequency. Recently, the first International Conference on Flow Analysis was held in Amsterdam (Sept., 1979) under the auspices of the Royal Netherlands Chemical Society, Analytical Division. The proceedings of the conference appeared in a special issue of Analytica Chimica Acta (24).

FIA is an offshoot of Continuous-Flow Analysis (CFA) which was first proposed by Skeggs in 1957 (25) and made famous by Technicon (Tarrytown, NY). Historically CFA has referred to methods in which the flowing solution containing the sample is divided into discrete segments by air bubbles (26). Analysis is based upon the attainment of steady-state conditions, i.e., homogeneity, within each liquid segment. The air bubbles are removed from the flow stream immediately prior to detection to minimize cross-contamination between liquid segments. In methods falling within the category of FIA, the sample is introduced into a nonsegmented stream. Results are obtained under nonsteady-state conditions. Hence, reproducible injection and control of dispersion of the sample within the flow stream are essential in most applications (27-31). Similiarities and differences between CFA and FIA have been reviewed by Snyder (32).

A very simple FIA system is shown in Figure I-1, and consists of four basic components. A pump, usually a peristaltic device, provides the flow of liquid through the system. The pump often has multi-channel capability so that additional reagents can be pumped into and mixed with

Figure I-1. Diagram of a simple Flow-Injection Analyzer

A - reservoirs for reagent solutions

B - pump

C - sample injector

D - mixing coil

E - detector

F - recorder

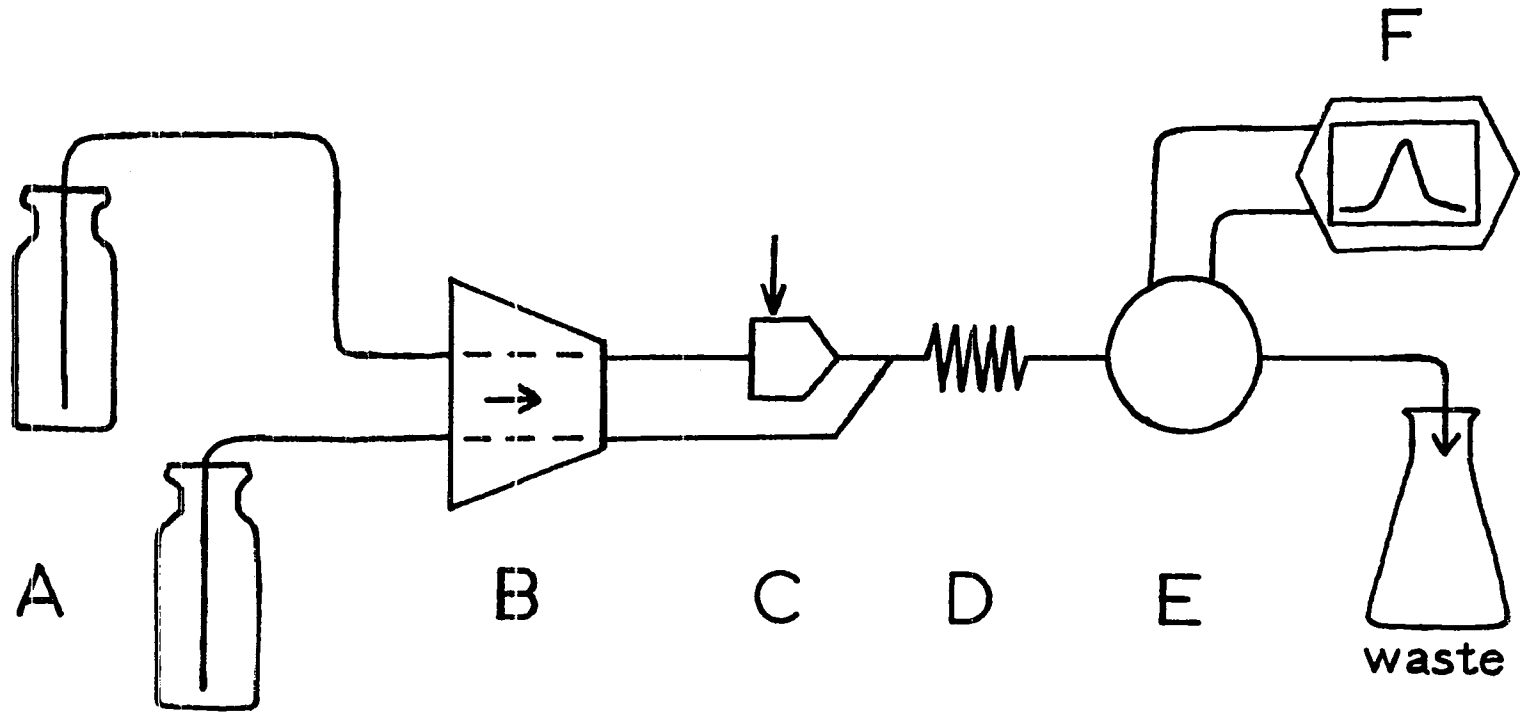
F
A
B
C
D
E
waste

the flow stream at some point after injection of the sample. The sample may be injected via syringe, or a variety of devices which directly insert a "plug" of solution containing the sample into the flow stream. The latter method provides a highly reproducible injection of fixed volume and is preferred over injections made by use of a syringe. Finally, the flow stream enters the detector and the analytical signal is recorded by the associated instrumentation. As depicted in Figure I-1, FIA systems were initially designed for straightforward analyses requiring only one phase and one or more reagent streams. However, in reviews of the development of FIA, Ruzicka and Hansen (27,28) discuss the expansion of the method into the areas of chemical separations (e.g., solvent extraction, low-pressure chromatography), physical separations (e.g., dialysis) and kinetic studies.

The major advantages of FIA are: 1) the simplicity of the apparatus; 2) the relatively low cost of the apparatus; and 3) the speed of analysis, i.e., high sample-throughput. Often, a simple FIA system can be constructed from equipment already available in the laboratory. Sampling rates of more than 400 samples per hour have been reported (33), but rates of 100-200 samples per hour are more common.

C. Summary of Research

Worldwide concern about the presence of mercurial contamination in the environment has spurred vigorous analytical research. The primary analytical methods for the determination of mercury have been

reviewed by several workers over the past decade, e.g., Jones in 1971 (2, Chap. 6), D'Itri in 1972 (7, Chap. 4), Allen in 1974 (34), Uthe and Armstrong in 1975 (35, Chap. 2), and the Panel on Mercury in 1978 (5, Appendix A), and will not be discussed in depth here.

Kissinger (36) has reviewed the use of EC detection in liquid chromatography (LC). The application of EC detection in FIA will be discussed in Section IV.A.

The research described in this dissertation has resulted in the development of an EC method utilizing Differential Pulse Anodic Stripping Voltammetry (DPASV) applied within the scheme of FIA. Selectivity for mercury was achieved by underpotential deposition (UPD) of the metal onto a Au electrode. The advantages of FIA in combination with the selectivity achieved by UPD followed by EC stripping analysis provides an attractive, alternate method to be added to the list of methods available for the determination of mercury. The proposed method yields a linear calibration with respect to the concentration of mercury(II) in the injected solution over the range 1.0×10^{-9} M $\leq C^{b}_{Hg(II)} \leq 2.0 \times 10^{-6}$ M (0.20 to 400 ppb). Routine determinations can be made at the ppb-Hg(II) level with a throughput of ~10 injections per hour. The limit of detection is on the order of 5×10^{-10} M (100 parts per trillion) Hg(II) using a deposition time of 5.0 min.

"Thus, the experiments on various radio-elements show that the nature of the electrode can strongly influence the deposition phenomena.... Even on a metal such as gold, which has generally a normal behavior, the deposition of polonium in extremely dilute solution is associated with an appreciable undervoltage. As the deposited amounts are here of the order of 10^{-7} of a monoatomic layer, it seems legitimate to think that this is due to the attractive action of some very rare spots...(on) the surface."

M. Haissinsky and A. Coche, 1949

II. THE UNDERPOTENTIAL DEPOSITION OF MERCURY ON GOLD

Noble metals, such as platinum and gold, are generally considered to be the materials of choice for use as indicating electrodes in EC measurements. This preference is based upon the assumption that the metal is inert, or indifferent, at the electrochemical potentials applied for obtaining the analytical signal. For example, in potentiometry the measured potential of the indicating electrode is assumed to be dependent only upon the relative ratio of electroactive species contained within the solution in which the electrode is placed. Similarly, in voltammetry the potentials at which reduction or oxidation of an electroactive species occurs should be dependent solely upon the position of the EC couple within the electromotive series, i.e., the thermodynamic reduction/oxidation potential, and not upon the identity of the indicating electrode.

When the identity of the indicating electrode does influence the EC reaction, an overpotential or underpotential phenomenon is observed.

Perhaps the best known example of such phenomena is the overpotential required at a mercury electrode for the reduction of hydrogen ion to hydrogen gas, the so-called hydrogen overpotential. This feature has made mercury electrodes the primary tools of electrochemists for investigation of metals more negative than hydrogen in the electromotive series.

UPD refers to the EC reduction and deposition of a metal at potentials which are more positive than those predicted on the basis of the electromotive series. Typically, UPD might be expected to be limited to the first monolayer of metal deposited, the quantity for which the interaction between the deposit and substrate is strongest. After the first monolayer has been deposited, deposition of macro (bulk) quantities of the metal occurs only at more negative potentials which are more in line with prediction from the electromotive series. However, there exists definite experimental evidence that, in some cases, significant UPD can also occur for several layers of the deposited metal beyond the first monolayer.

A. Literature Survey of Underpotential Deposition

A general survey of literature (37-142) which is pertinent to the subject of UPD is given in Table II-1. The list is not intended to be exhaustive, but rather to illustrate the scope of investigations which have been made during the past 70 years. The table was prepared by reference to Chemical Abstracts, and from literature cited in two Ph.D. Dissertations (114,127) on the subject of UPD. It is hoped that this

Table II-1. Literature for underpotential deposition of various metals on selected electrodes: a general reference base

Substrate	Metal Deposited	References
Ag	Au	117
	Bi	63,64,72,82,83,107,130,131
	Cd	38,82,83,130,131
	Cu	83,110,131
	Pb	38,39,82,83,88,105,107,117,130,131
	Po	72,81
	Tl	38,67,82,83,88,106,107,130,131
Au	Ag	52,54,56,82-84,97-99,101,104,117,123,125, 130,131
	Bi	56,61,63,64,72,82,83,101,130,131
	Cd	82,83,118,130,131
	Cu	56,82-84,110,117,130,131
	Hg	34,39,52,66,76,82,83,114-116,125,130,131, 137,138,148
	Ni	92
	Pb	82,108,109,111,117,118,127,129-131
	Po	72,78
	Pt	123
	Sn	127,128
	Tl	52,80,82-84,117,127,130,131
Carbon	Ag	96
	Cu	126
	Hg	66
Cu	Cd	82,83,130,131
	Pb	107
	Po	81
	Tl	82,83,107,130,131

Table II-1. Continued

Substrate	Metal Deposited	References
Ni	Fe	94
	Zn	94
Pt	Ag	37,41,54-56,58,69,82,83,89,93,95,98,101, 102,104,119,122,123,125,130,131
	Au	56,133
	Bi	45,46,56,59-61,73,77,82,83,101,130,131
	Cd	68,85,139
	Cu	43,44,49,50,56-58,65,82,83,90,91,93,95, 112,119-121,123,124,130,131
	Ge	136
	Hg	51,53,62,66,74,75,79,82,83,87,90,100,114, 130-132
	Ni	92
	Pb	48,56,58,60,61,77,93,95
	Po	60,71,78,81
	Ru	134,135
	Se	90
	Sn	47,82,83,130,131,136
	Tl	42,43,46,80,85,139
	Zn	70,139
Sn	Hg	39
Ta	Hg	66
Miscellaneous		103[a],113[b],140-142[a]

[a]Discussions of theoretical developments.

[b]Entry based on title only: "Multiple states of bonding of underpotentially deposited species on noble metal electrodes".

information will be useful as a "first-step" to the literature for anyone beginning an investigation of underpotential phenomena. The most recent, comprehensive work to appear is that by Kolb (142) in which 255 references are reviewed with respect to the physical and electrochemical properties of metallic monolayers on metallic substrates.

It is not the purpose of this dissertation to present in great detail the theory of UPD with respect to Hg(II) on Au, for that task has recently been accomplished by W. G. Sherwood (114) working in the laboratory of Professor Stanley Bruckenstein at the State University of New York at Buffalo. In this section, data will be presented most of which was obtained prior to, and simultaneously with, the publication of Sherwood's work and that of others (115,116,125). Rather than repeating their descriptions in different words, the discussion will center on additional EC studies which not only add support to some of the conclusions made by Sherwood, but further illustrate the utility of UPD for the electroanalytical determination of Hg(II).

B. Description of Experimental Parameters

The UPD of Hg(II) on Au from dilute solutions of nitric (HNO_3) and sulfuric (H_2SO_4) acid was investigated using rotating electrodes and flow-through detectors. The description of these electrodes, detectors and the associated apparatus is presented here.

1. Rotating electrodes

a. Rotating ring-disk electrode (RRDE) The RRDE was from Pine Instrument Company of Grove City, PA. Both the disk and the ring were constructed of Au. The pertinent geometrical parameters were as follows: R_1 = 0.3832 cm; R_2 = 0.4007 cm; R_3 = 0.4203 cm. The radius of the disk is denoted as R_1; the distance from the center of the disk to the inside edge of the ring as R_2; and the distance from disk-center to the outermost edge of the ring as R_3. The surface of the RRDE was polished to a mirror finish according to standard metallographic procedures (143).

b. Rotating disk electrode (RDE) The disk electrode was that of the RRDE described above. Since processes occurring at the ring do not affect those occurring at the disk, the ring electrode was not connected to the electronic control circuitry during investigations of UPD at the disk electrode.

c. Rotator and apparatus The synchronous rotator was a model PIR from Pine Instrument Company with nine speeds ranging from 400 to 10,000 rev min^{-1} in increments of $(20 + 10X)^2$ where X = 0,1,2,...,8.

The electrolysis cell was constructed from pyrex and had a capacity of approximately 500 mL. Typically the volume of solution used was 400 mL. The chamber containing the Pt auxiliary electrode was separated from the solution under investigation by a fritted glass disk and was filled with supporting electrolyte. The reference electrode was placed in a chamber connected to a Luggin capillary by a three-way stopcock. The Luggin capillary and reference chamber were filled with

the supporting electrolyte and the stopcock was turned to prevent flow of solution from the reference chamber into the electrolysis chamber. The tip of the Luggin capillary was placed approximately between the ring and disk electrodes as close as possible to the surface of the electrodes. A two-way stopcock, connected to a gas-dispersion tube, was used to direct flow of nitrogen through, or maintain a nitrogen atmosphere above, the solution under investigation.

The reference electrode was a miniature Saturated Calomel Electrode (SCE) commercially available from the Scientific Instruments Division of Corning Glass Works, Medfield, MA. The internal filling solution was saturated potassium chloride. All potentials reported in this dissertation are with respect to this reference electrode.

2. Flow-through detectors

The flow-through detectors described below were designed by this author and manufactured by the Chemistry Shop at Iowa State University.

a. Tubular electrode A cross-sectional diagram of the tubular Au electrode is shown in Figure II-1. The design eliminates the most troublesome problem associated with tubular detectors, i.e., leakage of the solution of electrolyte into the interface between the electrode and the inert material of the detector body. The body of the detector was constructed of Kel-F due to its mechanical strength, and consisted of two parts (B,G) which were screwed together. The action of the threads provided uniform pressure upon the Teflon compression seals (E).

Figure II-1. Cross-sectional diagram of the tubular detector

A - pressure ring

B - upper body of detector

C - FETFE compression ring for reference and auxiliary electrodes

D - exit port from reference/auxiliary electrode chamber

E - Teflon compression seals for Au tubular electrode

F - Au tubular electrode

G - lower body of detector

H - hole for Au wire, electrical contact to the Au tubular electrode

I - inlet for solution

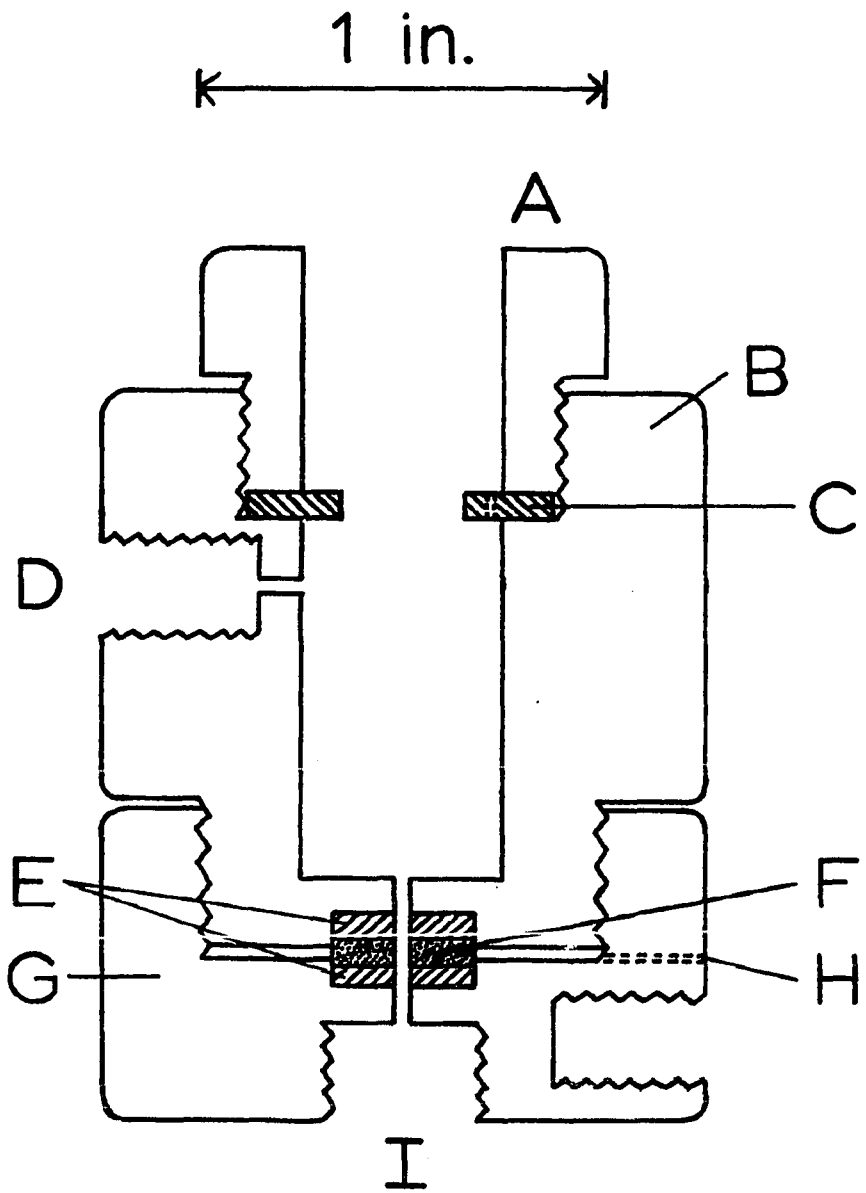
1 in.
A
B
C
D
E
F
G
H
I

The electrode (F) was positioned by two opposing recesses as the two parts came together. Furthermore, the recesses confined the somewhat pliable Teflon and maintained the integrity of the Teflon/electrode interface, even after disassembly and reassembly. The pressure ring (A), made of 25% glass-filled Teflon, and FETFE compression ring (C) were added later. The purpose was to cause solution to be directed from the reference electrode chamber to waste without the need of aspiration which can cause significant "noise" in the analytical signal during measurement of very small currents, e.g., ≤microamperes (μA). The tubular electrode was made from a button of Au which measured 0.15 cm in thickness by 0.9 cm in diameter. The tubular channel drilled through the detector was 0.10 cm i.d.

A detector based on this design has recently been used by Maitoza (144) in the development of a new electroanalytical technique called Reverse Pulse Amperometry.

b. Coulometric electrode A cross-sectional diagram of the coulometric Au electrode is shown in Figure II-2. The body of the detector (C) was constructed of 25% glass-filled Teflon due to its comparable machining properties and cost advantage over Kel-F. The Au chips (F) were made from 31-gauge Au wire, and spirals of the wire (H) were placed before and after the chips to act as retainers. The channel containing the chips was 0.48 cm i.d., and the chips were packed in the channel by gentle tamping with the blunt end of a 3/16-in. drill bit. The total length of the packed, Au chips was

Figure II-2. Cross-sectional diagram of the coulometric detector

A - Pt auxiliary electrode

B - FETFE seals

C - detector body

D - exit port from auxiliary electrode chamber

E - "No-flow" connection for reference electrode

F - Au chips

G - Au wire, electrical contact to Au chips

H - Au wire, spiral retainers

I - inlet for solution

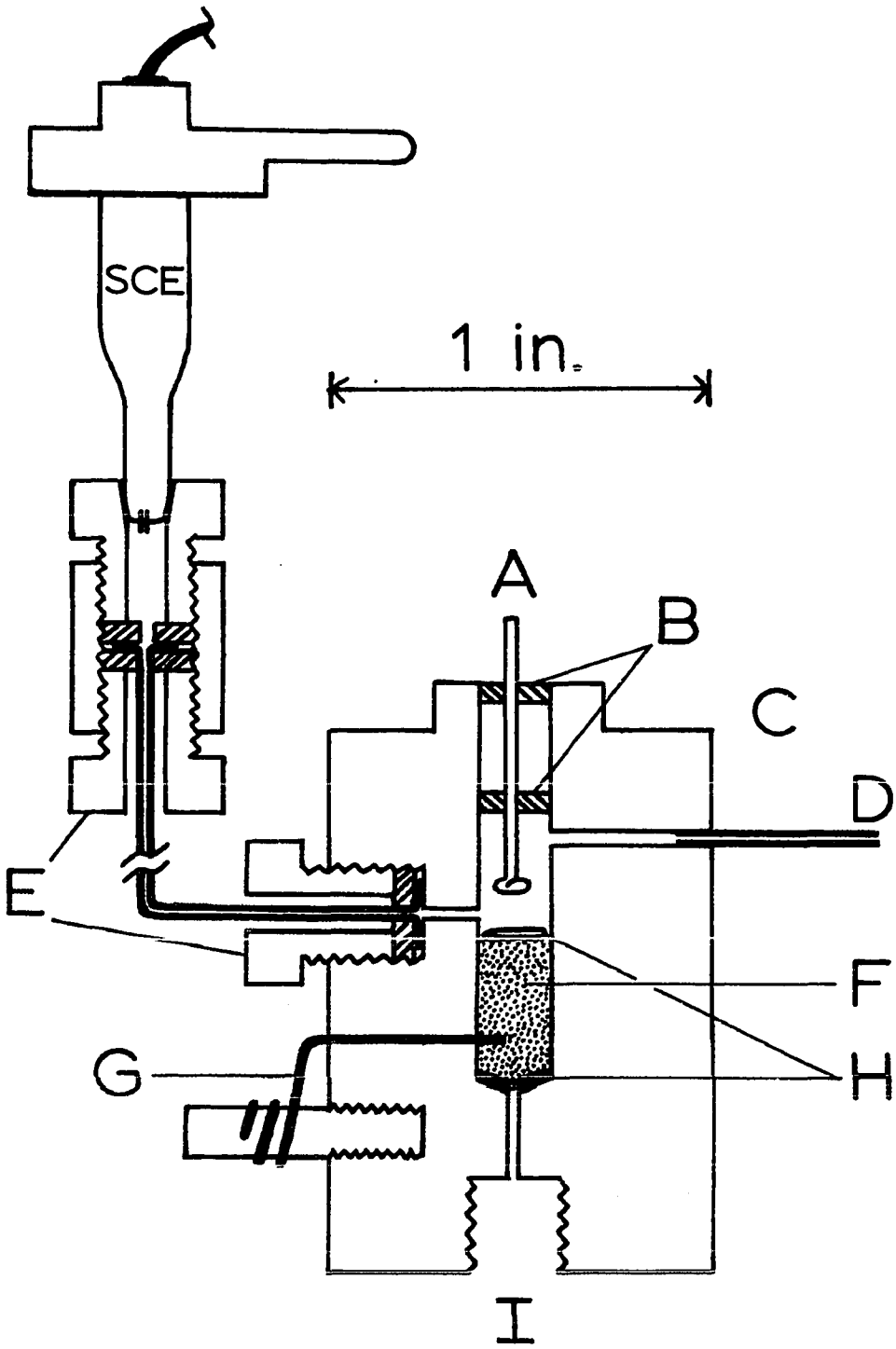
SCE
1 in.
A
B
C
D
E
F
G
H
I

~1.0 cm. Electrical contact to the chips was made by a 20-gauge Au wire (G) protruding through the detector body into the chips.

It was found that a simple connection for the reference electrode could be made from the tube-end fittings and Teflon tubing used in the flow systems which are described below in Part B.4 of this section. The connection, (E) in Figure II-2, is similar to a Luggin capillary. Solution was allowed to flow into the connector until contact was made with the tip of the reference electrode. The reference electrode was then pressed into the tube-end fitting, preventing any further flow of solution in the connector. Any leakage from the reference electrode which diffused into the auxiliary electrode chamber was continually directed to the exit port, away from the indicating electrode, by the flowing solution. The FETFE seals (B) around the Pt auxiliary electrode provided a liquid-tight seal so that aspiration to waste was not required.

3. Instrumentation

Potential control and current measurement were made with a Model RDE2 Potentiostat from Pine Instrument Co. This instrument was used in the experiments with the rotating electrodes and the tubular detector. A Model 174A Polarographic Analyzer from EG&G Princeton Applied Research, Princeton, NJ, was used for potential control and current measurement with the coulometric detector. The potential of the indicating electrode was monitored with a Model 361 digital multimeter from Data Technology Corporation, Palo Alto, CA.

Cyclic voltammograms obtained at the RDE and the tubular detector were recorded on a Model 1131 Variplotter from the Instrument Division of Electronic Associates, Inc., Long Branch, NJ. The data from studies performed with the RRDE were recorded on a Model Omnigraphic 2000 X-Y recorder from Houston Instruments, Bellaire, TX. Detection peaks for the reduction of Hg(II) at the tubular detector were recorded on a stripchart recorder, Model EU-20V from Heath (now Heath-Schlumberger), Benton Harbor, MI. Studies with the coulometric detector were recorded on another Heath-Schlumberger Strip Chart Recorder, Model SR-255 A/B.

Integration of current peaks during this research was performed electronically at the time of data aquisition, or calculated later from the recorded data using Simpson's Formula (145) according to Equation II-1. In this equation: $f_{(x)}$ is the continuous function; $f_{(x_i)}$ is the value of the function at regular intervals, h; and n must be an even number.

$$\int_{x_n}^{x_n} f(x)dx = \frac{h}{3}\left[f(x_o) + 4f(x_1) + 2f(x_2) + 4f(x_3) + \ldots + 2f_{(x_{n-2})} + 4f_{(x_{n-1})} + f_{(x_n)}\right] \qquad \text{II-1.}$$

The calculation was performed on a Hewlett-Packard, Model 19C, programmable calculator.

4. Flow systems

A diagram of the flow system used with the tubular electrode is shown in Figure II-3. All tubing, tube-end fittings and valves were Cheminert from Laboratory Data Control, Riveria Beach, FL. The tubing (0.918 mm i.d.) was used to make a sample loop on the injection valve (F). The sample loop was calibrated according to the method of acid-base titrimetry described by Morris (146), and had a volume of 0.507 mL. The flow rate (V_f) of the supporting electrolyte was controlled by an adjustable needle valve (D) which was designed by this author and manufactured in the Chemistry Shop. Recently, a cross-sectional diagram of the needle valve appeared in the Ph.D. Dissertation of a co-worker (147, Figure 4). The V_f was monitored by a flow meter (E) from Gilmont Instruments, Inc., Great Neck, NY. The flow meter was calibrated at several values of V_f by measuring the volume of solution collected in a buret during a known period of time.

A different flow system was used with the coulometric detector. A diagram of this system appears in Figure II-4. Pumping of the supporting electrolyte was provided by a calibrated Gilson HP Minipuls-2 Peristaltic Pump (B) from Gilson Medical Electronics, Inc., Middletown, WI. A vinyl manifold-tube (0.76 mm i.d.) was used to provide a range of flow rates from 0.2 to 1.2 mL min^{-1}. Two pressure pads for the manifold tubes were specially constructed of Al to provide more uniform pressure on a greater length of each tube than had the original pressure pads. This modification significantly increased the working life-time of each tube. The pulse dampener was an inverted T-tube (C) containing

Figure II-3. Flow system used with the tubular detector

A - helium tank

B - On-Off valve

C - reservoir for the supporting electrolyte

D - adjustable needle valve

E - flow meter

F - injection valve with sample loop

G - syringe

H - solution containing the sample

I - tubular detector

J - potentiostat

K - recorder

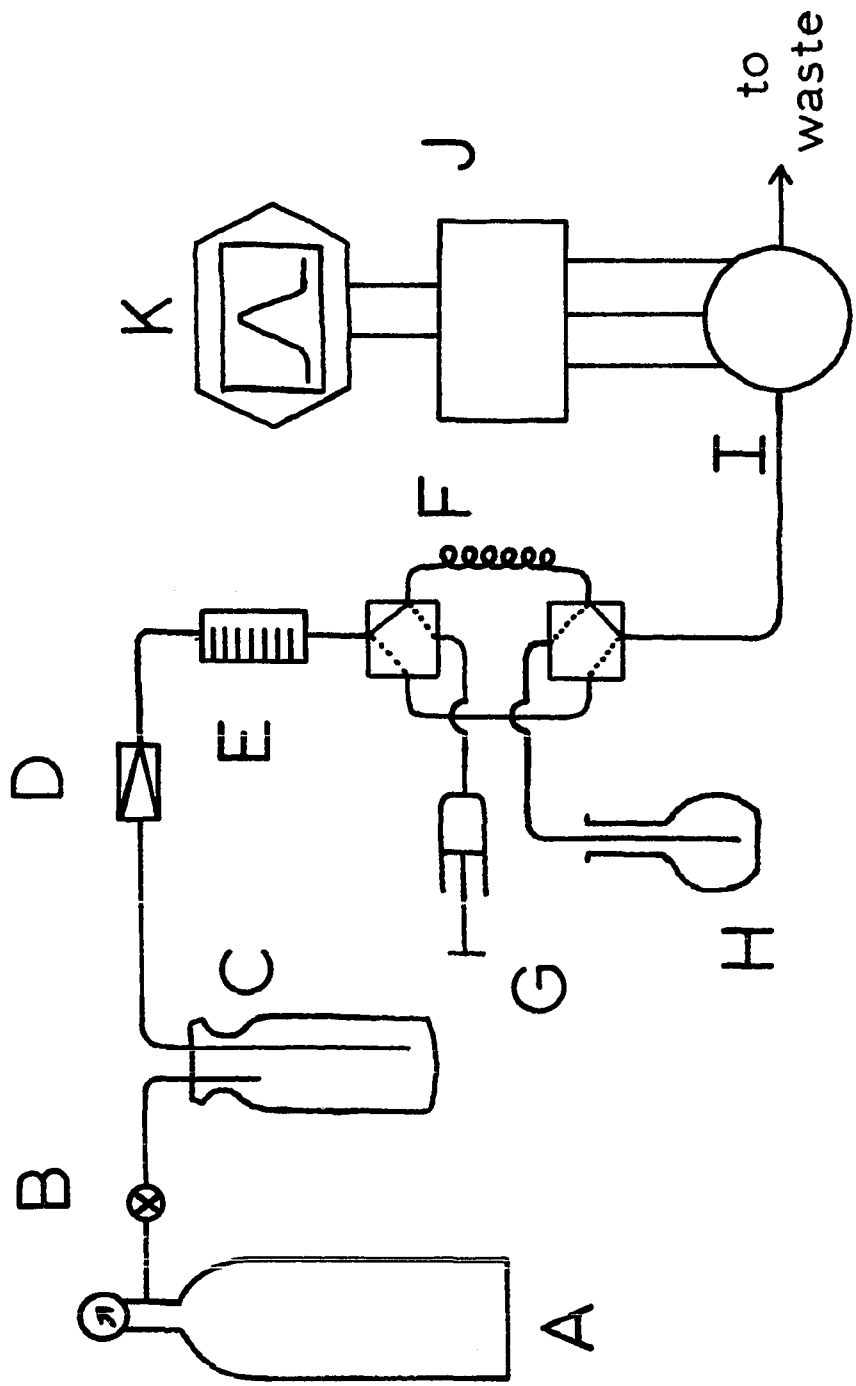
A
B
C
D
E
F
G
H
I
J
K
to
waste

Figure II-4. Flow system used with the coulometric detector

A - reservoir for the supporting electrolyte

B - peristaltic pump

C - inverted T-tube

D - adjustable needle valve

E - injection valve with sample loop

F - syringe

G - solution containing the sample

H - coulometric detector

I - potentiostat

J - recorder

K - electronic integrator

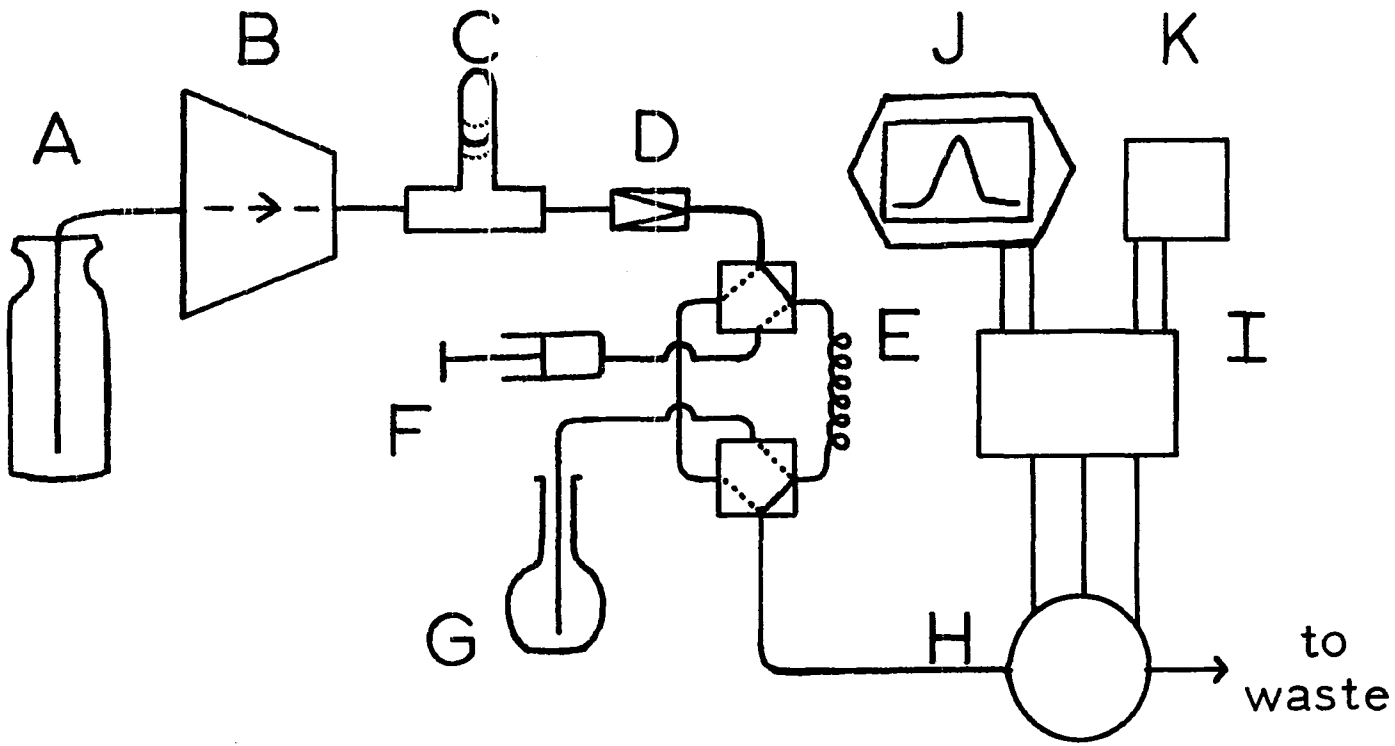
A
B
C
D
E
F
G
H
I
J
K
to
waste

a bubble of air (~0.25 mL) in series with the adjustable needle valve (D), described above, for generation of back pressure. The inverted T-tube was marked in such a way that the position of the meniscus gave an approximate indication of the back pressure supplied by the needle valve, e.g., 3,10,15,20 psi, etc. The sample loop for these experiments had a volume of 0.145 mL.

5. Chemicals and solutions

All solutions were prepared using triply-distilled water (TDW): dimineralization occurred after the first distillation; and the second distillation was from alkaline permanganate (0.10 M $KMnO_4$/0.1 M KOH). The supporting electrolyte was either 2.0 M HNO_3 or 1.0 M H_2SO_4 prepared from the Analytical Reagent Grade acid. The acids were obtained from either Mallinkrodt, Inc., Paris, KT, or from Fisher Scientific Co., Fair Lawn, NJ.

Solutions of Hg(II) were prepared by serial dilution with the supporting electrolyte of aliquots from a concentrated (10^{-1} M) stock solution. The stock solution was prepared as needed by dissolving an accurately weighed quantity of triply-distilled Hg in a sufficient volume of concentrated HNO_3 to yield, upon dilution, a final concentration of acid of ~2 M. The Hg was triply distilled by Chemistry Stores at Iowa State University. The determinations of mass were performed on an Ainsworth Type 28N Analytical Balance from Wm. Ainsworth and Sons, Inc., Denver, CO.

All volumes were measured with standard laboratory glassware. All glassware was cleaned using alcoholic potassium hydroxide followed by hot concentrated HNO_3 and thorough rinsing with TDW. Volumetric flasks, thus prepared, were completely filled with TDW and stored until needed.

The potassium dichromate ($K_2Cr_2O_7$) used to determine the V_f-independence of the Au-chip detector was Baker Analyzed Reagent from J. T. Baker Chemical Co., Phillipsburg, NJ. The reagent was dried at 100^0 C for several hours and then stored in a desiccator over Drierite from Midland Scientific, Inc., Omaha, NE. Stock solutions of $K_2Cr_2O_7$ were prepared by dissolving the dried salt in the supporting electrolyte.

C. Results and Discussion

Before presenting the data obtained by this author, it is appropriate to summarize the results of Sherwood (114) as reported by Sherwood and Bruckenstein (115), Sherwood, et al. (116), and Untereker, et al. (125) pertaining to the UPD of Hg(II) on Au.

Studies performed by Sherwood were conducted using solutions of 0.2 $\underline{M}$ H_2SO_4 as the supporting electrolyte. It was reported (114,115) that Hg(II) "adsorbs on a reduced gold electrode in acid media over a wide potential range, 1.0 V $\geq E_{dep} \geq$ 0.40 V," where E_{dep} refers to the potential of deposition. Furthermore, he found that the quantity of mercury deposited and/or adsorbed within the above range of potential was dependent upon E_{dep}. He calculated the equivalent of one monolayer of Hg(II) on Au to correspond to 339 $\mu C\ cm^{-2}$ of the true area and

demonstrated that a maximum surface coverage equivalent to one monolayer (θ_{max}) could be deposited at the Nernst potential, 0.40 V. Further comments will be made concerning this calculation in Parts C.1 and C.3 below. The Nernst potential was defined as that potential which is established at a Hg-pool electrode in contact with the supporting electrolyte containing Hg(II).

RRDE experiments reported by Sherwood demonstrated that approximately 84% of the first monolayer of mercury deposited on gold was Hg(0). The other 16% of the monolayer was deposited via a nonfaradaic process, i.e., a process which does not result in a net flow of current, as either adsorbed Hg(II) or Hg(I). EC oxidation, or stripping, of the deposited mercury in the underpotential region produced Hg(II) in four overlapping peaks. This latter observation had also been made by Allen (34), and was reported by Allen and Johnson (148) in 1973-1974. Further, calculations made by Allen and reported to this author by Johnson (149), also indicated that only about 80% of the expected current was observed for the UPD of Hg on a Au-film glassy-carbon electrode.

Although the studies reported by Sherwood are important for the understanding of the process of UPD of Hg(II) on Au, no attempt was made to show whether or not UPD could be analytically useful for the quantitative determination of Hg(II). The fact that the UPD of Hg(II) occurs at such positive potentials on Au offers two very attractive advantages: 1) the opportunity of performing the determination without

interference from dissolved oxygen; and 2) enhanced selectivity for Hg(II) via EC stripping analysis because few other metals are deposited on Au at potentials within the UPD region for Hg(II).

For any analytical method utilizing EC stripping, it is highly desirable, although not absolutely necessary, for the deposition step to be performed under conditions limited by the rate of mass transport of the analyte to the surface of the electrode. Primarily, such conditions permit a maximum rate of accumulation so that analysis time may be minimized.

1. Cyclic voltammograms for the underpotential deposition and stripping of Hg(II) at a rotating gold-disk electrode

One of the primary investigative tools which is used in the study of EC processes is the rotating electrode (150). The rotating electrode may be a RDE or RRDE depending upon the information desired. The relationship describing the mass transport-limited current obtained at a RDE for a reversible EC reaction is the Levich Equation, and is given by Equation II-2.

$$I_{D,lim} = 0.62nFAD_X^{2/3}\nu^{-1/6}\omega^{1/2}C_X^b \qquad \text{II-2.}$$

In Equation II-2:

$I_{D,lim}$ = limiting current at the disk (mA);

n = number of electrons involved in the EC process (equivalents $mole^{-1}$);

F = Faraday's constant (96487 coulombs equivalent^{-1}) (151);

A = true area of the electrode surface (cm^2);

D_X = diffusion coefficient of the electroactive species (cm^2 s^{-1});

ν = kinematic viscosity of the solution (cm^2 s^{-1});

ω = angular velocity of the electrode (radians s^{-1});

C_X^b = concentration of the electroactive species in the solution (moles L^{-1}).

According to Equation II-2, $I_{D,lim}$ should be directly proportional to $\omega^{\frac{1}{2}}$. This is confirmed experimentally for the reduction of Hg(II) at a Au RDE at potentials (E_D) $\leq$ 0.40 V, as illustrated in Figures II-5 and II-6, and Table II-2. For convenience, ω (radians s^{-1}) has been converted to rotation speed (W, revolutions min^{-1}) according to Equation II-3. The data for Figure II-6 and Table II-2 were taken from

$$W = \frac{60\omega}{2\pi} \qquad \text{II-3.}$$

Figure II-5. Since Equation II-2 applies only to the current resulting from transport of electroactive species to the surface of the electrode, the data were corrected for the residual current obtained in the absence of Hg(II) in the deaerated, supporting electrolyte. The occurrence of the small, cathodic, current peak in excess of the mass transport-limited current at $E_D \leq 0.4$ V, during the negative scan of potential, will be discussed later in relation to experiments performed using the Au RRDE. No further mention of this phenomenon will be made here.

Figure II-5. Effect of rotation speed of Au disk for Hg(II) in 2.0 $\underline{M}$ HNO_3

$C^b_{Hg(II)}$ - 5.00×10^{-5} $\underline{M}$

$\emptyset$ - 2.0 V min^{-1}

All solutions deaerated

A - 400 rev min^{-1}, residual current

B - 400 rev min^{-1}

C - 900 rev min^{-1}

D - 1600 rev min^{-1}

E - 2500 rev min^{-1}

F - 3600 rev min^{-1}

G - 4900 rev min^{-1}

H - 6400 rev min^{-1}

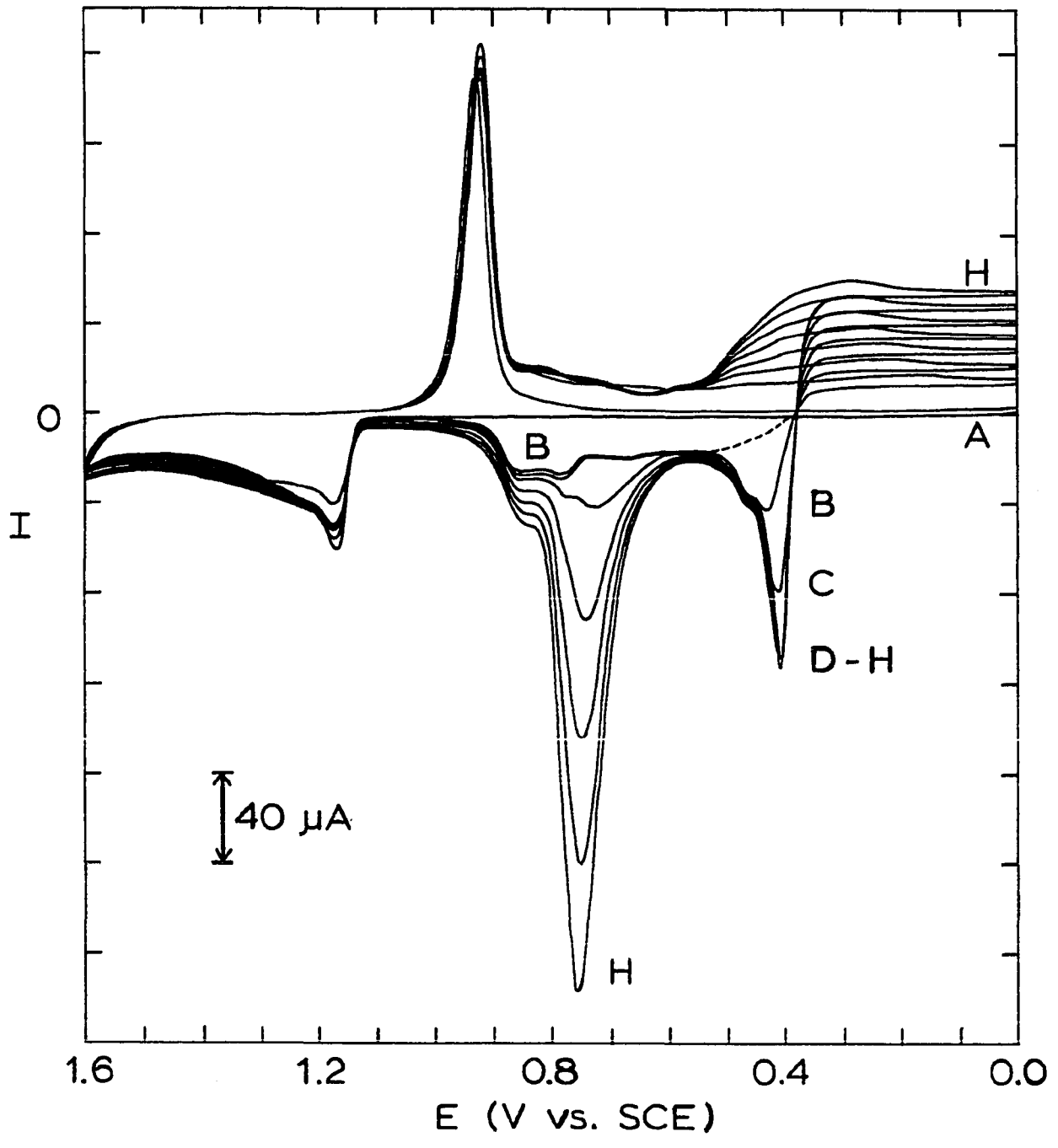
H
A
O
B
I
B
C
D-H
40 μA
H
1.6
1.2
0.8
0.4
0.0
E (V vs. SCE)

Figure II-6. Dependence of limiting current on rotation speed of Au disk during negative scan of potential for Hg(II) in 2.0 M HNO_3

$C^{b}_{Hg(II)}$ - 5.00×10^{-5} M

Ø - 2.0 V min^{-1}

● - 0.40 V vs. SCE

▲ - 0.0 V vs. SCE

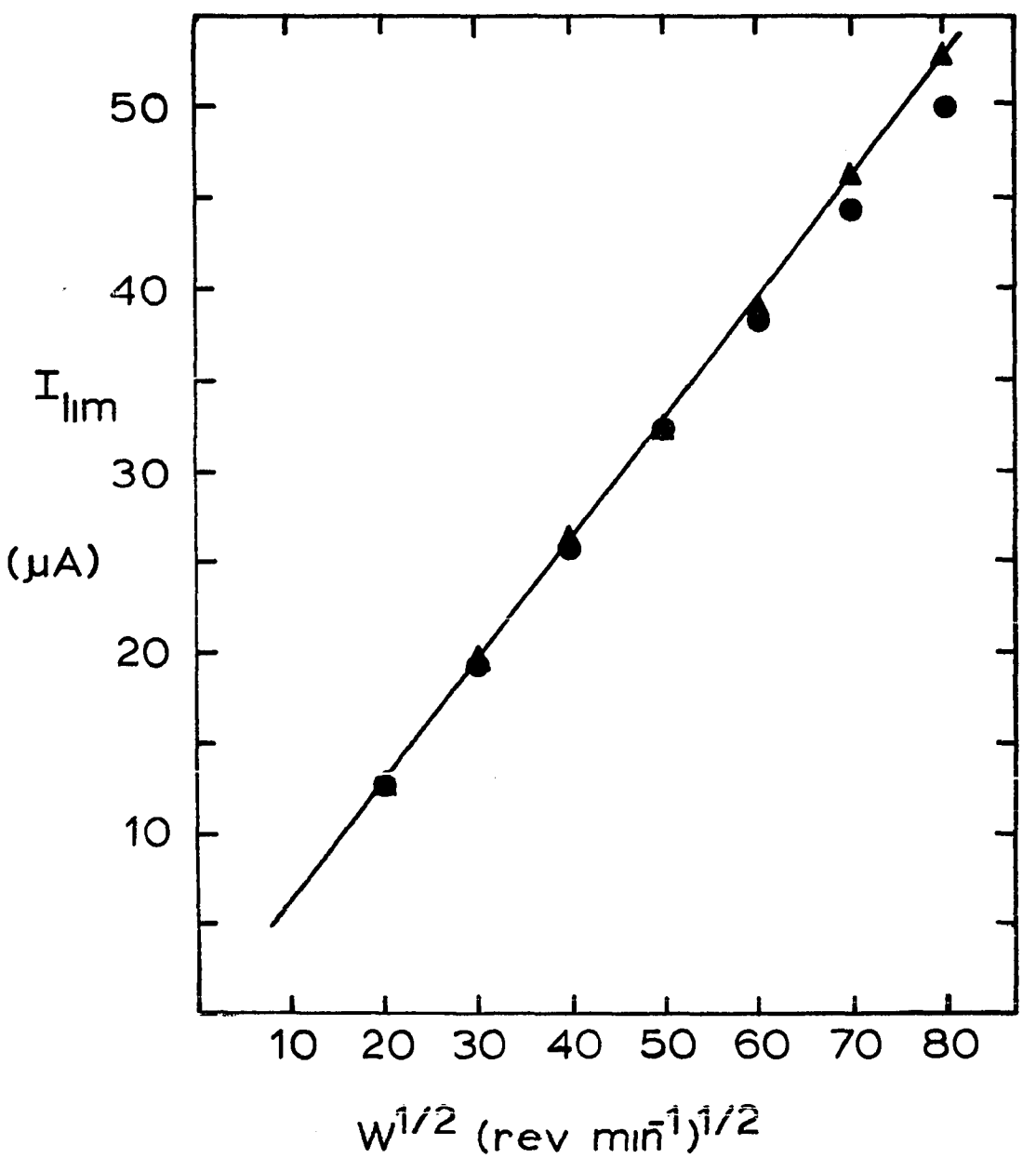
50
40
I_{lim}
30
(μA)
20
10
10 20 30 40 50 60 70 80
$W^{1/2}$ (rev min^{-1})$^{1/2}$

Table II-2. Dependence of limiting reduction current on rotation speed[a] of Au disk for Hg(II) in 2.0 M HNO_3

$W^{\frac{1}{2}}$ ($rev^{\frac{1}{2}}$ $min^{-\frac{1}{2}}$)	Potential (V)	I_{lim} (μA)
20	0.40	12.8
	0.0	12.8
30	0.40	19.2
	0.0	19.6
40	0.40	25.6
	0.0	26.4
50	0.40	32.4
	0.0	32.4
60	0.40	38.4
	0.0	39.2
70	0.40	44.4
	0.0	46.4
80	0.40	50.0
	0.0	52.8

[a]Other parameters as given in Figures II-5 and II-6.

The residual currents obtained at a Au electrode in deaerated, 2.0 M HNO_3 are illustrated in Figure II-5 (Curve A) and may be described as follows. At $E_D > 1.1$ V, the surface of the metal becomes oxidized with the concomitant flow of anodic current. For $E_D > 1.6$ V, destructive oxidation of water to oxygen gas begins. The film of surface oxide is reduced to Au metal at $1.0 \geq E_D \geq 0.8$ V, during the negative scan, with the peak of the reduction current appearing at ~0.95 V.

Only residual currents due to charging of the surface of the electrode are observed at potentials between 1.1 and 0.0 V for a reduced Au electrode. The current observed in the UPD region (1.0 - 0.4 V) during the negative scan of potential displays very little dependence upon the rotation speed of the electrode, as illustrated in Figure II-5. Without further evidence one might be led to conclude that the UPD of Hg(II) on Au is a process controlled only by the rate of adsorption of the reduced species to the surface of the electrode. Some additional evidence comes from the anodic currents obtained in response to the dissolution of the deposited mercury.

During the positive scan of potential, the stripping of mercury deposited as the bulk metal occurs at ~0.4 V. The stripping of the UPD species occurs at $0.95 > E_D > 0.5$ V. It may be observed (Curves B, C,D) that relatively no change occurs in the stripping of the UPD species until a certain quantity of the bulk metal, deposited on the surface of the electrode, is exceeded. After this, the continued deposition of metal apparently forces diffusion of Hg into the interior of the electrode, presumably due to a concentration gradient. The resulting amalgam species is stripped, during the positive scan, in an increasingly large anodic peak at 0.75 V. The fact that Curves B and C in Figure II-5 are nearly identical in the UPD region suggests that the maximum surface coverage equivalent to one monolayer, i.e., ~340 $\mu C\ cm^{-2}$ according to Sherwood, was obtained even at the slowest rotation speed for the conditions under which the data were procured.

Such a conclusion is supported by the following approximate calculation: The stripping charge corresponding to the area under Curve C, excluding the stripping of the bulk metal as indicated by the dashed curve in Figure II-5, was determined to correspond to 225 μC. The geometrical area of the disk electrode was 0.461 cm^2. Although the true, microscopic area was not determined by this author, a Au electrode polished to a mirror finish typically has a roughness factor (R.F. = true area/geometric area) of about 1.7 (127, Chap. 2). Hence, the true area of the disk electrode was estimated to be 0.78 cm^2. Dividing the charge passed during the stripping of the UPD species by the estimated true area of the electrode yields a coverage corresponding to 340 $\mu C\ cm^{-2}$. The agreement with Sherwood's value is remarkable in consideration of the uncertainties in the above calculation.

Equation II-2 also predicts that a plot of $I_{D,lim}$ vs. C_X^b should be linear for a process limited by the rate of mass transport. A linear relationship was verified experimentally for both the UPD of Hg(II), and the deposition at potentials more negative than the Nernst potential. The data are shown in Figure II-7, and the relationship is illustrated in Figure II-8 and Table II-3. In this experiment, the potential of the Au disk was not allowed to exceed 1.1 V. Hence, the reduction peak for the surface oxide is absent, revealing that UPD commences at ~0.9 V during the negative scan of potential. The half-wave potential ($E_{\frac{1}{2},UPD}$) is observed to be ~0.86 V, i.e., the potential at which the current is equal to one-half the limiting value. The value of $E_{\frac{1}{2}}$ has a qualitative significance in electroanalysis similar

Figure II-7. Cyclic voltammograms of Hg(II) in 2.0 M HNO_3 at a Au disk

Ø - 4.0 V min^{-1}

W - 3600 rev min^{-1}

All solutions deaerated

A - 2.0 M HNO_3, residual current

B - 5.00×10^{-6} M Hg(II)

C - 1.00×10^{-5} M Hg(II)

D - 1.50×10^{-5} M Hg(II)

E - 2.00×10^{-5} M Hg(II)

F - 2.50×10^{-5} M Hg(II)

G - 3.00×10^{-5} M Hg(II)

H - 3.50×10^{-5} M Hg(II)

I - 4.00×10^{-5} M Hg(II)

J - 4.50×10^{-5} M Hg(II)

K - 5.00×10^{-5} M Hg(II)

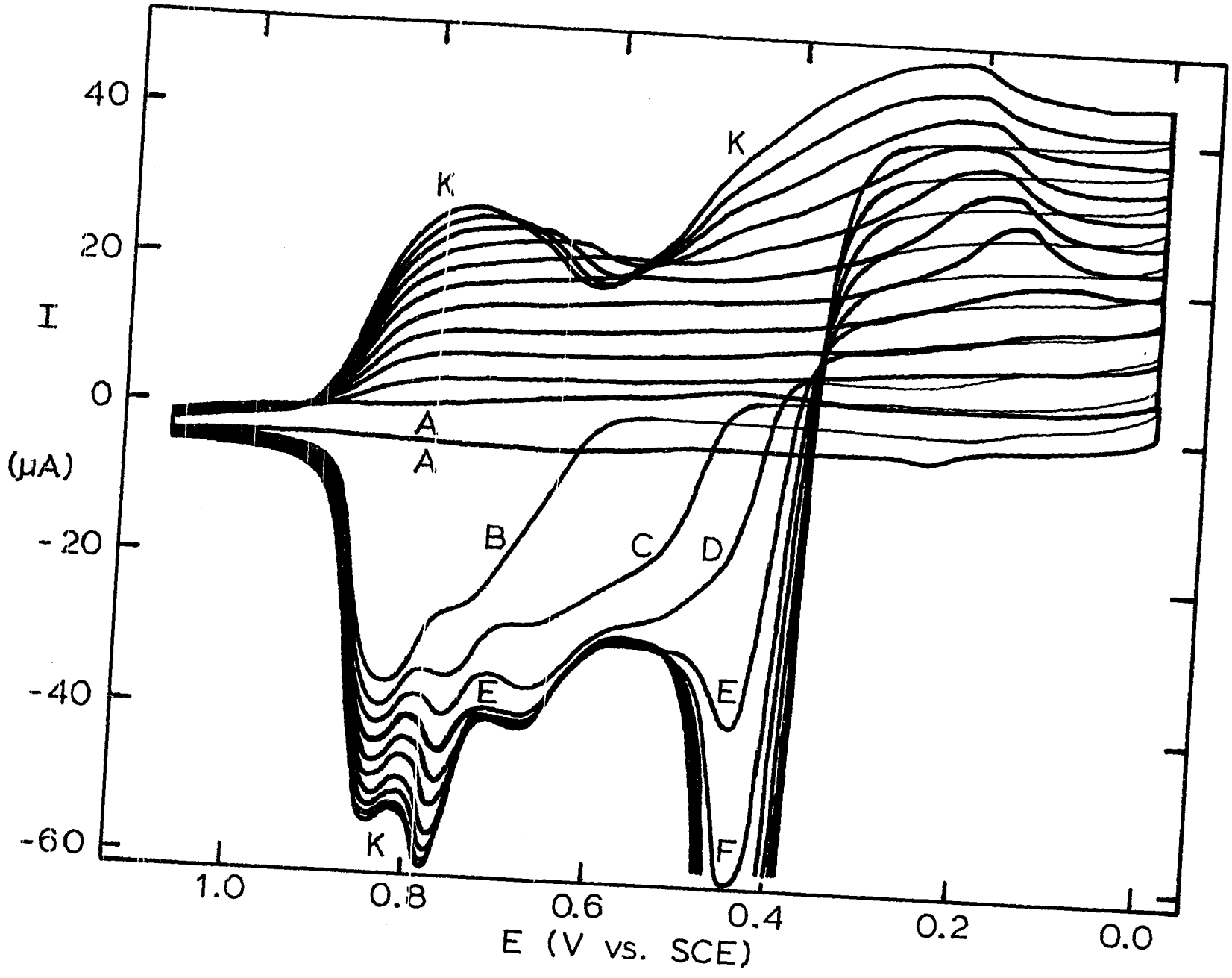
40
20
I
0
(μA)
-20
-40
-60
K
K
A
A
B
C
D
E
E
K
F
1.0
0.8
0.6
0.4
0.2
0.0
E (V vs. SCE)

Figure II-8. Limiting current produced at Au disk during negative scan of potential for various concentrations of Hg(II) in 2.0 M HNO_3

Ø - 4.0 V min^{-1}

W - 3600 rev min^{-1}

○ - 0.77 V vs. SCE

△ - 0.64 V vs. SCE

● - 0.40 V vs. SCE

▲ - 0.0 V vs. SCE

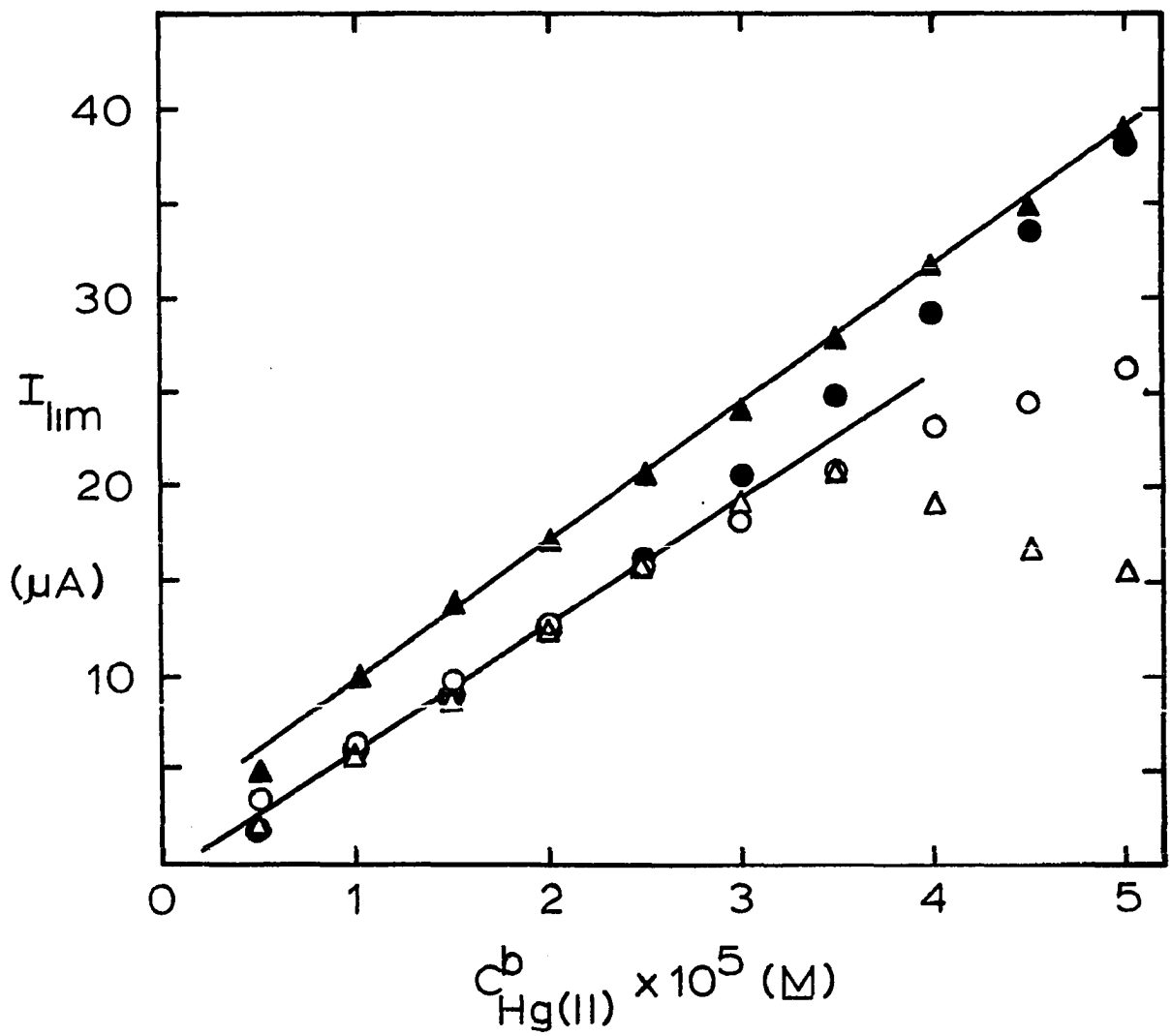
40
30
20
10
I_{lim}
(μA)
0
1
2
3
4
5
$C^{b}_{Hg(II)} \times 10^{5}$ (M)

Table II-3. Limiting reduction current produced at Au disk[a] for various concentrations of Hg(II) in 2.0 M HNO_3

$C^{b}_{Hg(II)}$ (M)	Potential (V)	I_{lim} (μA)
5.00×10^{-6}	0.77	3.4
	0.64	2.2
	0.40	2.2
	0.0	5.0
1.00×10^{-5}	0.77	6.6
	0.64	5.6
	0.40	5.8
	0.0	10.0
1.50×10^{-5}	0.77	9.8
	0.64	8.6
	0.40	9.0
	0.0	14.0
2.00×10^{-5}	0.77	12.8
	0.64	12.4
	0.40	12.6
	0.0	17.2
2.50×10^{-5}	0.77	15.8
	0.64	15.8
	0.40	16.4
	0.0	20.6
3.00×10^{-5}	0.77	18.2
	0.64	19.4
	0.40	20.6
	0.0	24.2
3.50×10^{-5}	0.77	20.8
	0.64	21.0
	0.40	24.8
	0.0	28.0

[a]Other parameters as given in Figures II-7 and II-8.

Table II-3. Continued

$C^{b}_{Hg(II)}$ (M)	Potential (V)	I_{lim} (μA)
4.00×10^{-5}	0.77	23.2
	0.64	19.4
	0.40	29.4
	0.0	31.8
4.50×10^{-5}	0.77	24.6
	0.64	16.8
	0.40	33.6
	0.0	35.0
5.00×10^{-5}	0.77	26.4
	0.64	15.6
	0.40	38.2
	0.0	39.0

to the wave number of an absorption band in infrared spectroscopy (152, Section IV). The fact that the value of $E_{\frac{1}{2},UPD}$ displays little, or no dependence upon the rate of mass transport is indicative of an EC process for which the transfer of electrons is kinetically fast, i.e., reversible. Furthermore, such behavior is expected for a reversible deposition when the activity of the deposited product is significantly less than unity, i.e., $\theta << \theta_{max}$.

Sherwood and Bruckenstein reported that the surface coverage for Hg(II) deposited at underpotential was a function of the potential applied to the Au disk (115). The data shown in Figure II-7 are in agreement with this observation. As the value of $C^{b}_{Hg(II)}$ increases, $I_{D,lim}$ increases until the rate of reduction of Hg(II) causes the

deposited quantity of metal to approach the maximum coverage allowed at the particular potential within the UPD region (θ_E). The current then decays (Curves F-K in Figure II-7) until the potential of the electrode becomes sufficiently negative to reduce Hg(II) to the bulk metal. The decay of the UPD reduction wave corresponds well with the appearance of the stripping peak for the bulk metal.

A linear relationship is observed in Figure II-8 between $I_{D,lim}$ and $C^b_{Hg(II)}$ at potentials within the UPD region until the conditions cited above are exceeded. This indicates that the UPD of Hg(II) on Au is limited by the rate of mass transport so long as $\theta < \theta_E < \theta_{max}$. Furthermore, it may be seen that $I_{D,lim}$, obtained in the UPD region, is consistently less than that obtained at more negative potentials, i.e., 0.0 V. Such a result implies that the UPD process does not occur with n = 2 equivalents $mole^{-1}$, which is the case for reduction of Hg(II) to the bulk metal. Actually one can not determine electrochemically whether all species deposited at underpotential retain a partial charge, or whether the deposit consists of both zero-valent metal and Hg(II), or Hg(I), ions (adions) adsorbed to the surface of the electrode. For now, this author defines n_{app} as the apparent, average value of n for the UPD of Hg(II) on Au, according to Equation II-4.

$$Hg^{2+} + n_{app}e \rightleftharpoons Hg(UPD) \qquad \text{II-4.}$$

This notation will be used later in the discussion of data obtained with the coulometric detector. Hg(UPD) refers to the deposited species, whether partially charged or a combination of Hg(0) and adions.

The dependence of $I_{D,lim}$ upon $W^{\frac{1}{2}}$ was studied again, using a more dilute solution of Hg(II). The data appear in Figures II-9 and II-10, and in Table II-4. Although the quality of the data is not the best possible, the linear relationship between $I_{D,lim}$ and $W^{\frac{1}{2}}$ is verified in the UPD region when $\theta < 0.7\theta_{max}$ (Curves B-E in Figure II-9). It should also be noted that the strong interaction between the Au surface and the very first, deposited quantities of mercury, e.g., $\theta < 0.25\theta_{max}$, seems to follow Equation II-4 even when the potential of the electrode is much more negative than the Nernst potential. For example, the dependence of $I_{D,lim}$ upon $W^{\frac{1}{2}}$ at E_D = 0.0 V, does not exhibit linearity until θ_{max} for UPD has been achieved. Hence, the quantitative determination of Hg(II) should not be based upon $I_{D,lim}$ for the deposition of trace quantities of the metal at $E_D < 0.4$ V. Furthermore, the quantitative evaluation of $I_{D,lim}$ for solutions containing Hg(II) at submicromolar concentrations (< 0.2 ppm) is severely hindered by the residual current due to charging of the electrode/solution interface as the scan of potential proceeds. Amperometric detection, i.e., the measurement of current with respect to time at constant potential, although eliminating the residual charging current, does not resolve the nonlinearity observed in $I_{D,lim}$ at $E_D < 0.4$ V as the deposited quantity of metal exceeds the equivalent of a few monolayers. The ramifications of the latter statement extend to the use of a Au electrode as an amperometric detector for Hg(II) in a flowing stream, as will be discussed below in Part C.2.

Figure II-9. Effect of rotation speed of Au disk for Hg(II) in 2.0 M HNO_3

$C^{b}_{Hg(II)}$ - 1.50×10^{-5} M

$\emptyset$ - 4.0 V min^{-1}

All solutions deaerated

A - 400 rev min^{-1}, residual current

B - 400 rev min^{-1}

C - 900 rev min^{-1}

D - 1600 rev min^{-1}

E - 2500 rev min^{-1}

F - 3600 rev min^{-1}

G - 4900 rev min^{-1}

H - 6400 rev min^{-1}

I - 8100 rev min^{-1}

J - 10000 rev min^{-1}

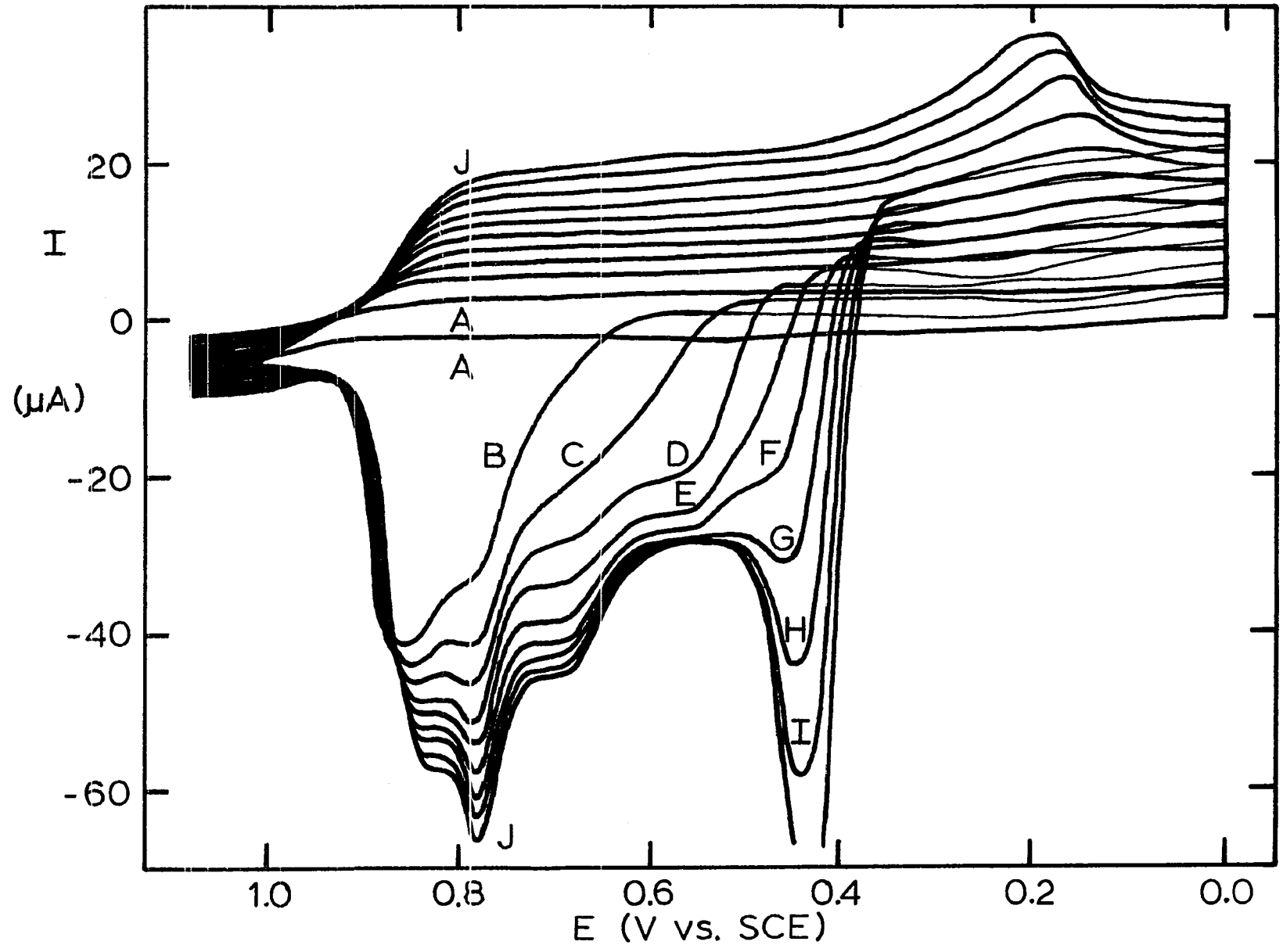
20
I
0
(μA)
-20
-40
-60
J
A
A
B
C
D
E
F
G
H
I
J
1.0
0.8
0.6
0.4
0.2
0.0
E (V vs. SCE)

Figure II-10. Dependence of limiting current on rotation speed of Au disk during negative scan of potential for Hg(II) in 2.0 M HNO_3

$C^b_{Hg(II)}$ - 1.50×10^{-5} M

ϕ - 4.0 V min^{-1}

○ - 0.77 V vs. SCE

△ - 0.64 V vs. SCE

● - 0.40 V vs. SCE

▲ - 0.0 V vs. SCE

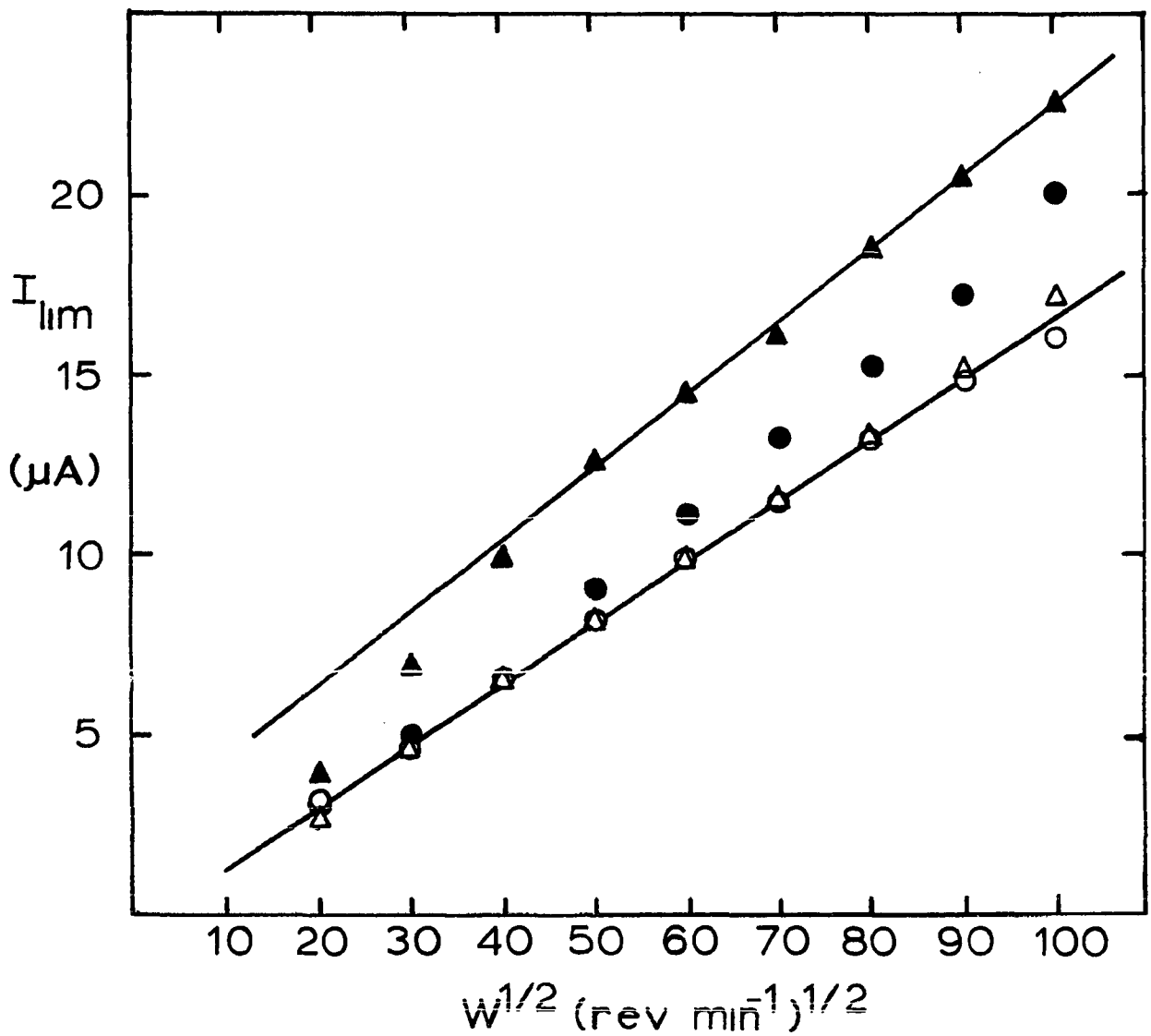
20
I_{lim}
15
(μA)
10
5
10 20 30 40 50 60 70 80 90 100
$w^{1/2}$ (rev min^{-1})$^{1/2}$

Table II-4. Dependence of limiting current on rotation speed[a] of Au disk for Hg(II) in 2.0 M HNO_3

$W^{1/2}$ ($rev^{1/2}$ $min^{-1/2}$)	Potential (V)	I_{lim} (μA)
20	0.77	3.2
	0.64	2.6
	0.40	3.0
	0.0	3.8
30	0.77	4.6
	0.64	4.6
	0.40	5.0
	0.0	6.8
40	0.77	6.6
	0.64	6.4
	0.40	6.6
	0.0	9.8
50	0.77	8.2
	0.64	8.0
	0.40	9.0
	0.0	12.6
60	0.77	9.8
	0.64	9.8
	0.40	11.0
	0.0	14.4
70	0.77	11.4
	0.64	11.4
	0.40	13.2
	0.0	16.2
80	0.77	13.2
	0.64	13.2
	0.40	15.2
	0.0	18.4

[a]Other parameters as given in Figures II-9 and II-10.

Table II-4. Continued

$W^{\frac{1}{2}}$ ($rev^{\frac{1}{2}}$ $min^{-\frac{1}{2}}$)	Potential (V)	I_{lim} (μA)
90	0.77	14.6
	0.64	15.2
	0.40	17.2
	0.0	20.4
100	0.77	16.0
	0.64	17.0
	0.40	19.8
	0.0	22.6

Using the same solution for which the data of Figure II-5 were obtained, a study was made to determine the relationship, if any, between the rate of potential scan ($\emptyset$) and the cathodic current obtained in the UPD region. The data were rather complex and are shown sequentially in Figures II-11, II-12 and II-13. Current values, measured at 1.5 V during the positive scan (surface oxide) and at 0.64 V during the negative scan (UPD), are plotted vs. $\emptyset$ in Figure II-14, and given in Table II-5.

The limiting current for an EC reaction which is limited by the rate of mass transport to the surface of the electrode will exhibit no dependence upon $\emptyset$. On the other hand, the current for a surface-controlled process which is dependent upon the potential of the electrode, e.g., the formation of the surface oxide on Au, will be proportional to $\emptyset$.

Figure II-11. Effect of rate of potential scan of Au disk for Hg(II) in 2.0 M HNO_3

$C^b_{Hg(II)}$ - 5.00×10^{-5} M

W - 3600 rev min^{-1}

All solutions deaerated

A - 1.0 V min^{-1}

B - 2.0 V min^{-1}

C - 3.0 V min^{-1}

D - 4.0 V min^{-1}

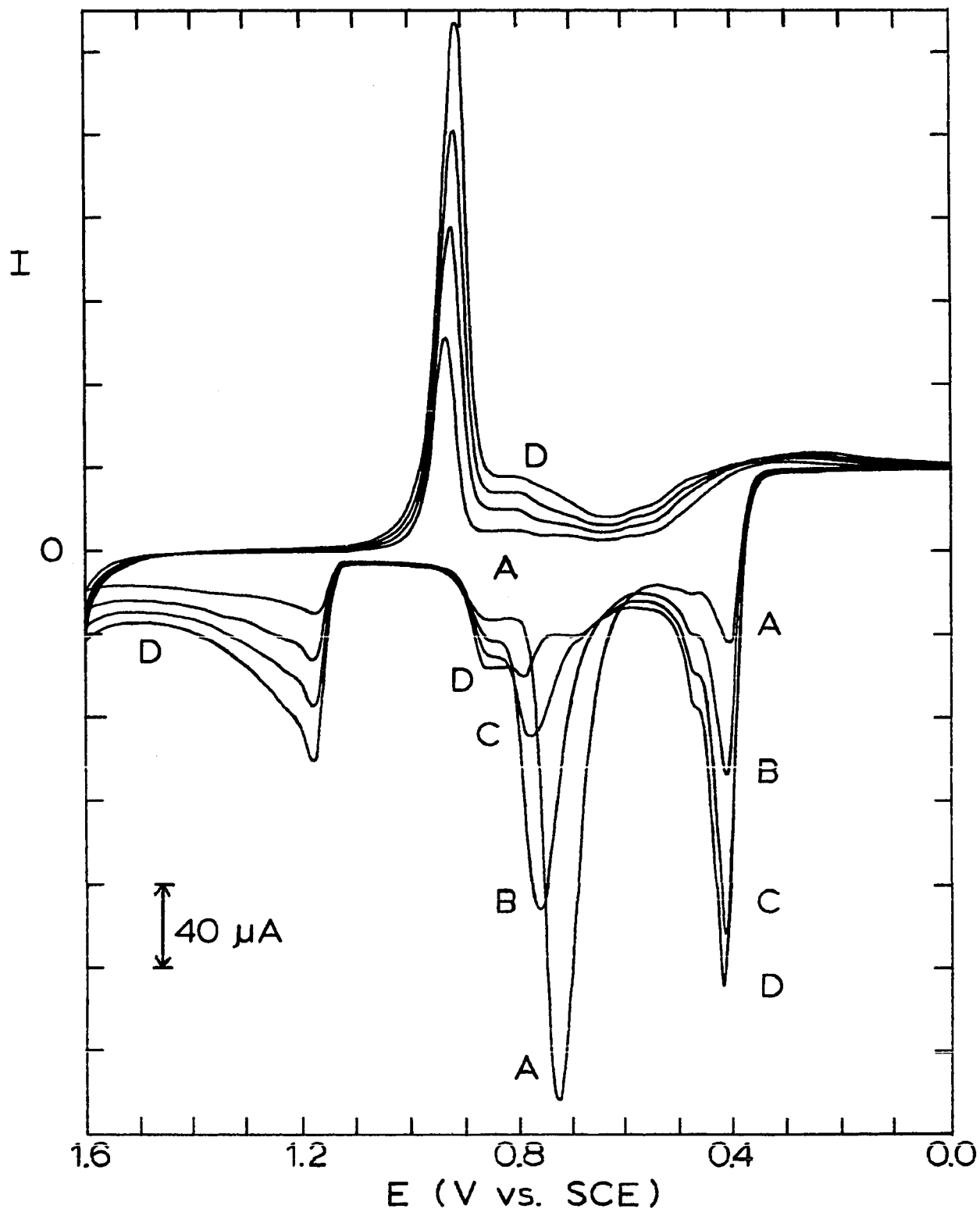
I
0
D
A
D
D
C
A
B
C
D
B
A
40 μA
1.6
1.2
0.8
0.4
0.0
E (V vs. SCE)

Figure II-12. Effect of rate of potential scan of Au disk for Hg(II) in 2.0 $\underline{M}$ HNO_3

$C^{b}_{Hg(II)}$ - 5.00×10^{-5} $\underline{M}$

W - 3600 rev min^{-1}

All solutions deaerated

A - 4.0 V min^{-1}

B - 5.0 V min^{-1}

C - 6.0 V min^{-1}

D - 7.0 V min^{-1}

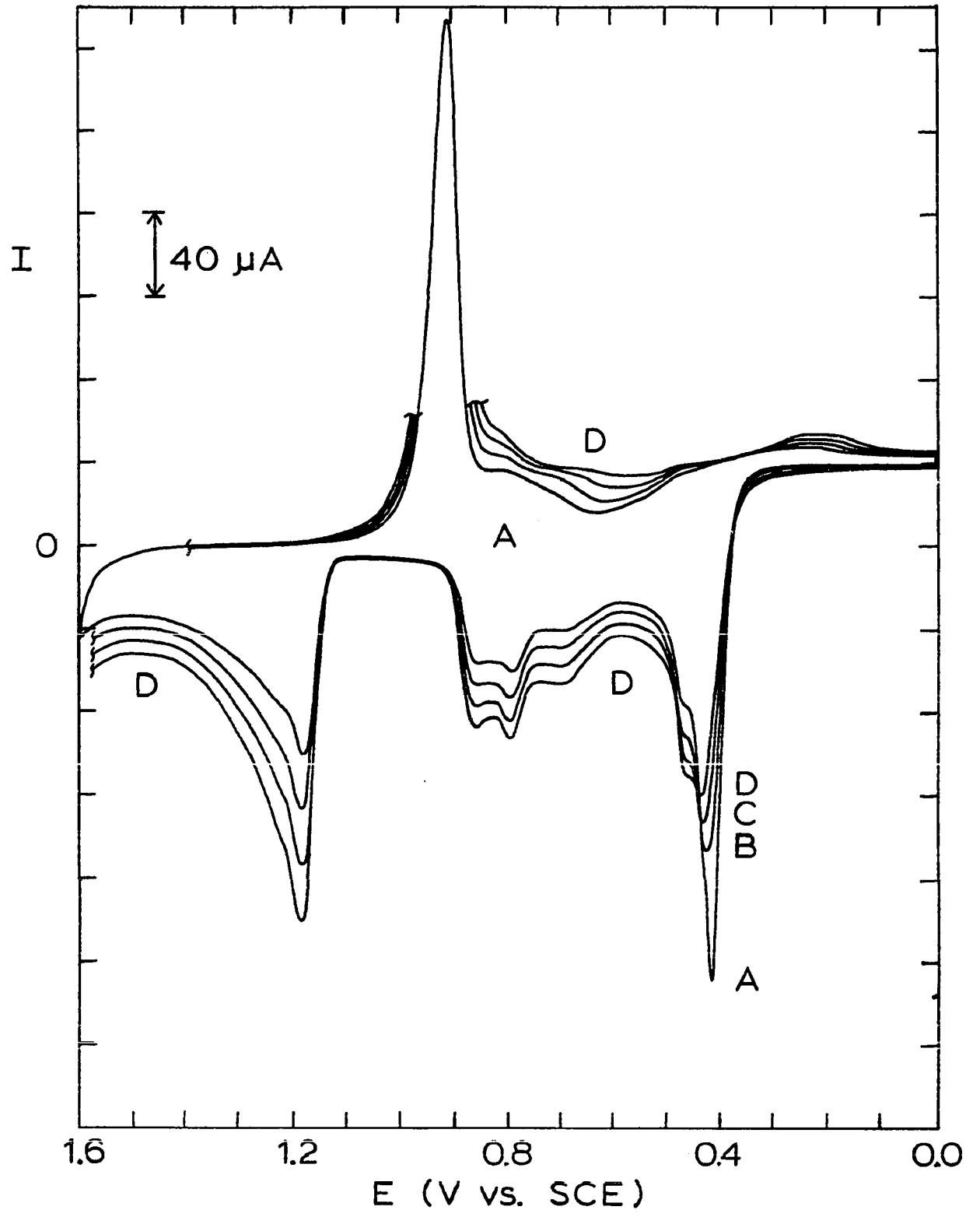
I
40 μA
0
D
A
D
D
D
C
B
A
1.6
1.2
0.8
0.4
0.0
E (V vs. SCE)

Figure II-13. Effect of rate of potential scan of Au disk for Hg(II) in 2.0 M HNO_3

$C^b_{Hg(II)}$ - 5.00×10^{-5} M

W - 3600 rev min^{-1}

All solutions deaerated

A - 7.0 V min^{-1}

B - 8.0 V min^{-1}

C - 9.0 V min^{-1}

D - 10.0 V min^{-1}

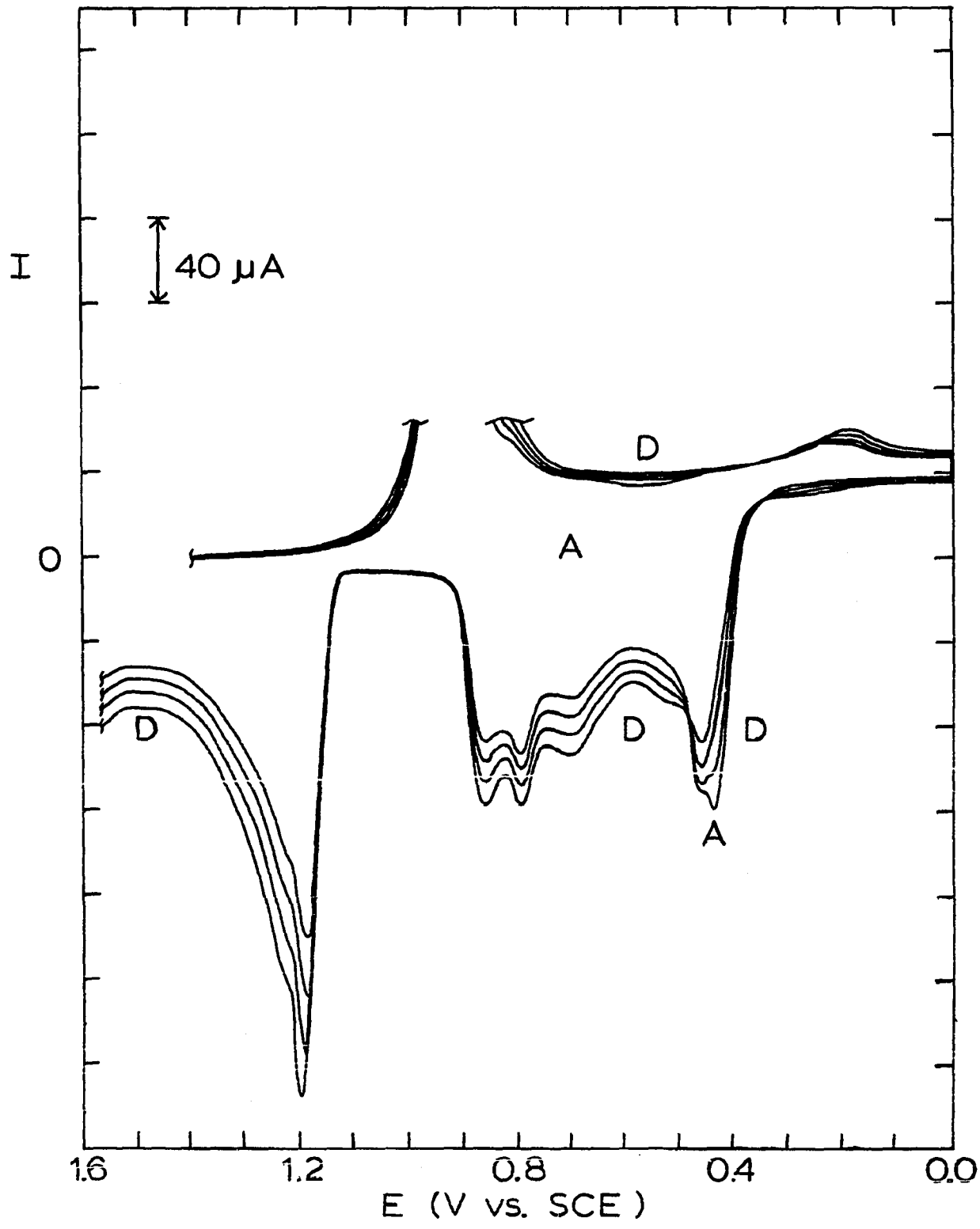
I
40 μA
0
D
A
D
D
D
D
A
1.6
1.2
0.8
0.4
0.0
E (V vs. SCE)

Figure II-14. Comparison of currents obtained at Au disk for a surface-controlled process and for UPD of Hg(II) in 2.0 M HNO_3 as function of rate of potential scan

$C^b_{Hg(II)}$ - 5.00×10^{-5} M

W - 3600 rev min^{-1}

● - 1.50 V vs. SCE, positive scan

○ - 0.64 V vs. SCE, negative scan

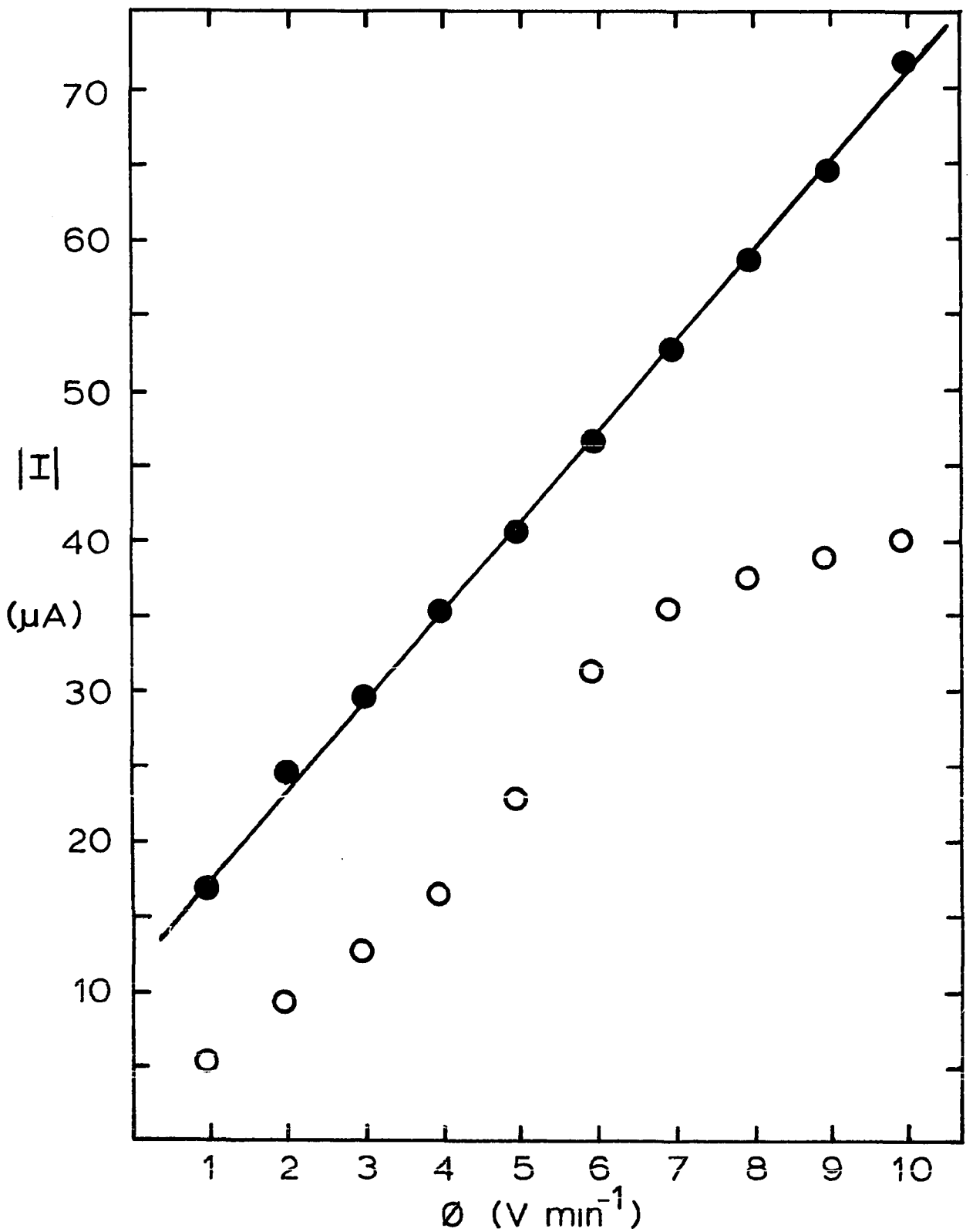
70
60
50
|I|
40
(μA)
30
20
10
1
2
3
4
5
6
7
8
9
10
Ø (V min⁻¹)

Table II-5. Comparison of currents obtained at Au disk[a] for a surface-controlled process and for UPD of Hg(II) in 2.0 M HNO_3 as function of scan rate

Scan Rate, Ø ($V\ min^{-1}$)	I (μA), E = 1.50 V positive scan	I (μA), E = 0.64 V negative scan
1.0	16.8	5.2
2.0	24.4	9.2
3.0	29.6	12.4
4.0	35.2	16.4
5.0	40.4	22.8
6.0	46.8	31.2
7.0	52.8	35.6
8.0	58.8	37.6
9.0	64.8	38.8
10.0	72.0	40.0

[a]Other parameters as given in Figures II-11 through II-14.

A linear relationship between Ø and the current due to the formation of the surface oxide at 1.5 V is clearly demonstrated in Figure II-14. One can not come to a definitive conclusion based upon the data for the UPD of Hg(II) in this figure. However, the nonlinearity of the data is indicative of a process under mixed control, i.e., surface-control at low Ø and mass transport-control at high Ø. The particular conditions chosen for W and $C^{b}_{Hg(II)}$, evidently provided a sufficiently high rate of mass transport such that θ_E was attained within the period of time in which E_D was scanned within the UPD region.

The limiting current is observed to decay at all but the faster rates of scan in a manner similar to that observed at higher concentrations in Figure II-7.

These data are consistent with the conclusion that UPD of Hg(II) on Au occurs at a rate which is limited by mass transport of Hg(II) to the surface of the electrode so long as the deposited quantity of metal does not approach θ_E for $0.9\ V > E_D > 0.4\ V$.

2. The underpotential deposition and stripping of Hg(II) at a tubular gold electrode

The voltammetric characteristics of an electroactive species are often investigated using rotating electrodes to determine the suitability of EC detection for the determination of that species by LC and/or FIA. The tubular detector, first introduced by Levich in the USSR (153), is ideally suited as an EC, flow-through detector. The quantitative relationship describing the response of the limiting, steady-state current, $I_{T,lim}$, at the tubular electrode is given by Equation II-5.

$$I_{T,lim} = 5.43nFL^{2/3}D_X^{2/3}V_f^{1/3}C_X^b \qquad \text{II-5.}$$

In Equation II-5:

L = length of the tubular electrode (cm);

V_f = flow rate of the fluid stream ($cm^3\ s^{-1}$);

and the other terms are as defined in Equation II-2.

Tubular electrodes, when applied in LC or FIA, are most often operated in the amperometric mode. Equation II-5 predicts a 1/3-root proportionality between $I_{T,lim}$ and V_f. However, due to the nature of LC and FIA, a steady-state response is very seldom achieved because of dispersion of the injected sample within the flow stream prior to the point of detection.

The problem of dispersion in FIA has recently come under extensive investigation by P. L. Meschi, working in the laboratory of Professor Dennis C. Johnson, at Iowa State University. Meschi has shown dispersion to be a very complex function of V_f and the design of the flow system, which usually causes the concentration of the species of interest at the detector to be less than the analytical concentration injected, i.e., C_X^b in Equation II-5. According to Meschi (154), the equation relating $I_{T,lim}$ to the smaller, peak current (I_p), observed after dispersion within a straight, tubular channel can be approximated by Equation II-6 for $V_s < V_r$.

$$I_p = I_{T,lim} V_s \left\{ 2\pi^{3/2} a^2 \left[\frac{a^2 \left(\frac{V_f}{\pi a^2} \right)^2}{48 D_X a^2} \right]^{1/2} \left[\frac{0.5V_s + V_r}{V_f} \right]^{1/2} \right\}^{-1} \qquad \text{II-6.}$$

Fortunately, by combining terms, Equation II-6 can be reduced to the somewhat simpler form given by Equation II-7.

$$I_p = I_{T,lim} \left[2.76 D_X^{1/2} V_s (V_s + 2V_r)^{-1/2} a^{-1} V_f^{-1/2} \right] \qquad \text{II-7,}$$

In Equations II-6 and II-7:

V_s = volume of sample solution injected (cm^3);

V_r = retention volume of the flow system, i.e., the internal volume of the connecting tubing between the injector and detector (cm^3);

a = radius of the tubular channel (cm).

The relationship of I_p to V_f in LC and FIA using a tubular electrode can not be expected to show the simple 1/3-root proportionality given for $I_{T,lim}$ by Equation II-5. However, under conditions of constant V_f, i.e., constant dispersion, the value of I_p may be used to indicate the potentials at which a limiting-current plateau may be observed for steady-state electrolysis of the solution containing the sample.

The experiments described thus far have shown that a reduction wave is observed in the current-voltage (I-E) curve for UPD of Hg(II) from very dilute solutions on a Au RDE at $E_D < 0.9$ V. This reduction wave was investigated amperometrically at a Au tubular electrode. The pseudo I-E curve, shown in Figure II-15, was constructed by plotting I_p as a function of E_{dep} for injections of constant concentration. The data are listed in Table II-6. The appearance of a pseudo limiting-current plateau in Figure II-15 is consistent with the data obtained at the RDE indicating that UPD of Hg(II) on Au is a process limited by the rate of mass transport. The value of $E_{\frac{1}{2},UPD}$ determined from Figure II-15 is ~0.88 V which, in view of the limited data in the vicinity of $E_{\frac{1}{2},UPD}$, is in good agreement with the value of ~0.86 V observed at the Au RDE (compare Figures II-7 and II-9).

Figure II-15. Pseudo I-E curve for UPD of Hg(II) at tubular Au electrode in 2.0 M HNO_3

$C^b_{Hg(II)}$ - 1.00×10^{-4} M

V_s - 0.507 mL

V_f - 1.5 mL min^{-1}

Air saturated solutions

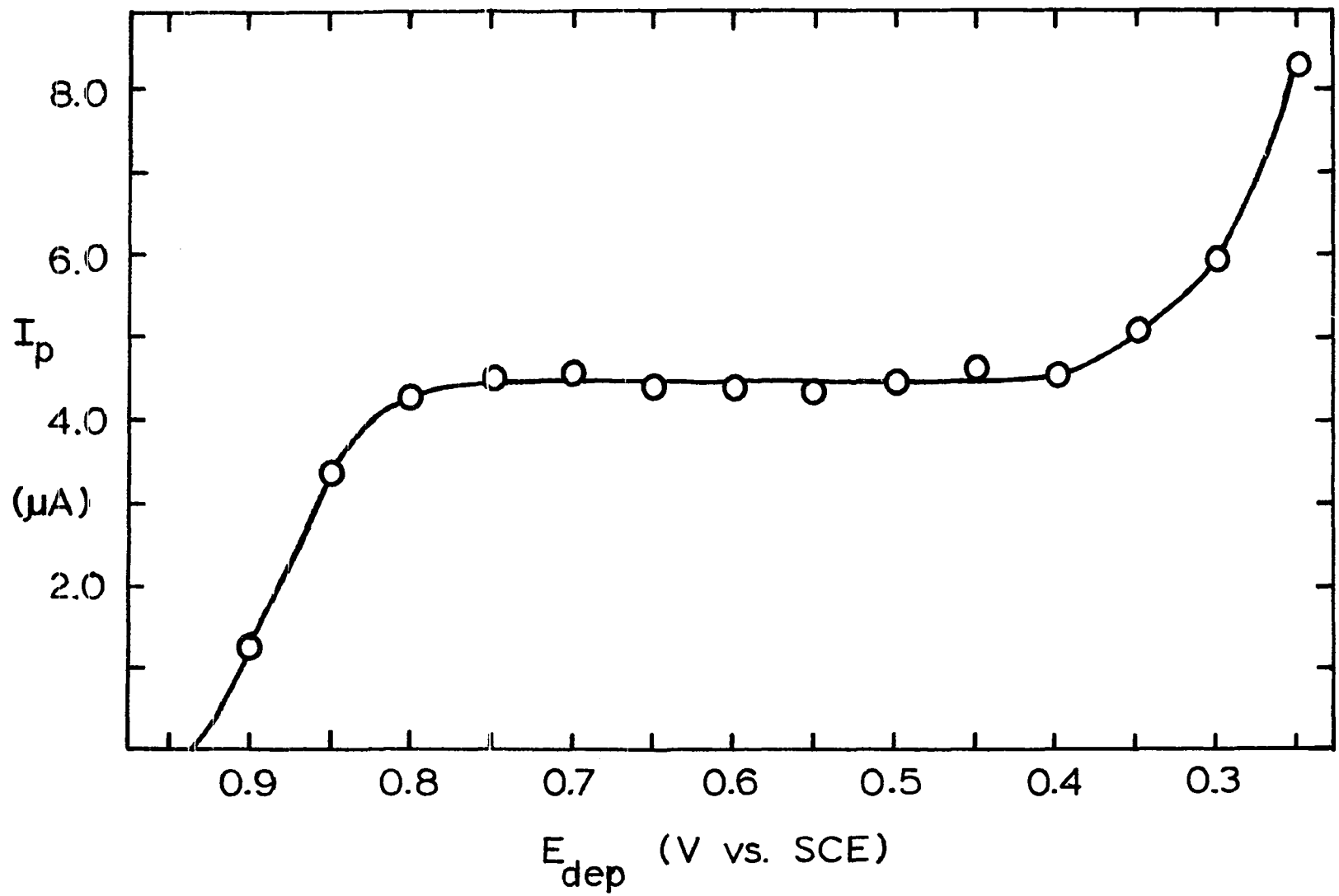
8.0
6.0
I_p
4.0
(μA)
2.0
0.9
0.8
0.7
0.6
0.5
0.4
0.3
E_{dep} (V vs. SCE)

Table II-6. Peak current for UPD of Hg(II) at tubular Au electrode[a] in 2.0 M HNO_3 as a function of E_{dep}

E_{dep} (V)	I_p (μA)	E_{dep} (V)	I_p (μA)
1.00	0.0	0.60	4.38
0.95	0.0	0.55	4.35
0.90	1.25	0.50	4.48
0.85	3.33	0.45	4.61
0.80	4.26	0.40	4.55
0.75	4.50	0.35	5.10[b]
0.70	4.57	0.30	5.95[b]
0.65	4.37	0.25	8.32[b]

[a]Other parameters as given in Figure II-15.

[b]Severe shift in baseline after peak due to reduction of dissolved oxygen at Hg-film Au electrode.

Interference from the simultaneous reduction of dissolved oxygen during the reduction of Hg(II) at a Au flow-through electrode makes questionable the interpretation of data obtained at $E_{dep} < 0.40$ V. Removal of dissolved oxygen from the flow stream is not easily accomplished; the Teflon tubing and other plastic components commonly used in the construction of flow systems are readily permeated by oxygen in the air. The problem of dissolved oxygen, more than any other, discourages the use of Au flow-through electrodes, operated at $E_{dep} < 0.4$ V (vs. SCE), for the direct determination of Hg(II) based upon the measurement of current for reduction to the bulk metal.

Alternatively, the UPD and stripping of Hg(II) is shown to be without interference from dissolved oxygen. Figure II-16 illustrates the stripping curves obtained at the Au tubular detector for different quantities of accumulated metal. The depositions were made at $E_{dep} < 0.4$ V, and quantitative evaluation of I_p was impossible due to the interference from dissolved oxygen. The area under the stripping curves represents the charge (Q_{strip}) necessary to remove the accumulated deposit. The data are plotted in Figure II-17, and given in Table II-7.

The slight, positive deviation from the straight line for greater than seven successive injections may be attributed to the transition from deposition according to Equation II-4, at $\theta < 0.7\theta_{max}$, to deposition of the bulk metal with n = 2 at $E_{dep} < 0.4$ V. For deposition and stripping from a potential within the UPD region, a plot of Q_{strip} vs. the injected quantity of Hg(II) would be expected to increase in a linear fashion until $\theta_E \leq \theta_{max}$ is approached, after which Q_{strip} would become independent of the number of successive injections.

Special notice should be taken that a single, symmetrical stripping peak is obtained when the deposited quantity of metal is very small, i.e., $\theta << \theta_{max}$, as would be expected for determinations at trace and ultratrace levels. This observation has also been made by Andrews, et al. (155). A single stripping peak is preferred over unresolved peaks, primarily for the purpose of recognizing possible interferences. A change in the appearance of a single, symmetrical

Figure II-16. Stripping curves for removal of various quantities of Hg deposited at a tubular Au detector in 2.0 $\underline{M}$ HNO_3

$C^b_{Hg(II)}$ - 1.00×10^{-5} $\underline{M}$

V_s - 0.507 mL

V_f - 1.2 mL min^{-1}

E_{dep} - 0.35 V vs. SCE

$\emptyset_{strip}$ - 2.0 V min^{-1}

1-10 Successive injections prior to stripping scan

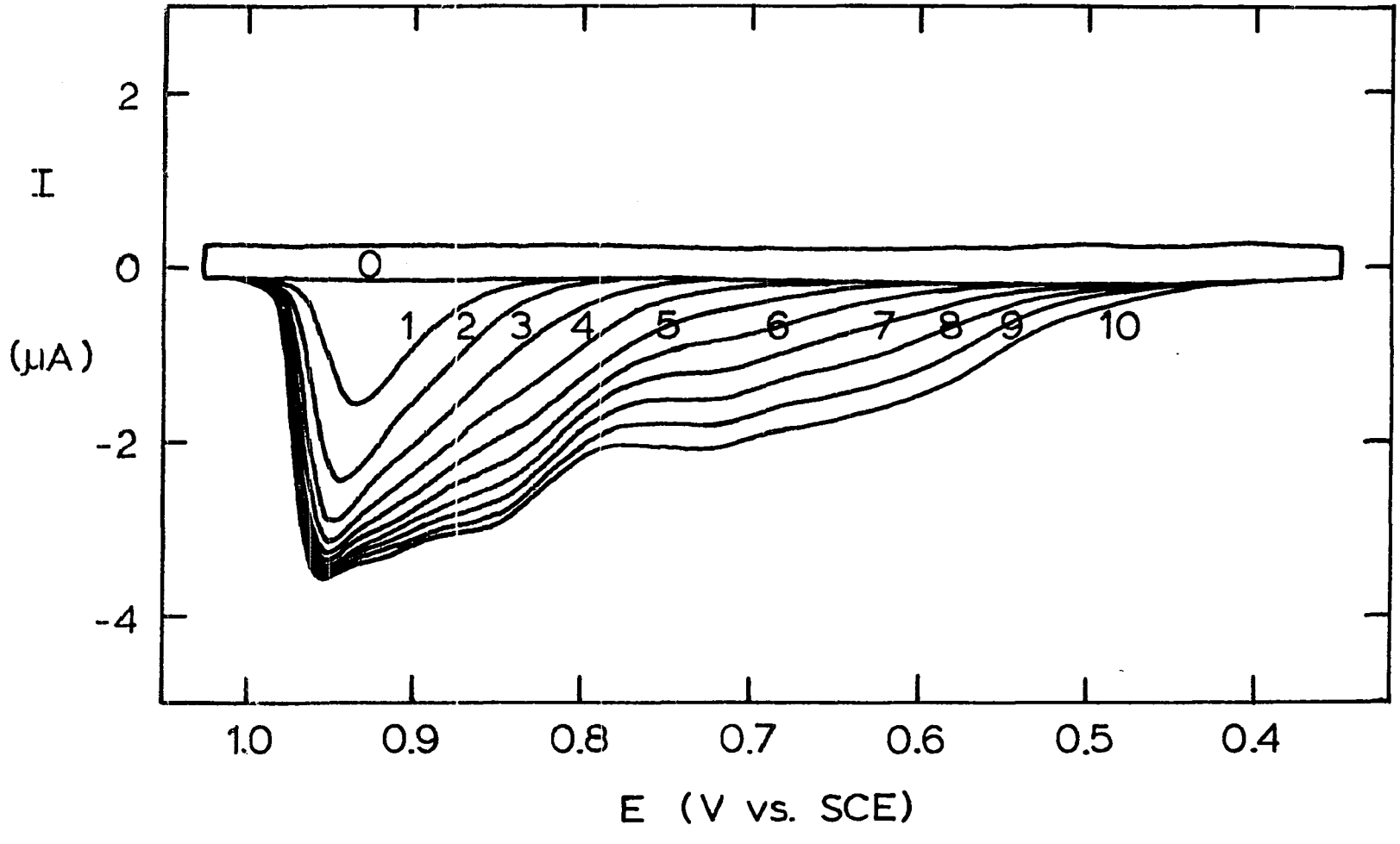
2
I
0
(μA)
-2
-4
0
1
2
3
4
5
6
7
8
9
10
1.0
0.9
0.8
0.7
0.6
0.5
0.4
E (V vs. SCE)

Figure II-17. Charge passed during stripping of UPD Hg from tubular Au electrode in 2.0 M HNO_3

$C^b_{Hg(II)}$ - 1.00×10^{-5} M

V_s - 0.507 mL

V_f - 1.2 mL min^{-1}

E_{dep} - 0.35 V vs. SCE

$\emptyset_{strip}$ - 2.0 V min^{-1}

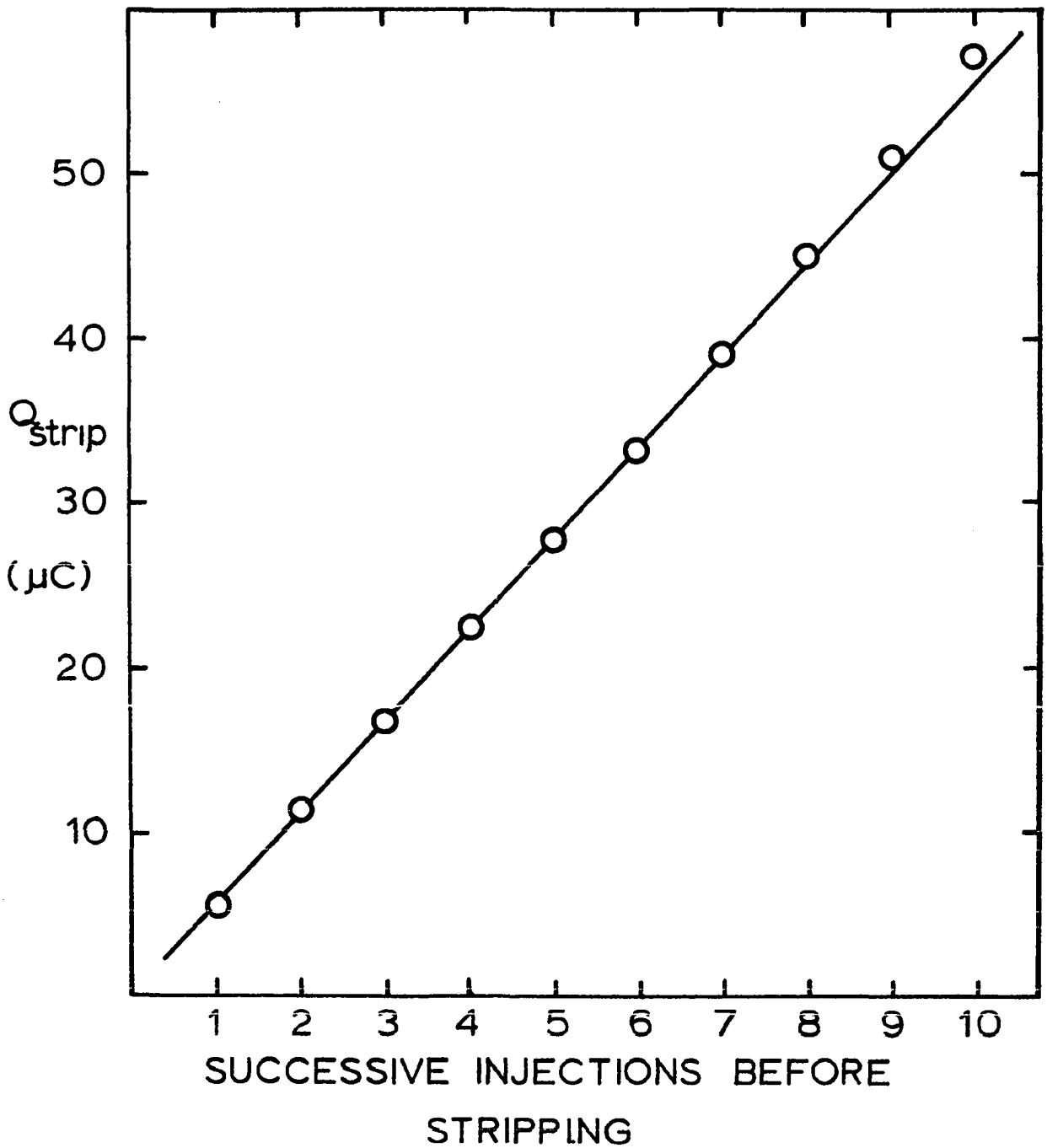
50
40
Q_{strip}
30
(μC)
20
10
1
2
3
4
5
6
7
8
9
10
SUCCESSIVE INJECTIONS BEFORE STRIPPING

Table II-7. Charge passed during stripping[a] of UPD Hg from tubular Au electrode in 2.0 M HNO_3

Injections (#)	Q_{strip} (μC)	Injections (#)	Q_{strip} (μC)
1	5.65	6	33.2
2	11.4	7	39.1
3	16.7	8	45.0
4	22.4	9	51.0
5	27.7	10	57.0

[a]Other parameters as given in Figures II-16 and II-17.

peak is more easily discerned than small changes in one or more unresolved stripping peaks.

3. The oxidation state of mercury stripped from a gold electrode

> "We dance around in a ring and suppose,
> But the Secret sits in the middle and knows."
>
> from "The Secret Sits"
> by Robert Frost

It was shown in Part C.1 of this section that the RDE can provide significant information on the voltammetric characteristics of the deposition of Hg(II) on Au. A major use of the RRDE is for the elucidation of kinetic parameters of multistep electrode processes (150). Rotation of the electrode results in convection of the solution from the vicinity of the disk electrode, across the surrounding ring

electrode. Because the insulating sheath between the two electrodes is generally very thin, e.g., < 0.05 cm, mass transport of soluble reaction products from the disk electrode reach the vicinity of the ring electrode in ≤ 40 ms at $W \geq 400$ rev min^{-1} (150). This makes the RRDE ideally suited for the EC investigation of highly unstable products of electrode reactions.

Quantitative investigations of the reduction of Hg(II) on Au using an RRDE were performed by Sherwood (114), and reported by Sherwood and Bruckenstein (115). Hence, the data presented here are qualitative in nature. Comment will be made, however, upon some of the observations and conclusions made by Sherwood, as they pertain to results obtained by this author.

A cyclic voltammogram is shown in Figure II-18 (Curve A) for the Au RDE in 2.0 M HNO_3 containing 3.90×10^{-5} M Hg(II). Plainly evident are: the decay of the limiting current within the UPD region (a); the small peak (b) in excess of $I_{D,lim}$ at $E_D < 0.3$ V; the stripping peak for removal of the bulk metal (c); and the unresolved stripping peaks for the oxidation of the UPD species (d). Curve B in Figure II-18, and Figure II-19, are records of the current, measured at the ring electrode (I_R), as a function of E_D for three different values of the potential applied to the ring electrode (E_R). For convenience only the data shown in Curve B of Figure II-18 will be discussed in detail. Further reference to Figure II-19 will be made as necessary in connection with the various portions of the data identified as (a) through (e).

Figure II-18. A - I_D-E_D curve of Hg(II) in 2.0 M HNO_3

B - I_R-E_D curve of Hg(II) in 2.0 M HNO_3 for E_R = 0.0 V

W - 3600 rev min^{-1}

ϕ_D - 4.0 V min^{-1}

$C^b_{Hg(II)}$ - 3.90 x 10^{-5} M

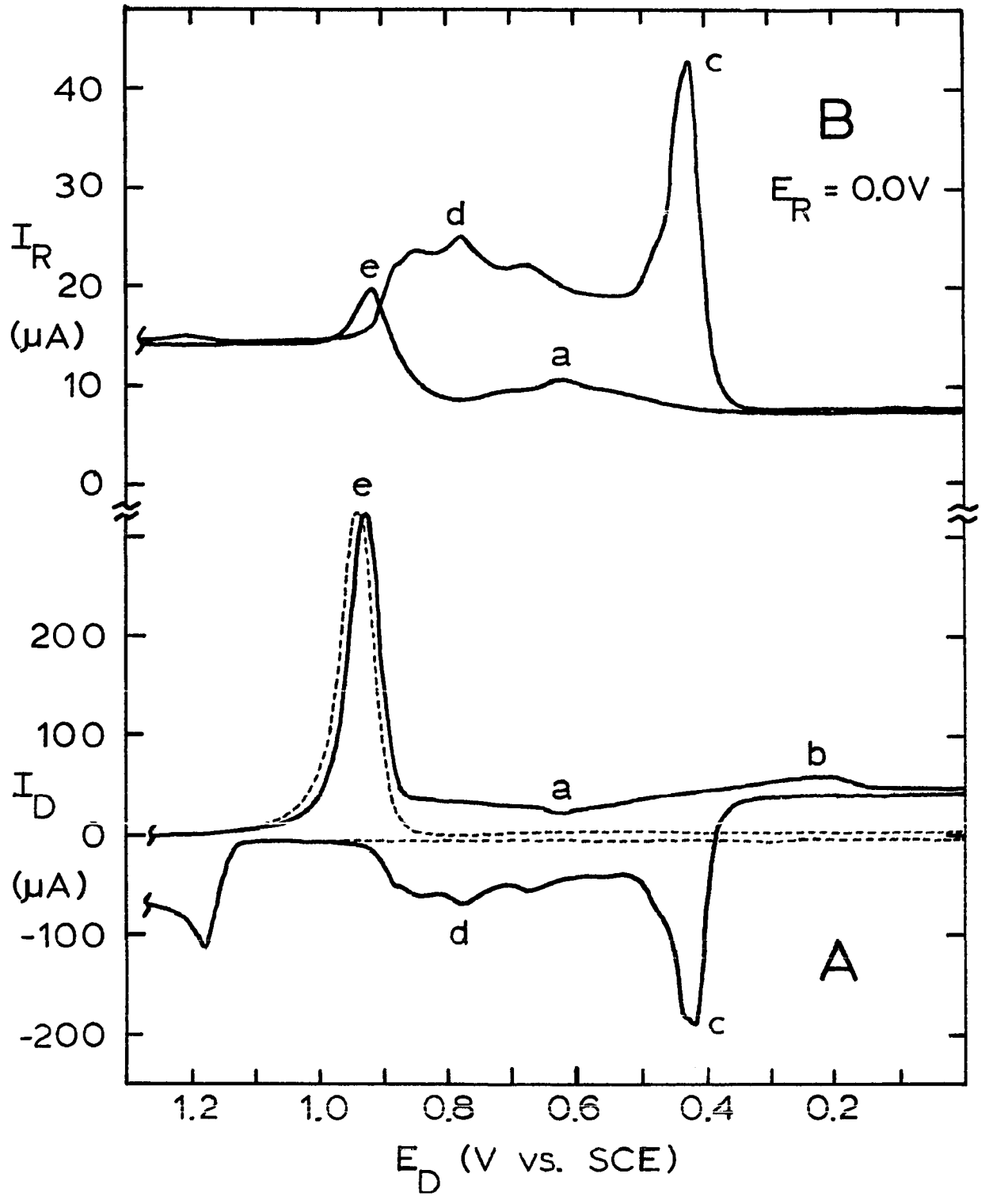
40
30
I_R
20
(μA)
10
0
c
B
E_R = 0.0V
d
e
a
e
200
100
I_D
0
(μA)
-100
-200
b
a
d
A
c
1.2
1.0
0.8
0.6
0.4
0.2
E_D (V vs. SCE)

Figure II-19. A - I_R-E_D curve for Hg(II) in 2.0 M HNO_3 for E_R = 0.40 V

B - I_R-E_D curve for Hg(II) in 2.0 M HNO_3 for E_R = 0.80 V

W - 3600 rev min^{-1}

ϕ_D - 4.0 V min^{-1}

$C^b_{Hg(II)}$ - 3.90 x 10^{-5} M

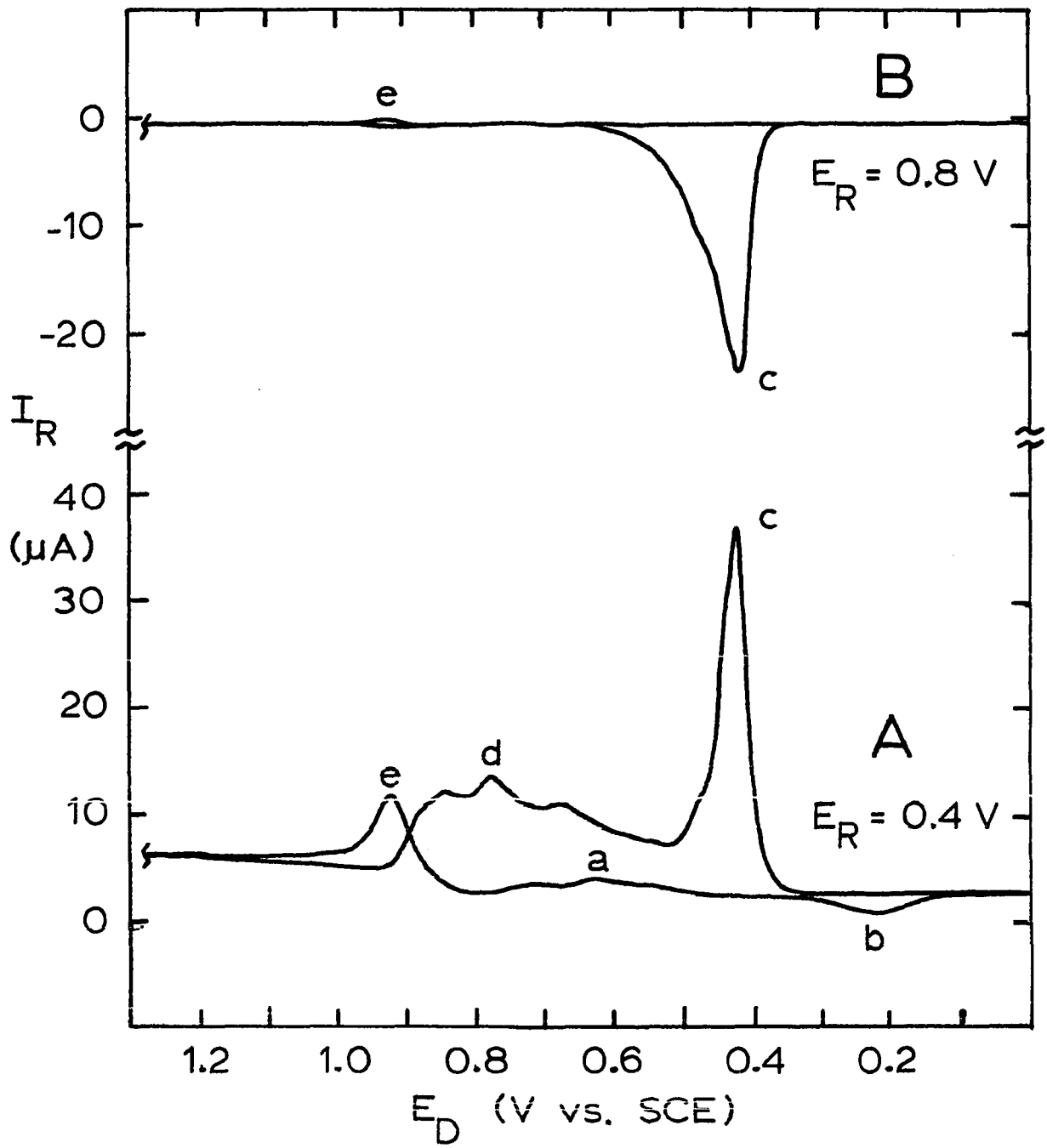
B
e
0
-10
-20
E_R = 0.8 V
c
I_R
40
(μA)
30
20
10
0
c
d
e
A
E_R = 0.4 V
a
b
1.2
1.0
0.8
0.6
0.4
0.2
E_D (V vs. SCE)

The mathematical relationship between $I_{D,lim}$ and $I_{R,lim}$ is given elsewhere (150; 152, Section VI) and the inclusion of such in the following qualitative discussion is unnecessary.

The I_R-E_D curve obtained at E_R = 0.0 V is shown in Figure II-18, Curve B. At this potential the reduction to the bulk metal occurs on the ring electrode at a rate which is limited by the rate of mass transport of Hg(II) to the surface of the electrode. The mass transport to the ring electrode is dramatically influenced by whatever reactions occur at the disk electrode. Hg(II) is not consumed at the disk electrode for $E_D > 0.9$ V and I_R is limited only by the mass transport of Hg(II) from the solution bulk. During the negative scan of E_D an increase in I_R is observed simultaneously with the current peak for the reduction of the surface oxide at the Au disk electrode (e). Peak (e) is observed in I_R when Hg(II) is absent from the supporting electrolyte, and may be concluded to result from the reduction of a soluble Au species produced during the reduction of the surface oxide at the disk electrode. Cadle and Bruckenstein (156) have studied the dissolution of Au electrodes in dilute solutions of H_2SO_4 during the formation and reduction of the surface oxide. I_R is decreased, i.e., "shielded", momentarily at E_D = 0.9 - 0.8 V, as UPD of Hg(II) begins at the disk electrode with the simultaneous decrease in the mass transport of Hg(II) to the ring electrode. Because of the conditions under which the experiment was performed, θ_E was approached at the disk electrode within the time frame that E_D was scanned within the UPD region. As θ_E is approached $I_{D,lim}$ for UPD decreases, and I_R

reflects the increased mass transport of Hg(II) to the ring electrode (a). For $E_D < 0.4$ V, the ring electrode is again shielded by reduction of Hg(II) to the bulk metal at the disk electrode.

During the positive scan of E_D, I_R remains fully shielded until the potential at which Hg(0) can no longer exist at the Au disk electrode (c). The current peaks observed in I_R in response to the stripping of the bulk mercury (c) at $E_D \sim 0.4$ V, and the UPD species (d) at $E_D = 0.5 - 0.9$ V indicate that a reducible mercury species is being produced at the disk electrode. I_R returns to the original "unshielded" value at $E_D > 0.9$ V when all processes related to the oxidation or reduction of Hg(II) at the disk electrode have ceased.

Comparison of peak (c) in the I_R-E_D curves for $E_R = 0.0$ V and $E_R = 0.80$ V reveals that the stripping of bulk Hg from the Au electrode produces a soluble species which can be both reduced and oxidized at the ring electrode. These data are consistent with the electrochemistry of Hg(I) as the product of the anodic dissolution of bulk Hg, and are in agreement with the conclusions of Allen (34) as reported by Allen and Johnson (148). Conversely, the species produced at the disk electrode during oxidation of the underpotential deposit (d) can only be reduced at the ring electrode. The conclusion made by this author and many others (34,114-116,148,155) is that oxidation of Hg(UPD) from a Au electrode results in the production of Hg(II).

RDE experiments performed by Sherwood (114) and reported by Sherwood and Bruckenstein (115) revealed that θ_{max} for the UPD of Hg(II)

on Au corresponded to 340 $\mu C\ cm^{-2}$. A theoretical calculation was made to determine the equivalent to a monolayer of Hg(0), assuming a closest-packed deposit with the atomic radii: r_{Au} = 1.44 Å and r_{Hg} = 1.57 Å. The result of this calculation was 336 $\mu C\ cm^{-2}$. However, the apparent agreement between the calculated and experimental value is unfounded. Subsequent experiments with an RRDE, performed by Sherwood, demonstrated that the actual quantity of Hg(II) produced upon oxidation of θ_{max} from the disk electrode, followed by collection on the ring electrode at E_R = 0.0 V, corresponded to 390 $\mu C\ cm^{-2}$. These results, appearing side-by-side in Table 2 of the report by Sherwood and Bruckenstein (115), indicated that either a partially charged species was deposited at underpotential, or that the underpotential deposit consisted of both Hg(0) and adions. Both of these cases are consistent with the observation made by this author that $I_{D,lim}$ for UPD of Hg(II) on Au is less than $I_{D,lim}$ for reduction of Hg(II) to the bulk metal. Whichever view is correct, the total charge density for the oxidation of one monolayer of the underpotential deposit could not be equal to the charge density calculated upon the assumption of a closest-packed deposit of Hg(0). Yet Sherwood and Bruckenstein state (115):

> "We calculate, then, that the charge required to strip one monolayer of mercury on gold as Hg(II) is 336 $\mu C/cm^2$. This value coincides, within experimental error, with the amount found...for the quantity of Hg(II) stripped after UPD 0.1 mV anodic of the Nernst potential. This remarkable result indicates that one atom layer of mercury on a gold substrate behaves as if it were bulk mercury in a potentiometric experiment."

Clearly, the conclusion of what constitutes the equivalent of a monolayer of mercury on Au is questionable. The appearance of multiple stripping peaks for the oxidation of "one monolayer" of Hg(UPD) is indicative of a deposit consisting of multiple states of activity, each having a different degree of interaction with the electrode. For example Andrews and Johnson (157) demonstrated that multiple stripping peaks for Se deposited at a Au electrode in 0.1 M perchloric acid ($HClO_4$) were not observed until more than the equivalent of one monolayer of Se atoms were deposited. A single stripping peak was observed for quantities of deposited Se less than the equivalent of one monolayer.

The data shown in Figures II-7 and II-9, indicate that a single stripping peak for the oxidation of Hg(UPD) may correspond to $\theta \leq 0.25\theta_{max}$. Further, following the reasoning of Andrews and Johnson, it can be postulated that θ_{max} may actually correspond to the equivalent of four atom layers; hence the observation made by this author and many others (34,114,115,148) that the stripping of Hg(UPD) produces Hg(II) in four, overlapping current peaks.

The small, cathodic current peak (b) in excess of the mass transport-limited current at $E_D < 0.3$ V, is observable in Figure II-18, Curve A, and also in Figures II-5, II-7, II-9, and II-11 through II-13. Sherwood was able to demonstrate that the charge corresponding to this peak was equal to the difference in charge between anodic stripping curves for the oxidation of Hg(UPD) from the disk electrode and the collection data obtained at the ring electrode. Hence, he concluded that peak (b) corresponds to the reduction of an adsorbed, charged

species of mercury. Presently, this author is in agreement with this conclusion. However, while this conclusion is supported by all of the data reported by Sherwood, this author has obtained some conflicting results.

The reduction of a charged mercury species adsorbed at the Au disk electrode should not affect in any way the mass transport of Hg(II) to the ring electrode. I_R-E_D curves obtained by Sherwood at E_R = 0.0 V and E_R = 1.0 V showed no change in I_R when peak (b) was observed at the disk electrode. The same observation can be made from the data shown in Figure II-18, Curve B for E_R = 0.0 V, and Figure II-19, Curve B for E_R = 0.80 V. However, when E_R = 0.4 - 0.5 V, an I_R-E_D curve such as that shown in Figure II-19, Curve A was obtained. Here, it appears that the mass transport to the ring electrode is momentarily decreased below the "shielded" value simultaneous with the appearance of peak (b) at the disk electrode. It must be reported that, to date, a satisfactory explanation for this phenomenon has not been found.

4. <u>The evaluation of n_{app} for the underpotential deposition of Hg(II) at a coulometric gold electrode</u>

The value of amperometric LC detectors, which electrolyze 100% of the electroactive species of interest, has been demonstrated by several workers at Iowa State University (158-160), especially J. H. Larochelle (161). The advantage of a coulometric electrode (100% efficiency) is that it is an absolute detector. The general equation for the

steady-state response of flow-through, amperometric detectors is given by Equation II-8, in which the proportionality constant k' is a function

$$I_{lim} = k'nFV_f^{\alpha}C_X^b \qquad \text{II-8.}$$

of experimental parameters such as the design of the electrode, etc., and α describes the dependence of I_{lim} upon the rate of mass transport via convection to the electrode. Tubular electrodes function with $\alpha = 1/3$ as indicated in Equation II-5, or with $\alpha = -1/6$ according to Equation II-7 if I_p is taken as the analytical signal.

It has been shown (158) that the charge (Q) passed during a detection peak follows the relationship given in Equation II-9 for an amperometric detector operating at less than 100% efficiency. The dependence of Q to changes in V_f is eliminated by a detector operating

$$Q = k'nFV_f^{\alpha-1}\cdot(\text{moles}) \qquad \text{II-9.}$$

at 100% efficiency. For the coulometric electrode, k' and α in Equation II-8 are unity and Equation II-9 becomes Equation II-10.

$$Q = nF(\text{moles}) \qquad \text{II-10.}$$

Hence, if n is known the quantity of the species to be determined may be calculated directly without the need of calibration. Conversely, the response of the coulometric detector may be used to evaluate n for an EC process such as the UPD of Hg(II) on Au. Because Q is the time integral of current, the value of n obtained from the response of a

coulometric electrode corresponds to the average value of n for the EC process giving rise to the detection peak, and as such will not reveal whether the UPD metal has a uniform, fractional valence or consists of a mixture of Hg(0) and adions.

The precision and V_f-independence of the Au coulometric detector was determined from the results of four-to-five injections of $Cr_2O_7^{2-}$ at each of several values of V_f in the range of 0.3 - 1.1 mL min^{-1}. The potential used was 0.40 V which was determined to be on the limiting-current plateau for the reduction of Cr(VI) to Cr(III), according to Equation II-11. The results are given in Table II-8. The relative

$$Cr_2O_7^{2-} + 14H^+ + 6e \rightleftharpoons 2Cr^{3+} + 7H_2O \qquad \text{II-11.}$$

standard deviation for the series of determinations was 0.18%.

The determination of the value of n_{app} in Equation II-4, was calculated from the response of the coulometric detector to standard injections of Hg(II) in the supporting electrolyte at V_f = 0.8 mL min^{-1} and selected values of E_{dep} between 0.9 and 0.3 V. Data were first obtained for 2.0 M HNO_3 as the supporting electrolyte, but a severe drift in the baseline response of the detector at $E_{dep} < 0.65$ V made questionable the accurate correction of the electronic integration of peak area. The drift was suspected to be caused by a soluble, electroactive species (probably NO_2) in the dilute acid and produced by the photodecomposition of HNO_3 upon long-standing. Other experiments

Table II-8. Efficiency of coulometric detector[a] for the reduction of Cr(VI) to Cr(III) in 1.0 M H_2SO_4 as a function of V_f

Flow Rate, V_f (mL min^{-1})		Charge, Q (mC)	Std. Dev., s (mC)	Efficiency (%)
1.10		1.090	0.001[b]	99.7
1.00		1.093	0.001[b]	100.0
0.90		1.093	0.002[b]	100.0
0.80		1.092	0.001[b]	99.9
0.70		1.091	0.001[b]	99.8
0.60		1.091	0.002[c]	99.8
0.50		1.090	0.001[c]	99.7
0.40		1.090	0.001[c]	99.7
0.30		1.089	0.001[c]	99.7
	Mean	1.091[d]	0.002[d]	99.8[d]

[a]Conditions were as follows: $C^{b}_{Cr(VI)} = 1.302 \times 10^{-5}$ M; $V_s = 0.145$ mL; and $E_{dep} = 0.40$ V vs. SCE.

[b]n = five determinations.

[c]n = four determinations.

[d]n = 41 determinations, total.

demonstrated that this interfering species could be removed by dispersing nitrogen through the solution of 2.0 M HNO_3 prior to use of the acid.

The value of n_{app} was also determined using 1.0 M H_2SO_4 as the supporting electrolyte. No drift in the baseline response of the detector was observed until $E_{dep} < 0.40$ V. As cited above in Part C.2 of this section, the simultaneous reduction of dissolved oxygen in the flow stream interferes in the evaluation of data for the reduction of Hg(II) on Au at potentials less than 0.4 V.

The data obtained for the evaluation of n_{app} are plotted in Figure II-20, and given in Table II-9. It may be observed from Figure II-20 that the value of n_{app} remains relatively unchanged for $0.75\ V \geq E_{dep} \geq 0.40$ V, which is the region of potential in which a limiting-current plateau is observed for UPD of Hg(II) on Au electrodes. The value of n_{app}, taken from the data for H_2SO_4 as the supporting electrolyte, is 1.60 ± 0.02 equivalents $mole^{-1}$ throughout this range of potential.

The significance of this result is that the UPD of Hg(II) on Au apparently occurs via the same mechanism at any potential within the UPD region, and at a rate which is limited by convective-diffusional mass transport.

D. Summary

EC studies have been presented which demonstrate that UPD of Hg(II) occurs at a Au electrode at $0.9\ V > E > 0.4$ V in either 2.0 M HNO_3 or

Figure II-20. Evaluation of n_{app} for UPD of Hg(II) on Au in 2.0 M HNO_3 and 1.0 M H_2SO_4

$C^b_{Hg(II)}$ - 1.03×10^{-5} M

V_s - 0.145 mL

V_f - 0.80 mL min^{-1}

○ - HNO_3

● - H_2SO_4

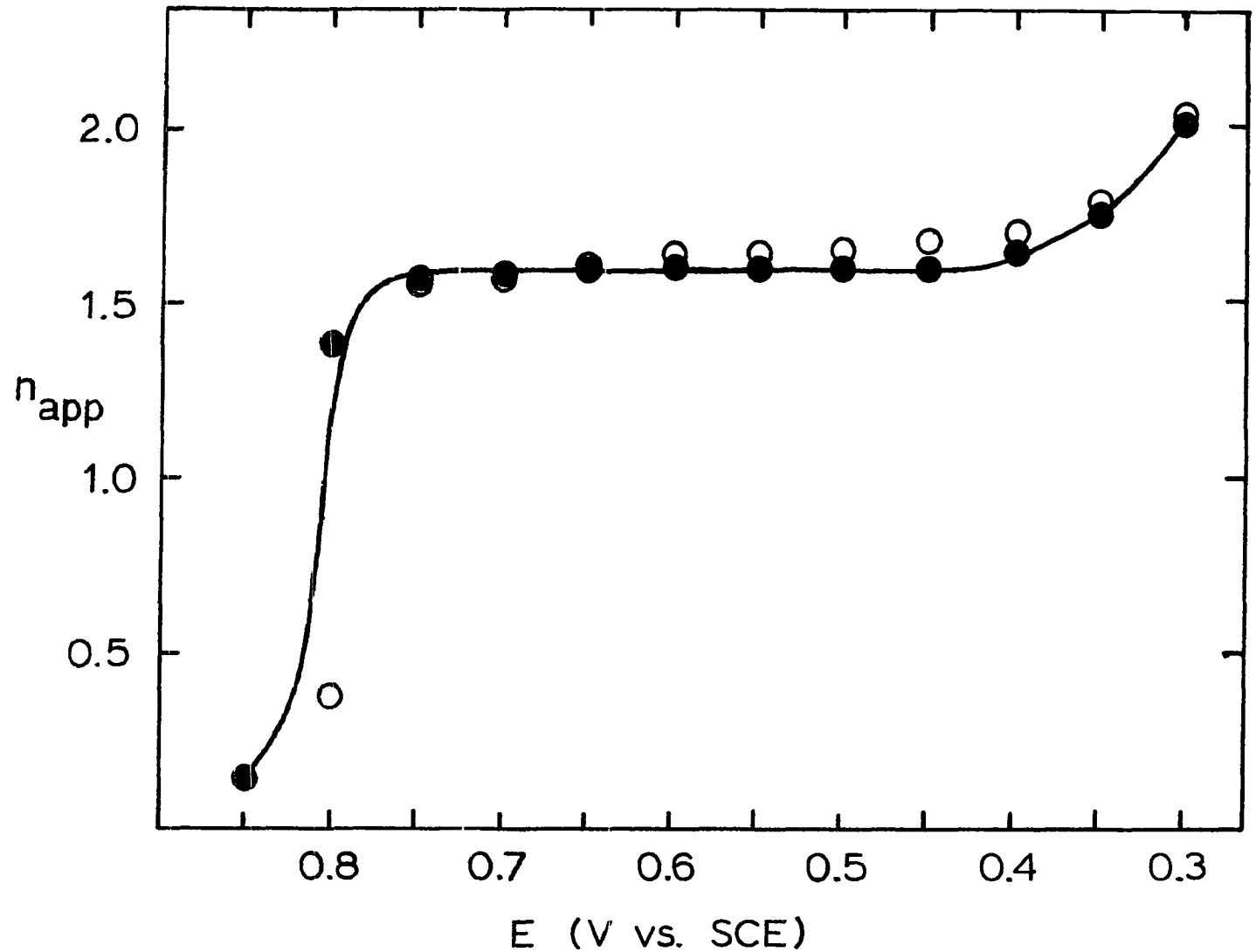
2.0
1.5
1.0
0.5
n_{app}
0.8
0.7
0.6
0.5
0.4
0.3
E (V vs. SCE)

Table II-9. Evaluation of n_{app} for UPD of Hg(II) on Au[a] from 2.0 M HNO_3 and 1.0 M H_2SO_4 using the coulometric detector

Potential (V)	2.0 M HNO_3[b]		1.0 M H_2SO_4[b]	
	Q (μC)	n_{app}	Q (μC)	n_{app}
0.90	---[c]	---[c]	7.29	0.05
0.85	---[c]	---[c]	22.0	0.15
0.80	52.8[d]	0.37[d]	199	1.38
0.75	252[e]	1.75[e]	226	1.57
0.70	226	1.57	227	1.58
0.65	231	1.60	230	1.59
0.60	236	1.64	229	1.59
0.55	238	1.65	231	1.60
0.50	239	1.66	231	1.60
0.45	242	1.68	232	1.61
0.40	248	1.72	236	1.64
0.35	260	1.80	252	1.75
0.30	296	2.05	292	2.03

[a]Other parameters as given in Figure II-20.

[b]Detector response to first of four injections at each potential after removal of previous deposit, except where noted.

[c]Not determined.

[d]Second consecutive injection; First peak not evaluated.

[e]Although this value seems high, the average for the four consecutive injections was: Q, 225 μC; and n_{app}, 1.56.

1.0 $\underline{M}$ H_2SO_4. Further, for surface coverages less than the potential-dependent equilibrium-coverage, UPD occurs at a rate which is limited by mass transport of Hg(II) to the surface of the electrode. The reduction process occurs with n_{app} = 1.60 equivalents $mole^{-1}$ at all potentials within the UPD region.

Mercury deposited as the bulk metal is stripped from the Au electrode as Hg(I). The EC stripping of mercury deposited at underpotential produces Hg(II) in four overlapping peaks for the maximum UPD surface coverage. For a surface coverage much less than the maximum coverage for UPD, the oxidation of the deposit results in a single, symmetrical stripping peak at ~0.9 V.

The conclusions drawn by this author from the data presented have been compared with results obtained by W. G. Sherwood (114), and reported by Sherwood and Bruckenstein (115). The observations made by this author are in support of most of the conclusions drawn by Sherwood. When the data presented here appeared to conflict with those obtained by Sherwood, the differences were discussed. These differences pertain to the following: 1) the calculation of the equivalent of a monolayer of mercury deposited at underpotential on Au; and 2) the interpretation of RRDE data concerning the reduction at $E < 0.4$ V of the ionic mercury species assumed to be adsorbed to the Au surface during UPD.

> "...(The) square-wave method for eliminating the capacity current has been developed.... The square-wave voltage, after appropriate attenuation, is fed into the cell modulator circuit where it is combined with a slowly changing voltage supplied by the linear voltage-sweep generator.... The combined polarizing voltage...(is) connected to the electrodes of the polarographic cell and the resulting (alternating) current waveform...is passed to the input terminal of the current detector. (The) amplitude of the waveform at a predetermined time after each change of applied voltage...is proportional to the difference between the two values observed in each complete cycle of the sqaure wave."
>
> G. C. Barker, 1952

III. DIFFERENTIAL PULSE ANODIC STRIPPING VOLTAMMETRY OF MERCURY DEPOSITED AT UNDERPOTENTIAL ON A GOLD ELECTRODE IN A FLOWING STREAM

Since 1922, the year in which Heyrovsky (162) first reported the use of a dropping mercury electrode (DME) for electroanalysis (polarography), the polarographic technique has become widely accepted throughout the scientific community and extensive research has been performed toward the development of instrumental methods which dramatically increase the sensitivity and selectivity of the technique. Many of the instrumental methods used nowadays in EC applications of solid electrodes are simply extensions of earlier polarographic research. Such is the case for applications in which the analytical signal arises from the use of a pulsed potential waveform. Differential pulse voltammetry began as "Square-Wave Polarography" which was developed by Barker and reported in 1952 by Barker and Jenkins (163). The

concept of the method is illustrated in the quotation which appears at the beginning of this section. An increase in the ratio of analytical signal to background noise was accomplished by minimizing the effect of the nonfaradaic, charging current (I_{ch}) on the analytical measurement.

Further sensitivity may be obtained by applying the differential pulse, voltammetric method with the technique of stripping analysis. In stripping analysis the species of interest is deposited (preconcentrated) on the electrode at constant potential, E_{dep}, over a certain deposition period, T_{dep}. Subsequently, the potential of the electrode is scanned from E_{dep} toward more positive potentials in a linear fashion with respect to time. The analytical signal is based upon the measurement of the current peak, produced during the stripping scan, which is recorded as a function of potential. The measured current is the sum of I_{ch} and the current due to the oxidation of the deposited metal. Hence, as the quantity of deposited metal becomes smaller, i.e., from more dilute solutions or shorter T_{dep}, the charge passed to oxidize the deposit eventually becomes comparable in magnitude to I_{ch}. Further distinction of the stripping peak is impossible without modification of the instrumentation.

When differential pulse voltammetry is applied to stripping analysis, a pulsed potential ramp is applied to the electrode during the stripping step. The waveform is illustrated in Figure III-1.A. The pulses are usually positive, equal in amplitude, ΔE, and of equal duration, t_p, and are applied at regular intervals of time, T_c.

Figure III-1. Potential waveforms for Differential Pulse Anodic Stripping Voltammetry (DPASV) using the PAR 174A Polarographic Analyzer

A - Normal DPASV

Typical parameters:

T_c - 0.5 s

$\emptyset$ - 5 mV s^{-1}

ΔE - +50 mV

B - Reverse DPASV

Parameters:

T_c - 0.114 s = $2t_p$

$\emptyset$ - 20 mV s^{-1}

ΔE - -50 mV

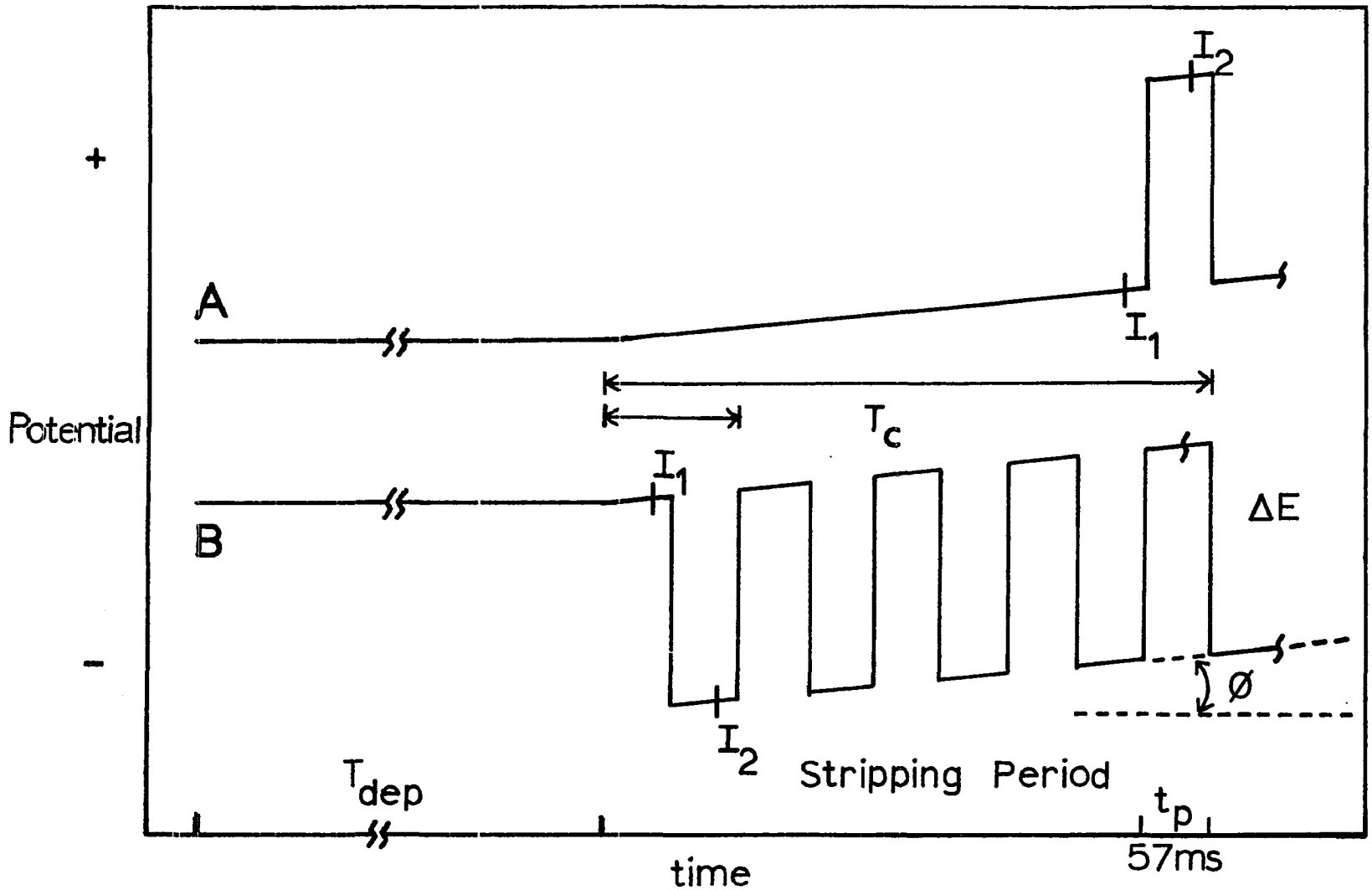
+
Potential
-
A
B
I_1
I_2
T_c
I_1
I_2
ΔE
Ø
T_{dep}
Stripping Period
t_p
57ms
time

The current, I_1, measured just prior to application of the pulse is subtracted from I_2, the current measured just prior to the conclusion of the pulse. The difference is amplified and passed to the recorder as ΔI according to Equation III-1.

$$\Delta I = k\ (I_2 - I_1) \qquad \text{III-1.}$$

ΔI is recorded as a function of the potential of the ramp, E_{ramp}, upon which the pulse is superimposed.

Figure III-2 is a representation of the current response to the potential waveform shown in Figure III-1.A. The dashed lines represent the response of the electrode in the absence of a deposit, i.e., the charging currents. The current spike associated with the re-establishment of the charge at the surface of the electrode, following a pulsed change in potential, is relatively short in duration, typically on the order of 20 ms, as observed by this author. The remaining value of I_{ch} is due to charging of the surface of the electrode as the potential is changed in response to the potential ramp. Note that by the time of each current measurement, I_{ch} is virtually unchanged whether or not the pulse has been applied. The solid line represents the total current, i.e., the sum of the faradaic and charging currents, when a portion of the deposited metal is stripped from the electrode during the pulse. The anodic current corresponding to the oxidation of the deposit decays more slowly than the charging current. Hence, the effect of I_{ch} in each individual measurement is very nearly eliminated, and ΔI reflects the analytical signal corresponding to the oxidation of the deposit.

Figure III-2. Current response to potential waveform for DPASV using the PAR 174A Polarographic Analyzer

T_c - 0.5 s

t_p - 57 ms

Current sampling interval - 17 ms

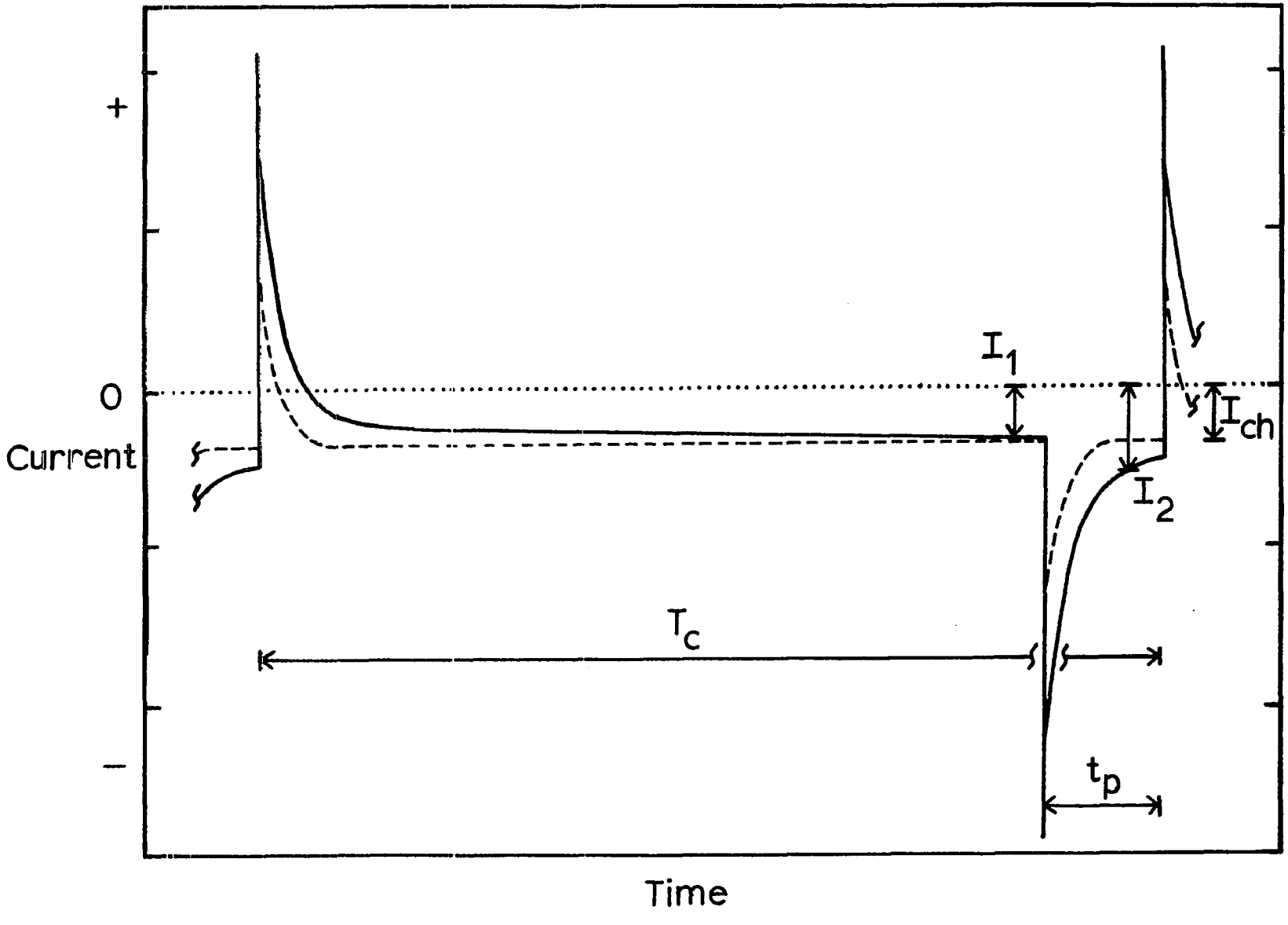
+
0
−
Current
Time
I_1
I_2
I_{ch}
T_c
t_p

A. Literature Survey of Differential Pulse Anodic Stripping Voltammetry (DPASV)

It has long been known that voltammetric stripping analysis offers increased sensitivity over direct amperometric measurements for the detection of species which can be deposited on an electrode. However, not until the past 10-15 years has there been realized a need for accurate analytical methods which are capable of monitoring environmental contaminants, such as Hg, at trace (ppm) or ultratrace (ppb) levels. Even as Barker and Jenkins were reporting the development of differential pulse polarography in 1952, they realized the possibilities of DPASV, but saw no need for it (163):

> "Indeed, there is some doubt in the authors' minds as to whether there is any real need for higher sensitivity. If there were, one might mention a recent development that can lead to a large increase in sensitivity for the detection of many of the species that form metallic amalgams. Briefly, this involves the use of a single mercury drop.... At the start of an experiment the drop electrode is polarized...(and) metallic impurities in the solution then tend to be concentrated in the drop.... After a suitable amount of concentration has been effected, the circulation of the solution is stopped and a (differential) polarogram is recorded....
>
> ...(The) method is of interest as it is readily applicable to the estimation of concentrations as small as 10^{-9} M and, if pressed to its limit, one might expect the smallest amount of a single species that could be detected to be of the order of 10^{-11} moles."

Yet analytical chemists seem to be ever intrigued with the possibility of lower and lower limits of detection, and thus DPASV became the

subject of continued research although the method apparently was not considered analytically useful until nearly 20 years later. Barker gave only cursory mention to DPASV as a method for obtaining increased sensitivity when he published a review of square-wave polarography and some related techniques in 1958 (164).

One of the first workers to publish a report on the specific subject of DPASV was Christian (165) in 1969. He studied the stripping of Cd from a hanging mercury-drop electrode (HMDE). By 1972, the use of the differential pulse waveform for polarography and stripping analysis was receiving more and more attention by analytical chemists who were interested in the detection of metals. Flato (166) reviewed both differential pulse polarography and DPASV in an article published in the Instrumentation series in Analytical Chemistry. Siegerman and O'Dom (167) demonstrated that Cd(II), Cu(II), Pb(II) and Zn(II) in tap water could be determined simultaneously using DPASV from a HMDE with $T_{dep} \leq 5$ min at concentrations ranging from 1.5 ppb Pb(II) to ~1 ppm Cu(II). They also reported the use of a wax-impregnated graphite (WIG) electrode coated with a thin film of Hg which proved to be five times as sensitive than the HMDE due to the relatively higher concentration of the deposited metals within the low-volume Hg-film. Lund and Onshus (168) applied DPASV from a glassy carbon RDE coated with Hg for the simultaneous determination of Cd(II), Cu(II), and Pb(II) in sea water at concentrations $\leq$ ppb. The rotating mercury-film electrode (MFE) has become the most popular electrode for EC investigations utilizing DPASV.

Copeland and others (169,170), working in the laboratory of Professor R. A. Osteryoung at Colorado State University about seven years ago, performed extensive research toward the evaluation of DPASV from MFEs. Turner, et al. (171) further confirmed and extended the findings of Copeland through computer-controlled data acquisition during DPASV from MFEs. Since about 1975 Nurnberg and co-workers, working in the Federal Republic of Germany, have done a great deal of work in the area of environmental analysis for toxic metals (172). Nurnberg has become a great proponent of the use of DPASV in such studies, e.g., see References 173 and 174. Valenta, Mart and Reutzel (175) presented a fairly thorough discussion of the optimization of parameters used in DPASV from MFEs. While some of the observations and conclusions of Valenta, et al., were in agreement with those made earlier by Copeland, et al. (170), other conclusions were not in agreement. Such contradiction is illustrative of the difficulty which has been encountered in the development of a unified theory for DPASV.

De Angelis and co-workers (176,177) applied DPASV to the determination of toxic metals using a thin-layer electrochemical cell with a WIG electrode coated with a thin film of Hg. Although the thin-layer cell was constructed in such a way that it might have been used in a flow system, these workers apparently failed to recognize this possibility.

Andrews, Larochelle and Johnson (155) applied DPASV to the detection of Hg(II) in 0.1 M $HClO_4$ using a Au RDE and reported a detection limit of 0.02 ppb Hg(II). Sipos, et al. (178,179) used an alternate

version of DPASV from a Au RDE for the simultaneous determination of Cu(II) and Hg(II) in sea water. Their method involved deposition upon a Au disk that had been divided into two, "twin" halves. The deposit was removed from one half of the twin electrode, and then the response of this "clean" half was subtracted from the response due to the stripping of the deposit from the other half as the pulsed potential waveform was applied to both. Apparently this "subtractive mode" DPASV provides even greater discrimination against residual charging currents during the stripping scan. The detection limit reported was 0.001 ppb for Hg(II). A glassy carbon RDE was successfully applied to the determination of 1.5 ppb Hg(II) in river water by DPASV as reported by Kritsotakis, Laskowski and Tobschall (180).

The majority of the available literature on the subject of DPASV deals with the use of Hg electrodes of different types, viz., HMDE, MFE, etc. However, this author has found in the literature only one account of work in which DPASV was applied to the determination of metals from a flowing stream (27). Very little information can be found pertaining to the evaluation of the parameters of DPASV when the deposit, itself, is a thin film, e.g., one monolayer, on a solid substrate.

The work presented in this section is intended to be a qualitative evaluation of the parameters which affect the stripping signal obtained by the DPASV of Hg(UPD) from a Au electrode in a flowing stream.

B. Description of Experimental Parameters

1. Flow-through detectors

a. Tubular electrode The tubular electrode was described in Section II.B.2.a.

b. Flow-through disk detector A cross-sectional diagram of a flow-through disk (FTD) detector employing a miniature Au disk is shown in Figure III-3. Again, the design was conceived by this author from experience gained through the designing and construction of the tubular electrode and adjustable needle valve mentioned earlier. The design is a further modification of the wall-jet electrode described by Fleet and Little (181), and the FTD detector used by G. A. Sherwood, Jr. (182).

The main body of the detector was constructed of 25% glass-filled Teflon and consisted of two parts (B and C) which were screwed together. The nozzle (A) was constructed from regular Teflon in which a channel, ~0.09 cm i.d., was drilled. The miniature disk-electrode (D) was constructed by silver-soldering a small button of Au, e.g., 0.3 cm o.d. x 0.15 cm in thickness, to a stainless steel shaft and encasing the entire assembly in a shroud of Teflon. It was found necessary to first apply heat-shrinkable, Teflon tubing around the electrode to insure a liquid-tight seal against the sides of the Au button. Then the remainder of the Teflon shroud was easily pressed over the electrode. Two electrodes were constructed: one with a radius (r_D) of 1.50 mm and the other with a radius of 1.72 mm. The exposed surface of the Au was polished to a mirror finish as described

Figure III-3. Cross-sectional diagram of the flow-through disk detector

A - inlet for solution stream and nozzle of detector, Teflon

B - upper body of detector, glass-filled Teflon

C - lower body of detector, glass-filled Teflon

D - Au mini-disk-electrode (MDE) assembly

E - exit port from reference/auxiliary electrode chamber

F - Pt auxiliary electrode

G - Neoprene compression seals

H - micrometer movement for positioning of MDE

I - electrical contact to MDE

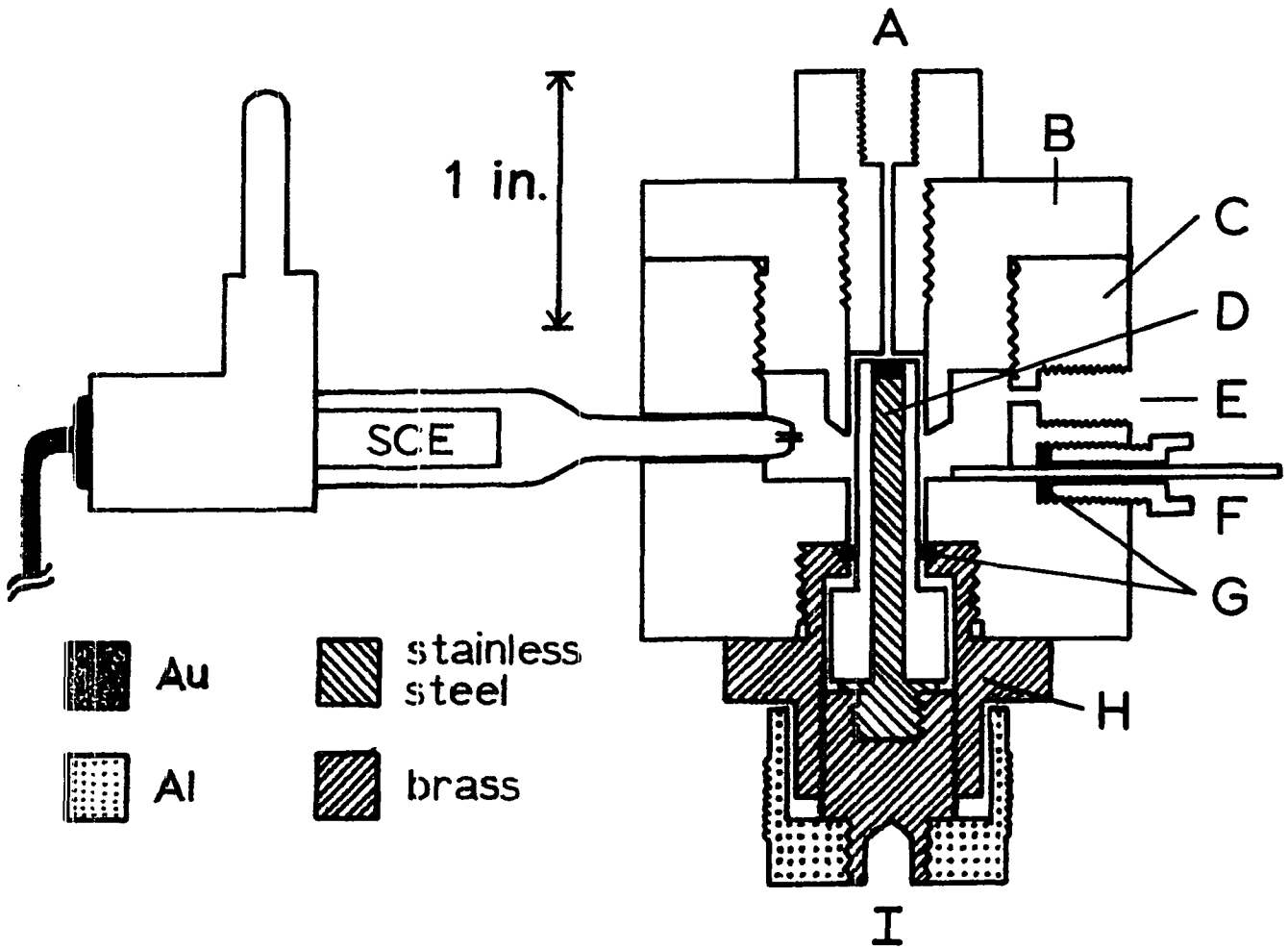
A
B
C
D
E
F
G
H
I
1 in.
SCE
Au
Al
stainless steel
brass

in Section II.B.1.a. The miniature disk was positioned perpendicular to the orifice of the nozzle such that the solution entering the detector impinged onto the center of the disk. Solution was then caused to flow radially over the disk and down into the reference and auxiliary electrode chamber before being diverted to waste. The distance, d, from the disk to the orifice of the nozzle was determined by the micrometer movement (H), constructed of brass, with an action on the order of 0.04 cm $turn^{-1}$ (64 threads in^{-1}).

The advantages of this type of electrode and detector are at least two-fold. First, extremely small volumes may be obtained in the vicinity of the Au disk electrode, e.g., $<1\ \mu L$, even though the area of the exposed surface of the Au may be relatively large. This provides maximum velocity of the solution flowing past the electrode, i.e., greater mass transport, and hence, greater sensitivity for the stripping of the accumulated deposit. Second, and perhaps the most significant, the miniature electrode can be removed from the FTD detector so that the surface of the Au disk may be polished for maximum reproducibility of EC response. Furthermore, if desired, the electrode may be fully characterized in use as a small RDE in other applications for which a flow stream is not required.

The major difference between this design and those of Fleet and Little (181), and Sherwood (182), is the manner in which the solution leaves the vicinity of the indicating electrode, i.e., the Au disk. The previous detectors were constructed such that the solution had

only two avenues of escape from the confining space around the tip of the indicating electrode. These exit channels extended in opposite directions away from the indicating electrode, the reference electrode making contact with one channel and the auxiliary electrode in contact with the other. Although the positioning of the reference and auxiliary electrodes on opposite sides of the indicating electrode is necessary to minimize potentiostatic losses due to solution resistance, it was thought that only two exit channels, extending from the indicating electrode might preferentially restrict the flow toward the exits rather than permit the preferred, uniform, radial flow over the entire surface of the disk. Therefore, the FTD detector used in this work was designed such that solution would flow over the disk electrode and down into a much larger, concentric chamber in which both the reference and auxiliary electrodes were contained. The opposing configuration of reference and auxiliary electrodes was maintained. Solution was directed from this larger chamber to waste without aspiration.

2. Instrumentation

Potential control and current measurement were made with the Model 174A Polarographic Analyzer. In the DIFFERENTIAL PULSE mode this instrument utilizes a pulse duration, t_p, of 57 ms and a current-sampling interval of 17 ms. The value of other parameters such as ΔE, $\emptyset$ and T_c may be varied by the operator in discrete intervals (usually a 1,2,5 sequence).

The circuitry of the instrument (183) was modified in two ways. The first was to replace R66, a 100-KΩ resistor in the T_c-timing circuit, with a 100-KΩ, 10-turn potentiometer. This modification allowed selection of T_c, continuously variable, ≤0.5 s. The second modification was the addition of two leads across R47, a 100-KΩ ± 1% resistor in the ΔE circuit. By connecting a second 100-KΩ ± 1% resistor to these leads, in parallel with R47, ΔE was increased from 100 mV to 200 mV. Addition of a third 100-KΩ ± 1% resistor in parallel with the other two gave ΔE = 300 mV. A 150-mV modulation was obtained when a 200-KΩ resistance was placed in parallel with R47. The polarity of ΔE was determined by the SCAN DIRECTION switch which has two positions, either positive or negative. When the SCAN DIRECTION switch is in the negative position, a positive potential ramp may still be obtained, without changing the negative polarity of ΔE, by selection of the REVerse-SCAN function.

The potential of the indicating electrode was monitored only when necessary, with a Model PDM 35 digital multimeter from Sinclair Radionic, Inc., New York. The multimeter compared the potential of the lead connected to the indicating electrode with respect to the potential of the lead connected to the reference electrode.

The data from studies performed with the tubular electrode were recorded on a Model 7035B X-Y recorder from Hewlett-Packard, Palo Alto, CA. The Model Omnigraphic 2000 X-Y recorder was used to record the studies made using the FTD detector.

3. Flow systems

A diagram of the flow system used with the tubular electrode for the preliminary investigation of DPASV is shown in Figure III-4. The sample loop had a volume of 0.507 mL. The syringe pumps were from Pine Instrument Co., and each provided a continuously variable rate of flow between 0 and 1.0 mL min^{-1}. By combining the stream from both pumps, values of $V_f \leq 2.0$ mL min^{-1} were obtained. Alternately, the use of two pumps permitted experiments to continue for longer periods of time before the pumps had to be refilled with supporting electrolyte.

Due to the inconvenience of periodically refilling the syringe pumps and the inflexibility regemented by the fixed sample volume, a different flow system was eventually chosen which permitted control of injection times rather than specific values of V_s. This flow system will be described in Section IV.B.1.

4. Chemicals and solutions

The preparation of solutions used for the evaluation of DPASV in a flowing stream was as described in Section II.B.5.

C. Results and Discussion

1. Evaluation of experimental variables

a. Flow rate during the stripping scan, $V_{f,strip}$ Since its inception, DPASV has been performed in quiescent solution, e.g., see quotation from Barker and Jenkins (163) above. Presumably, the

Figure III-4. Preliminary flow system used for investigation of DPASV

A - syringe pumps containing the supporting electrolyte

B - T-connector

C - injection valve with sample loop

D - syringe

E - solution containing the sample

F - tubular electrode

G - potentiostat

H - recorder

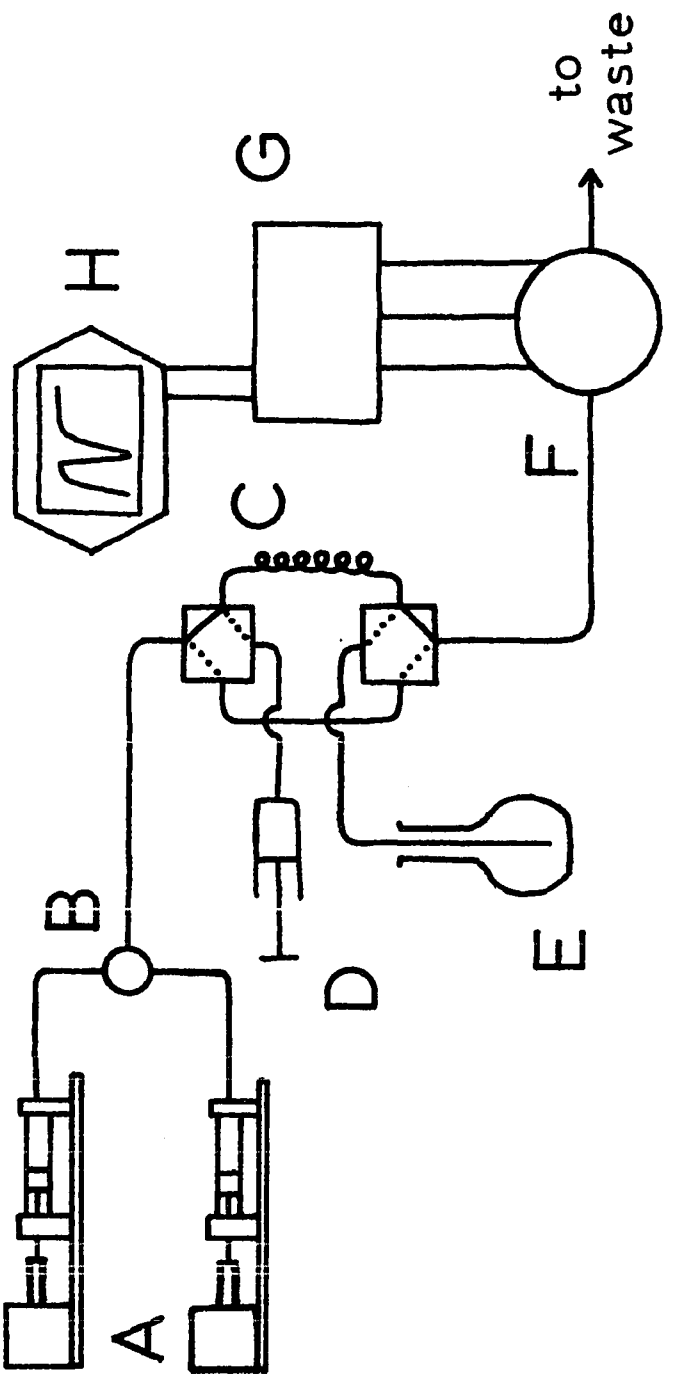
to
waste
G
H
F
C
B
D
E
A

reasoning for this was traditional because of the use of a HMDE. Perturbations of the drop under nonquiescent conditions would have led to significant background currents, making quantitative evaluation of the data most difficult. However, such problems would not occur for a MFE, and yet research continued using quiescent conditions for DPASV with MFEs. Here the reasoning apparently was to prevent background noise caused by the electrical contact to the rotating shaft of the RDE which serves as the substrate for the thin film of Hg.

Many workers have recognized that the nature of the potential waveform used for DPASV results in redeposition at E_{ramp} of material stripped during the pulse to more positive potentials (e.g., 168,171, 172,175). It seems likely that these same workers would have recognized also that convection during the stripping scan would affect the redeposition from the layer of solution adjacent to the surface of the electrode. However, this author has not found in the literature a report of work in which a relationship between the rate of mass transport during the stripping scan and the DPASV stripping signal was investigated.

Immediately upon beginning the evaluation of parameters in application of DPASV to a flow system for the determination of Hg(II), it was discovered that maintaining solution flow during the stripping scan dramatically decreased the observed stripping peak. The data are shown in Figure III-5, plotted in Figure III-6, and listed in Table III-1. Increasing $V_{f,strip}$ causes a decrease in the stripping peak

Figure III-5. Effect of $V_{f,strip}$ on the peak obtained for Hg by DPASV at a tubular Au electrode in 0.2 M HNO_3

Deposition:

$C^{b}_{Hg(II)}$ - 1.00×10^{-5} M

V_s - 0.507 mL

$V_{f,dep}$ - 1.0 mL min^{-1}

E_{dep} - 0.50 V vs. SCE

Stripping:

ΔE - 100 mV

$\emptyset$ - 2 mV s^{-1}

T_c - 0.5 s

A - 0.78 mL min^{-1}

B - 0.38 mL min^{-1}

C - 0.19 mL min^{-1}

D - 0.09 mL min^{-1}

E - 0.04 mL min^{-1}

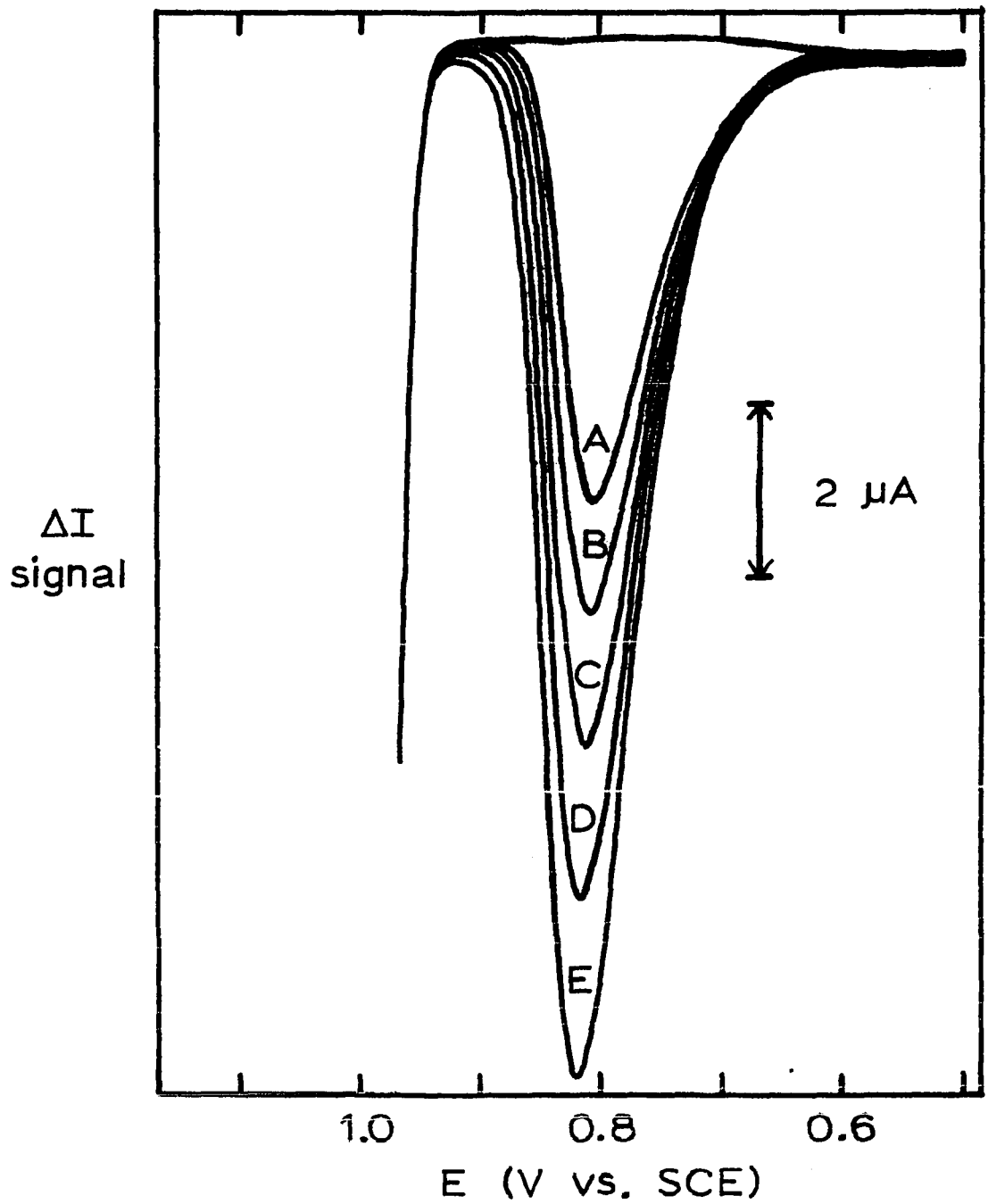
ΔI
signal
A
B
C
D
E
2 μA
1.0
0.8
0.6
E (V vs. SCE)

Figure III-6. Dependence of the DPASV peak-area on $V_{f,strip}$

Parameters as given in Figure III-5.

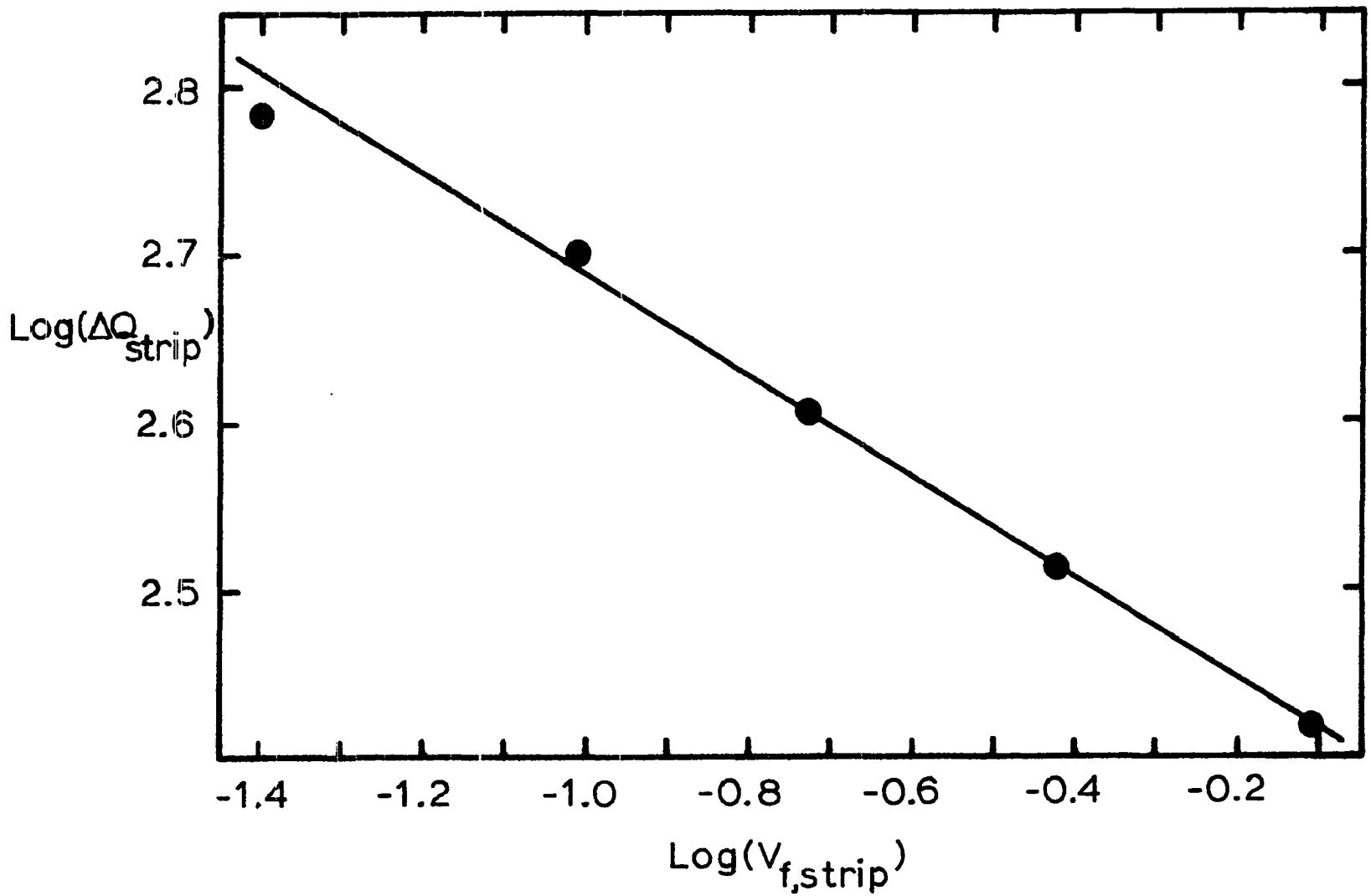
2.8
2.7
2.6
2.5
Log(ΔQ strip)
-1.4
-1.2
-1.0
-0.8
-0.6
-0.4
-0.2
Log(V f,strip)

Table III-1. Dependence of the peak obtained for Hg by DPASV[a] on $V_{f,strip}$ at a tubular Au electrode in 0.2 M HNO_3

Flow Rate, $V_{f,strip}$ (mL min^{-1})	Log $V_{f,strip}$	ΔQ_{strip} (μC)	Log ΔQ_{strip}
0.78	-0.108	262.9	2.420
0.38	-0.420	327.7	2.515
0.19	-0.721	405.4	2.608
0.09	-1.046	501.8	2.701
0.04	-1.398	605.6	2.782

[a]Other parameters as given in Figure III-5.

because significant quantities of Hg(II), produced during the pulse, pass through the thin, quiescent layer of solution immediately adjacent to surface of the electrode and are swept away by the flowing stream. Ions of Hg(II) lost in this way can not be redeposited at the conclusion of the pulse, then to be restripped during the next pulse. Hence, the depletion of the deposit occurs more rapidly under conditions of solution flow with the resultant decrease in the stripping peak. Under quiescent conditions the same material can be oxidized and redeposited many times before the accumulated deposit is completely removed from the electrode.

For the instrumental conditions and range of $V_{f,strip}$ studied with the tubular Au electrode, the area of the stripping peak was found to be proportional to the -0.30 power of $V_{f,strip}$ as indicated by the

slope of the plot in Figure III-6. However, the fact of true significance is that these data clearly indicate that, regardless of the type of electrode, the maximum stripping signal for DPASV will be obtained when quiescent conditions are maintained during the stripping scan, i.e., in this case when solution flow is completely interrupted.

Unfortunately, the geometry of the design of the tubular electrode did not permit the use of stopped-flow. When $V_{f,strip} = 0$, leakage of the internal filling solution (saturated KCl) from the reference electrode evidently diffused into the vicinity of the Au indicating electrode. Au is anodically dissolved at potentials more positive than ~0.75 V vs. SCE in the presence of significant quantities of Cl^-. Hence, data for the stripping of Hg could not be obtained unless a finite value of $V_{f,strip}$ was maintained to prevent the interference from Cl^-.

The tubular electrode was used for the majority of the data reported in this section. However, the realization of the Cl^- problem at $V_{f,strip} = 0$, led to the eventual design and construction of the FTD detector in which the Au indicating electrode is geometrically above the reference electrode. Because a solution saturated with KCl is more dense than the supporting electrolyte, any leakage from the SCE tends to remain at the bottom of the reference and auxiliary electrode chamber (refer to Figure III-3). The FTD detector functioned at $V_{f,strip} = 0$ without difficulty within the period of time necessary to complete the stripping scan.

b. Modulation amplitude, ΔE The effect of increasing ΔE on the observed stripping peak is shown in Figure III-7. The increase in both peak height and peak area is quite dramatic. Note that the separation between the stripping peak for Hg and the oxidation of the Au surface is decreased as ΔE increases, but resolution remains excellent even when ΔE = 100 mV. A decrease in the separation of two processes which occur at two different potentials is expected as ΔE increases. This is because as ΔE increases, the current sampled as I_1 (at E_{ramp}) may be due to the first process, while I_2 (at $E_{ramp} + \Delta E$) may be due to the second process. According to Equation III-1, ΔI then would be a function of both processes and resolution would be lost.

Another observation is that the potential at which the maximum stripping signal, ΔI_p, is observed shifts toward more negative potentials as ΔE increases. This effect may be attributed to the fact that ΔI is plotted as a function of E_{ramp}. As ΔE increases the maximum anodic current, sampled as I_2 (at $E_{ramp} + \Delta E$) causes ΔI_p to occur earlier in the stripping scan at less positive values of E_{ramp}. The effect is similar to that observed in differential pulse polarography for the reduction of metals at a DME (184).

Reports in the literature (e.g., 165,168,170,171) are generally in agreement that increasing ΔE increases the observed stripping peak for DPASV. However, data for the use of $\Delta E > 50$ mV is inconsistent among different workers. Christian (165) and Copeland, et al., (170) reported a significant increase in ΔI_p when ΔE = 100 mV over that

Figure III-7. Effect of ΔE on the peak obtained for Hg by DPASV at a tubular Au electrode in 0.2 M HNO_3

Deposition:

$C^{b}_{Hg(II)}$ - 1.00×10^{-5} M

V_s - 0.507 mL

$V_{f,dep}$ - 1.00 mL min^{-1}

E_{dep} - 0.50 V vs. SCE

Stripping:

$V_{f,strip}$ - 0.05 mL min^{-1}

$\emptyset$ - 1 mV s^{-1}

$\bar{T}_c$ - 1 s

A - 25 mV

B - 50 mV

C - 100 mV

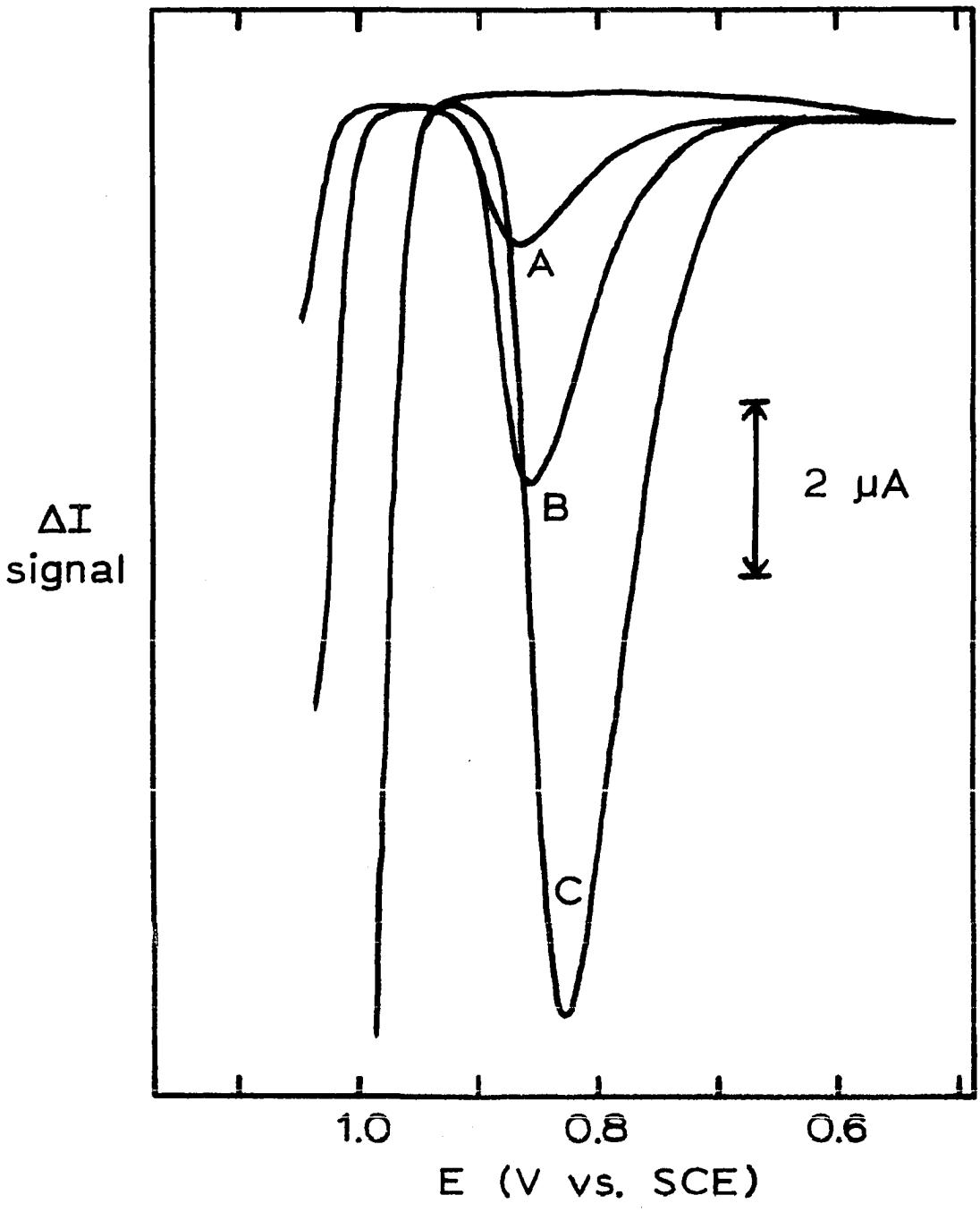
ΔI
signal
A
B
C
2 μA
1.0
0.8
0.6
E (V vs. SCE)

observed when $\Delta E \leq 50$ mV. On the other hand, Lund and Onshus (168) and Turner, et al. (171), concluded from their observations that use of $\Delta E > 50$ mV did not increase ΔI_p to an appreciable extent to make the use of larger modulation amplitudes worthwhile. To quote Turner, et al.:

> "There is a practical limit to the increase in sensitivity that can be obtained by increasing the square-wave amplitude. By considering a double-step chronoamperometric experiment, the largest possible current difference is given by a step from in front of the wave on to the diffusion plateau and back to the front again.... Any larger jump further into the wave and back to the front results in a broadening of the peak, but not an increase in its height."

Referring to Figure II-16 for the stripping peak obtained by conventional stripping analysis at the Au tubular electrode, the difference in potential between the beginning and maximum of Peak 1 is observed to be about 100 mV. Hence it was concluded that $\Delta E = 100$ mV was the maximum value of modulation amplitude which would lead to a significant increase in the stripping peak for Hg by DPASV from a Au electrode. This conclusion was confirmed in later experimentation which will be discussed below in Part C.1.f of this section.

c. Rate of potential scan, $\emptyset$ The effect of increasing $\emptyset$ on the stripping peak is shown in Figure III-8. Once again the peak is observed to increase. However, integration of the area of each peak to determine the stripping charge detected by the measurement of ΔI reveals that the largest peak corresponds to the smallest charge. The data are tabulated in Table III-2.

Figure III-8. Effect of Ø on the peak obtained for Hg by DPASV at a tubular Au electrode in 0.2 M HNO_3

Deposition:

$C^{b}_{Hg(II)}$ - 1.00×10^{-5} M

V_s - 0.507 mL

$V_{f,dep}$ - 1.00 mL min^{-1}

E_{dep} - 0.50 V vs. SCE

Stripping:

$V_{f,strip}$ - 0.05 mL min^{-1}

ΔE - 50 mV

T_c - 1 s

A - 1 mV s^{-1}

B - 2 mV s^{-1}

C - 5 mV s^{-1}

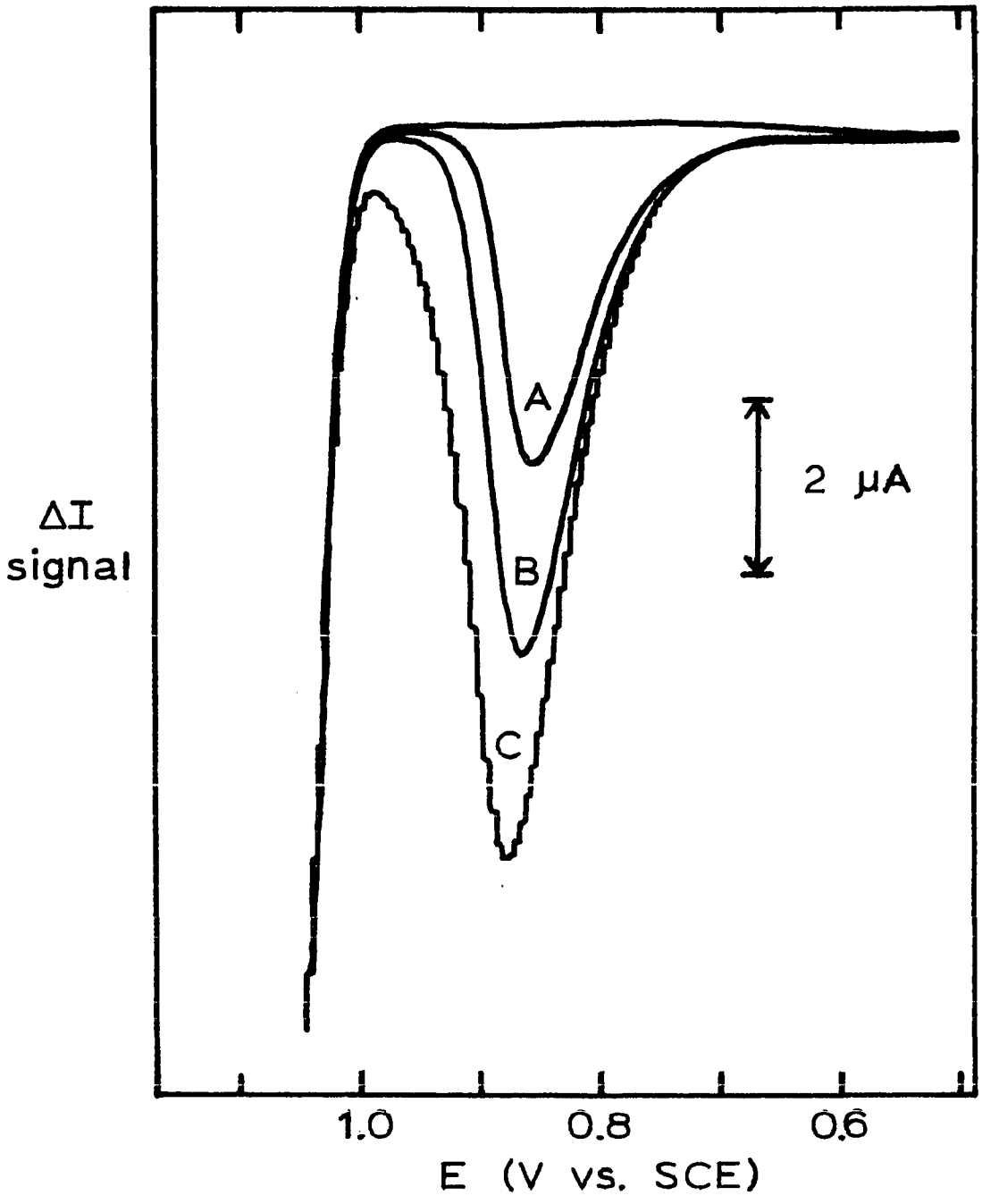
ΔI
signal
A
B
C
2 μA
1.0
0.8
0.6
E (V vs. SCE)

Table III-2. Dependence of peak obtained for Hg by DPASV[a] on $\emptyset$ at a tubular Au electrode in 0.2 M HNO_3

$\emptyset$ (mV s^{-1})	ΔI_p (μA)	ΔQ_{strip} (μC)
1	3.9	368
2	6.1	301
5	8.4	190

[a]Other parameters as given in Figure III-8.

The increase in ΔI_p with increasing $\emptyset$ occurs primarily because the individual measurements of I_2 are increased. The complete oxidation of the accumulated Hg must occur within a specific range of potential, e.g. 0.75 - 0.95 V. For a constant, deposited quantity of Hg, the more rapidly the potential of the electrode traverses the stripping range, the larger must be the rate at which the deposit is oxidized, i.e., the larger the anodic current. Current measured as I_2 is a sampling of the anodic current for oxidation of the deposit.

However, although the values of I_2 are increased, the number of pulses (and increments of ΔI) which define the stripping peak at constant T_c, are decreased as $\emptyset$ increases. In other words, a larger range of potential is traversed, and more information is lost, during the portion of T_c in which the current is not being measured. Hence the charge corresponding to the area under the stripping peak is actually less for the larger peaks at faster $\emptyset$. The deterioration of

peak definition is plainly evident for $\emptyset$ = 5 mV s^{-1}, when T_c = 1 s. Data not shown (185) for $\emptyset > 5$ mV s^{-1} indicated that the loss of peak definition eventually resulted in a decrease of ΔI_p. A rough rule to follow is that the product (in mV) of $\emptyset$ and T_c should not be greater than 10% of ΔE to maintain acceptable peak definition and resolution.

It follows from this conclusion that as T_c is decreased $\emptyset$ may be increased to yield a larger stripping peak so long as the relationship of Equation III-2 is maintained.

$$\emptyset T_c \leq 0.1 \Delta E \qquad \text{III-2.}$$

d. Cycle period of pulses, T_c The effect of decreasing T_c on the definition and resolution of the stripping peak is clearly illustrated in Figure III-9. For T_c = 2 s, the value of $\emptyset T_c$ is 10 mV, or 20% of ΔE, and both ΔI_p and resolution are severely affected (Peak A). Peaks B and C for which Equation III-2 is satisfied exhibit little difference in ΔI_p although resolution continues to improve with shorter T_c.

The fact that Peaks B and C display nearly identical values of ΔI_p implies that the contribution of I_1 to ΔI is approximately the same for T_c = 0.5 or 1 s. According to Figure III-2, this means that the cathodic current, due to redeposition of the material stripped during the pulse, has decayed to a negligible value within the 440 ms prior to each application of ΔE. It is apparent from Figure III-2,

Figure III-9. Effect of T_c on the peak obtained for Hg by DPASV at a tubular Au electrode in 0.2 M HNO_3

Deposition:

$C^b_{Hg(II)}$ - 1.00×10^{-5} M

V_s - 0.507 mL

$V_{f,dep}$ - 1.00 mL min^{-1}

E_{dep} - 0.50 V vs. SCE

Stripping:

$V_{f,strip}$ - 0.05 mL min^{-1}

ΔE - 50 mV

$\emptyset$ - 5 mV s^{-1}

A - 2 s

B - 1 s

C - 0,5 s

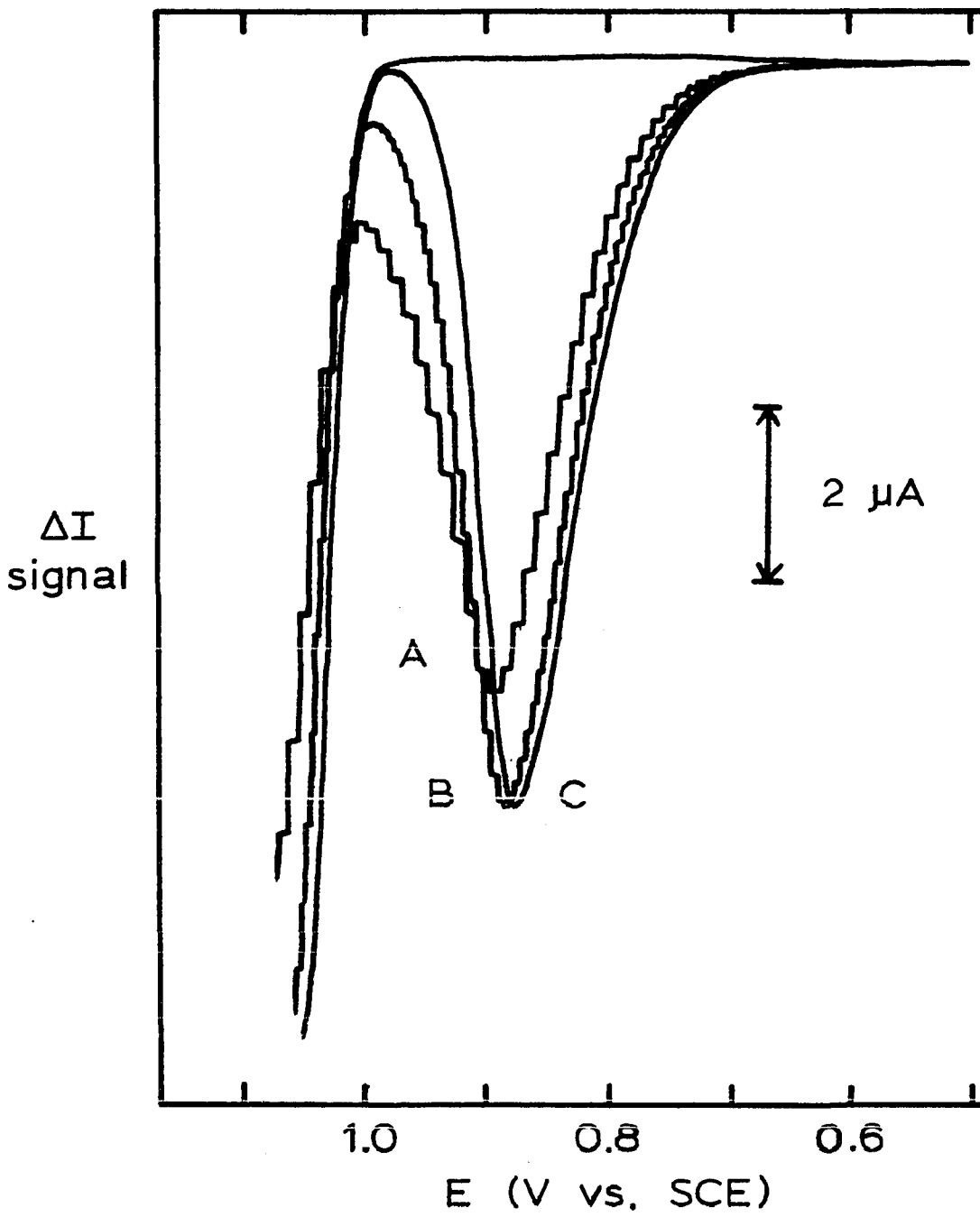
ΔI
signal
2 μA
A
B
C
1.0
0.8
0.6
E (V vs. SCE)

that a further decrease in T_c, to the order of twice t_p, should result in an approximately two-fold enhancement of ΔI.

Later experimentation (185), which was performed after the PAR 174A was modified to provide $T_c \leq 0.5$ s, as described in Part B.2 above, confirmed the enhancement of ΔI_p at $T_c = 2t_p$. Rates of scan ≤ 20 mV s^{-1} may be used for $T_c = 2t_p$ and $\Delta E \geq 50$ mV. Although the selection of $\emptyset = 50$ mV, $T_c = 2t_p$, and $\Delta E = 100$ mV does not violate the condition required by Equation III-2, it was observed that the X-Y recorder was not able to accurately follow ΔI when the parameters were so chosen. Therefore it is recommended that $\emptyset$ not exceed 20 mV s^{-1} even though Equation III-2 may be valid at larger values of $\emptyset$.

Reports in the literature, as in the case of $\Delta E > 50$ mV, are inconsistent in predicting the effect of decreasing T_c on the observed stripping peak. Observations made by Turner, et al. (171) and Valenta, et al. (175) using a MFE, and Lund and Onshus (168) using a HMDE are in agreement with the observations of this author. However, Lund and Onshus reported an improvement in ΔI_p of about 1/3-1/4 by increasing T_c from 0.5 to 2 s when they used an MFE. Copeland, et al. (170) also reported a decrease in ΔI_p at $T_c < 0.5$ s for DPASV at a MFE.

e. Flow rate, $V_{f,dep}$, and time of deposition, T_{dep} Equation II-9 predicts, for a given V_s, the charge passed during a detection peak for an amperometric detector operating at less than 100% efficiency. Q_{dep} corresponds to the charge equivalent to the quantity of metal deposited at the electrode, and Q_{strip} is the charge passed when the deposit is oxidized from the surface of the electrode during the

stripping scan. Ideally, Q_{dep} and Q_{strip} are equal, but this does not necessarily have to be true, e.g., when the metal is deposited from one valence state, but subsequently oxidized to another. Stripping of Hg deposited at underpotential on a Au electrode closely approximates the ideal case, and the area of the stripping peak is predicted to follow the α-1 power of $V_{f,dep}$. For the tubular electrode, $\alpha = 1/3$ and a plot of $Log(Q_{strip})$ vs. $Log(V_{f,dep})$ is predicted to be linear with a slope of -0.67, when the volume and concentration of sample injected remains constant.

The data obtained when the effect of $V_{f,dep}$ was investigated are shown in Figure III-10. Figure III-11 is the graphical representation of the results, and the data is contained in Table III-3. A linear relationship between $Log(\Delta Q_{strip})$ and Log $(V_{f,dep})$ was indeed observed. However, the slope of the line in Figure III-11 is -0.77, rather than -0.67 as predicted. The disparity between the theoretical and experimental $V_{f,dep}$ dependence is not too surprizing in light of the fact that the DPASV stripping peak represents not only charge passed during stripping of the deposit, but also reflects the redeposition of Hg(II) during the portion of T_c in which ΔE is not applied.

Obviously, from Figure III-10, the use of large $V_{f,dep}$ with a fixed V_s is detrimental to the signal obtained for a given concentration of Hg(II) injected. The much longer period of time which must be allowed for the entire sample plug to pass through the detector at low $V_{f,dep}$ severely limits the number of injections which can be made per unit time, i.e., the sample through-put. Modification of the flow

Figure III-10. Effect of $V_{f,dep}$ with fixed V_s on the peak obtained for DPASV at a tubular Au electrode in 0.2 M HNO_3

Stripping:

$V_{f,strip}$ - 0.01 mL min^{-1}

ΔE - 2 mV s^{-1}

$\emptyset$ - 2 mV s^{-1}

T_c - 1 s

Deposition:

$C^b_{Hg(II)}$ - 1.00×10^{-6} M

V_s - 0.507 mL

E_{dep} - 0.50 V vs. SCE

A - 0.98 mL min^{-1}

B - 0.48 mL min^{-1}

C - 0.24 mL min^{-1}

D - 0.11 mL min^{-1}

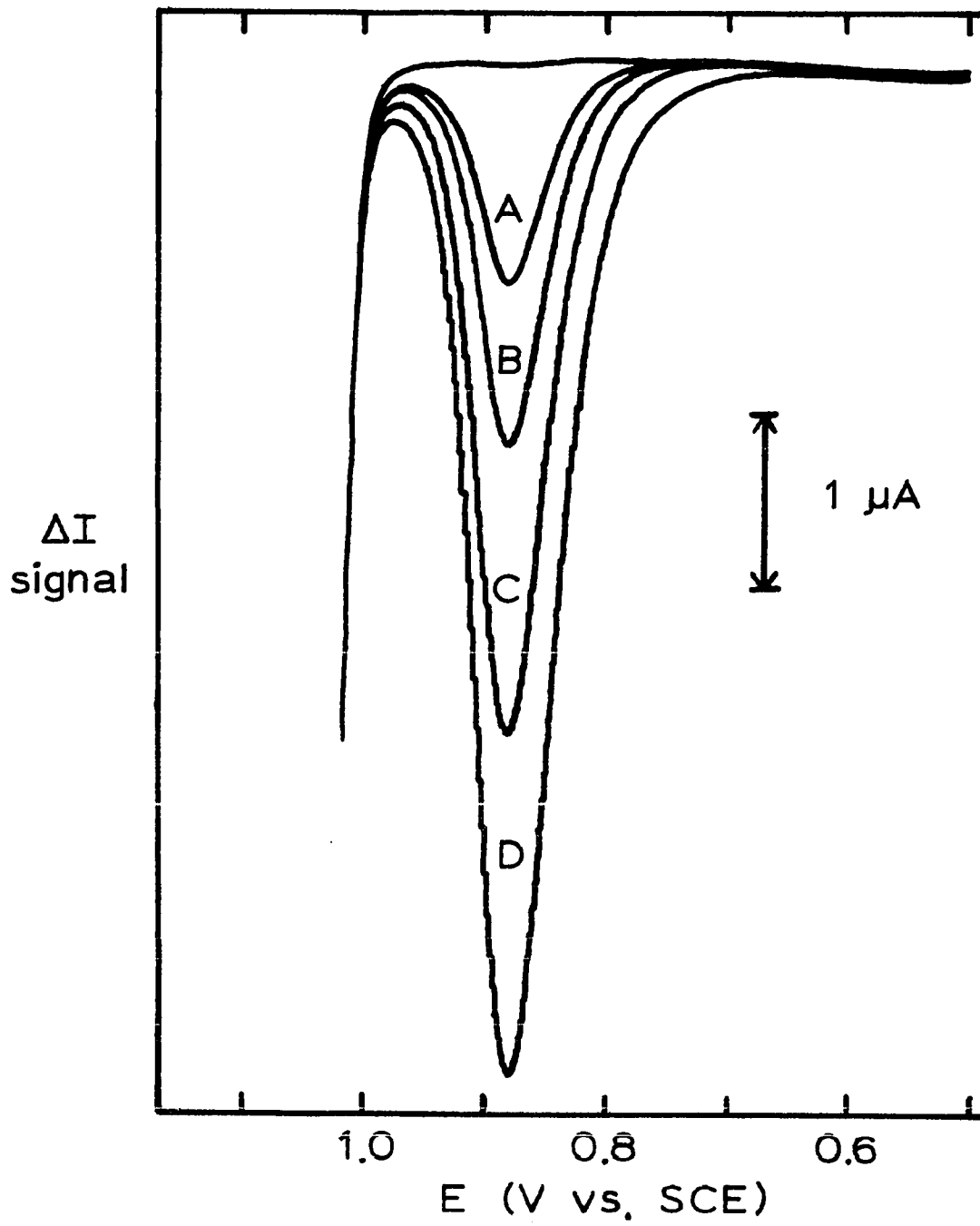
ΔI
signal
A
B
C
D
1 μA
1.0
0.8
0.6
E (V vs. SCE)

Figure III-11. Dependence of the DPASV peak-area on $V_{f,dep}$, at constant V_s

Parameters as given in Figure III-10.

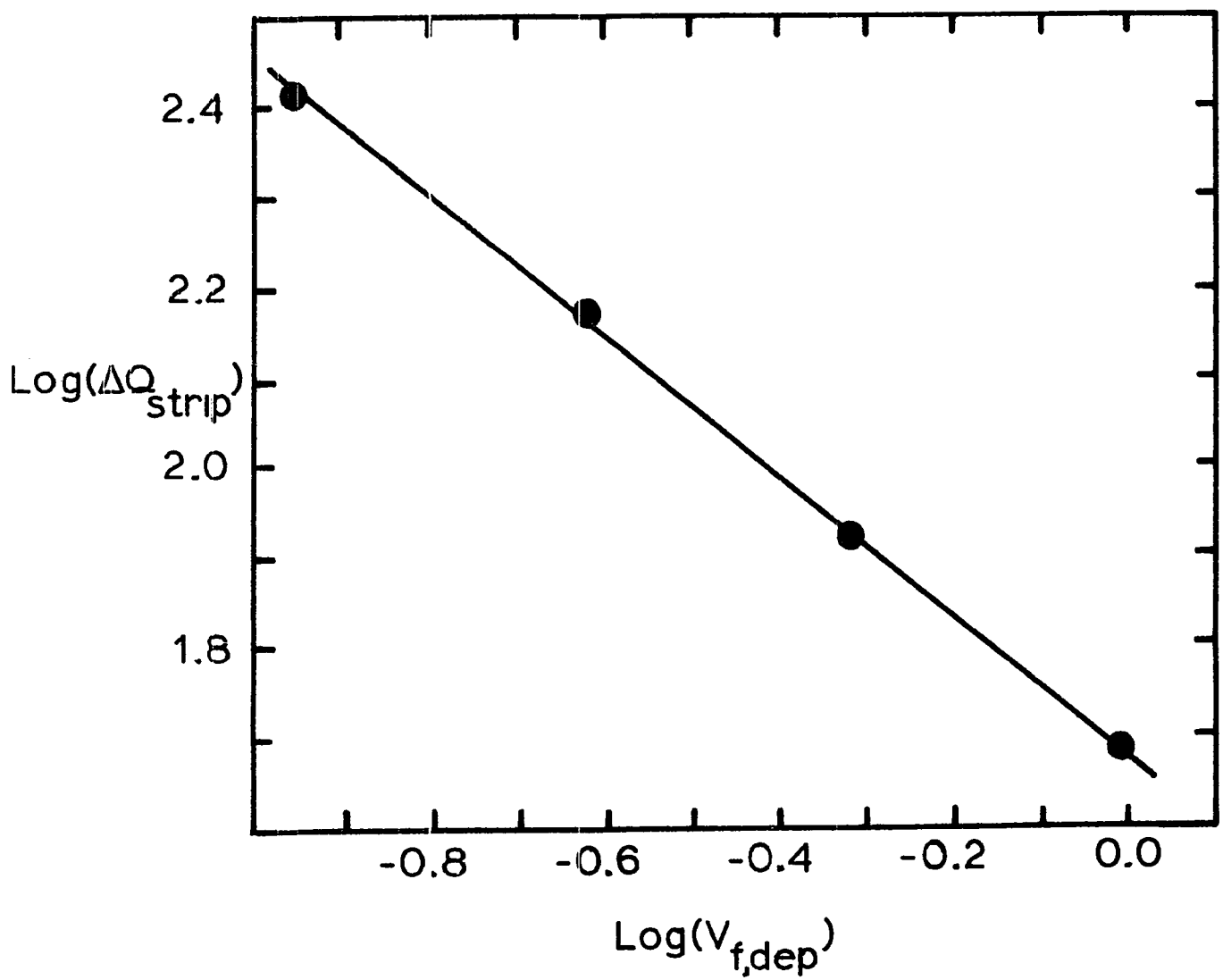
2.4
2.2
2.0
1.8
Log(ΔQ strip)
-0.8
-0.6
-0.4
-0.2
0.0
Log(V f,dep)

Table III-3. Dependence of peak obtained for Hg by DPASV[a] on $V_{f,dep}$ with constant V_s at a tubular Au electrode in 0.2 M HNO_3

Flow Rate, $V_{f,dep}$ (mL min^{-1})	Log V_f	ΔQ_{strip} (μ C)	Log ΔQ_{strip}
0.98	-0.009	48.4	1.685
0.48	-0.319	83.6	1.922
0.24	-0.620	148.3	2.171
0.11	-0.959	260.4	2.416

[a]Other parameters as given in Figure III-10.

system, as will be described in Section IV.B.1, permitted control of T_{dep} (actually injection time) independent of $V_{f,dep}$. The modified flow system permitted the use of both large $V_{f,dep}$ for maximum rate of deposition (recall Equation II-8) and long T_{dep}, when required by the most dilute solutions of Hg(II). The slope of 1.0 in Figure III-12 illustrates the direct proportionality between ΔQ_{strip} and T_{dep}, and the data are given in Table III-4. The concentration of Hg(II) was chosen such that a symmetrical stripping peak was obtained for all values of T_{dep}.

f. Reverse DPASV vs. Normal DPASV It was thought worthwhile to investigate again the effects of ΔE upon the stripping peak using $T_c = 2t_p$. The PAR 174A was modified to provide $\Delta E \geq 100$ mV as described above in Part B.2 of this section, and the FTD detector was

Figure III-12. Dependence of the DPASV peak-area on T_{dep} with nonconstant V_s using the FTD detector

Supporting electrolyte - 1.0 M H_2SO_4

Deposition:

$C^b_{Hg(II)}$ - 2.06×10^{-8} M

$V_{f,dep}$ - 1.16 mL min^{-1}

E_{dep} - 0.45 V vs. SCE

d - 0.07 mm

r_D - 1.50 mm

Stripping:

$V_{f,strip}$ - 0 mL min^{-1}

ΔE - 100 mV

$\emptyset$ - 5 mV s^{-1}

T_c - 0.5 s

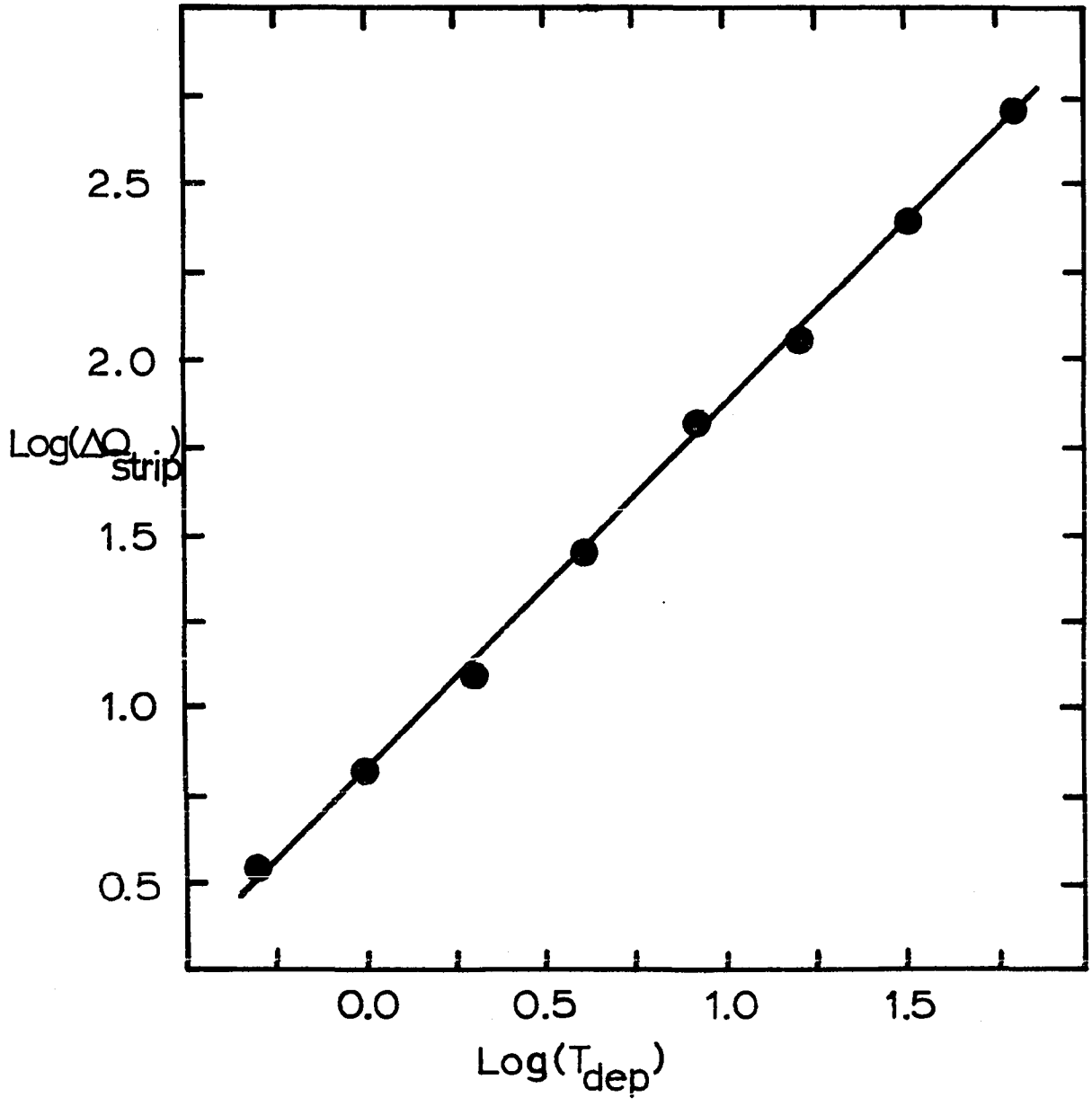
2.5
2.0
1.5
1.0
0.5
Log(ΔQ strip)
0.0
0.5
1.0
1.5
Log(T dep)

Table III-4. Dependence of peak obtained for Hg by DPASV[a] on T_{dep} with nonconstant V_s using the FTD detector

T_{dep} (min)	Log T_{dep}	ΔQ_{strip} (μC)	Log ΔQ_{strip}
0.5	-0.301	3.58	0.554
1.0	0	6.60	0.820
2.0	0.301	12.5	1.096
4.0	0.602	28.1	1.449
8.0	0.903	61.4	1.809
16.0	1.204	126	2.100
32.0	1.505	247	2.392
64.0	1.806	511	2.708

[a]Other parameters as given in Figure III-12.

used because flow could then be completely interrupted during the stripping scan. Although the data for Normal DPASV (NDPASV) were obtained first, according to the potential waveform of Figure III-1.A, but with $T_c = 2t_p$, the explanation for the observed effects was not apparent to this author until the data for Reverse DPASV (RDPASV) had been evaluated. The waveform used for RDPASV is illustrated in Figure III-1.B, and the data obtained are shown in Figure III-13. Curve F in Figure III-13 was off-set for clarity and does not represent an increase in ΔI_p.

Three effects are clearly seen in Figure III-13: first, the potential of ΔI_p is independent of ΔE; second, the selection of

Figure III-13. Effect of ΔE for Reverse DPASV

Deposition, FTD detector:

$C^{b}_{Hg(II)}$ - 1.03×10^{-7} M; 1.0 M H_2SO_4

$V_{f,dep}$ - 1.16 mL min^{-1}

T_{dep} - 1.0 min

E_{dep} - 0.45 V vs. SCE

d - 0.07 mm

r_D - 1.50 mm

Stripping:

$V_{f,strip}$ - 0 mL min^{-1}

Ø - 10 mV s^{-1}

T_c - 0.114 s

A - -25 mV

B - -50 mV

C - -100 mV

D - -150 mV

E - -200 mV

F - -300 mV

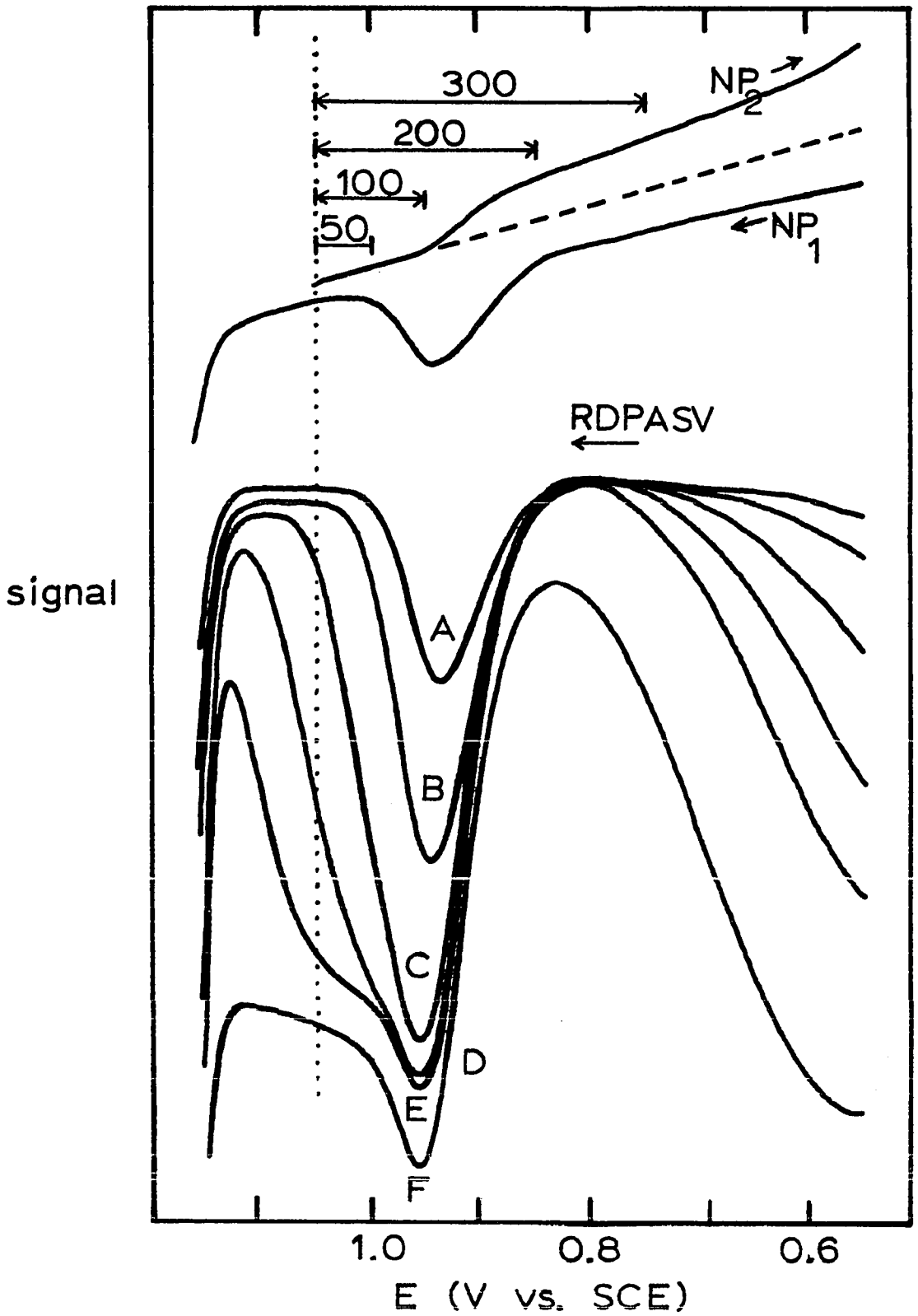
300
200
100
50
NP2
NP1
RDPASV
signal
A
B
C
D
E
F
1.0
0.8
0.6
E (V vs. SCE)

$|\Delta E| > 100$ mV does not significantly increase ΔI_p; and third, a distortion of the peak occurs at more positive potentials than that of ΔI_p when $|\Delta E| > 100$ mV.

Because the second effect was anticipated from the discussion in Part C.1.b, no further comment will be made here. The first and third effects both arise from the manner in which ΔI is determined and plotted as a function of potential using the PAR 174A. In the DIFFERENTIAL-PULSE mode the output of the PAR 174A relates the value of ΔI to the value of E_{ramp} at the time ΔE is applied. For RDPASV E_{ramp} is the more positive side of the pulsing potential waveform. Hence, ΔI is now plotted vs. the stripping potential rather than the redeposition potential as is the case for NDPASV. The stripping potential, being E_{ramp}, is independent of ΔE and hence, the potential of ΔI_p is also independent of ΔE.

The Curve labeled NP_2 in Figure III-13 was obtained in the following manner: Following the deposition step, the potential of the electrode was stepped to E_i = 1.05 V, and a pulsing waveform begun in which pulses of increasing negative amplitude were applied to E_i with $T_c = 2t_p$. Current was sampled only during the pulse, simulating the measurement of I_2, and plotted as a function of the potential of the pulse. Curve NP_1 simulates the measurement of I_1, and was obtained by applying a pulsing waveform similar to that used for NP_2, but with pulses of increasing positive amplitude from E_{dep}. The waveform and sequence of current measurements for RDPASV result in a combination of the currents simulated in NP_1 and NP_2. Note, however, that during

the stripping scan, redeposition can not occur until E_{ramp} is positive enough to cause oxidation of the deposit. On the other hand, redeposition may still occur, depending on ΔE, even after E_{ramp} has become so positive that no appreciable stripping current is detected as I_1 by the time of the sampling interval, e.g. at 1.05 V in NP_1.

The above discussion leads to the conclusion that the distortion of the stripping peak for $|\Delta E| > 100$ mV is the direct result of the redeposition current measured as I_2 during the pulse in RDPASV. For $|\Delta E| > 100$ mV the redeposition component of ΔI, e.g., plotted at 1.05 V, becomes significant and a small shoulder appears on the stripping peak (Curve D). The shoulder becomes quite apparent for $|\Delta E| = 200$ mV (Curve E) and reflects the fact that the potential pulses are extending sufficiently negative to attain the limiting-current plateau for the redeposition of Hg(II). When $|\Delta E| = 300$ mV, the pulses are still extending into the limiting-current plateau at the time E_{ramp} attains a value sufficient to begin oxidation of the Au surface. The result appears to be a small stripping peak superimposed on a large shift in the baseline (Curve F).

The data obtained for a similar series of experiments using NDPASV are shown in Figure III-14. The peak shapes obtained are virtually identical to those shown in Figure III-13. However, a direct interpretation of the three effects, especially the distortion of the peak shape, is made more difficult to visualize by the shift in potential of ΔI_p in NDPASV.

Figure III-14. Effect of ΔE for Normal DPASV

Deposition, FTD detector:

$C^{b}_{Hg(II)}$ - 1.03×10^{-7} M; 1.0 M H_2SO_4

$V_{f,dep}$ - 1.16 mL min^{-1}

T_{dep} - 1.0 min

E_{dep} - 0.45 V vs. SCE

d - 0.07 mm

r_D - 1.50 mm

Stripping:

$V_{f,strip}$ - 0 mL min^{-1}

Ø - 10 mV s^{-1}

T_c - 0.114 s

A - +25 mV

B - +50 mV

C - +100 mV

D - +150 mV

E - +200 mV

F - +300 mV

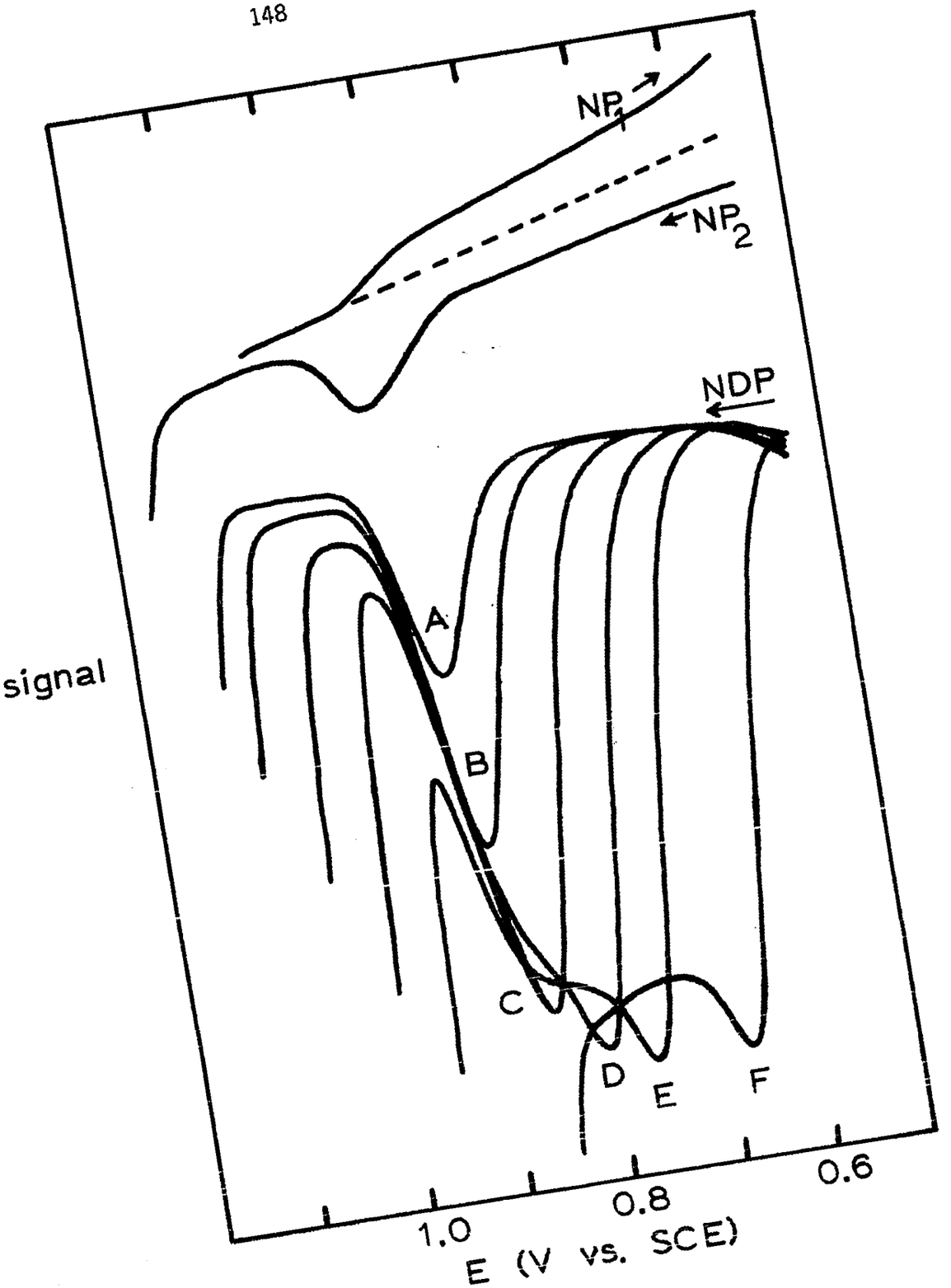
NP1
NP2
NDP
A
B
C
D
E
F
signal
1.0
0.8
0.6
E (V vs. SCE)

Table III-5. Optimum values for parameters of DPASV applied to the determination of Hg(II) at a flow-through Au electrode

Parameter			Comment
$V_{f,strip}$	=	0 mL min^{-1}	
ΔE	=	50-100 mV	$\emptyset T_c \leq 0.1\Delta E$
$\emptyset$	$\leq$	20 mV s^{-1}	$\emptyset T_c \leq 0.1\Delta E$
T_c	=	0.114 s	$T_c = 2t_p$ for PAR 174A
$V_{f,dep}$	=	slow	when V_s is constant
		fast	when V_s is determined by T_{dep}
T_{dep}	$\leq$	5 min	selected for sample through-put of $\geq$10 samples hr^{-1}

D. Summary

EC studies have been presented for the evaluation of parameters of DPASV applied to the determination of Hg(II) at a flow-through Au electrode. The effects of $V_{f,strip}$, ΔE, $\emptyset$, T_c, $V_{f,dep}$ and T_{dep} on the stripping peak were investigated. The optimum values found for these parameters are summarized in Table III-5.

The observations made by this author were compared to the observations of other workers using different types of Hg electrodes when such comparisons were applicable. No attempt was made to present a unified theory for the stripping peak obtained by DPASV.

The effect of ΔE on the stripping peak was discussed in detail for the case in which the DPASV waveform was applied in a "reverse" fashion, i.e., RDPASV. Three effects were observed: 1) no dependence on ΔE for the potential at which ΔI_p is observed; 2) no significant increase in ΔI_p at $|\Delta E| \geq 100$ mV; and 3) peak distortion was observed at $|\Delta E| \geq 150$ mV. The results of RDPASV were compared to those obtained by DPASV performed in the conventional manner.

IV. A FLOW-INJECTION ANALYZER FOR APPLICATION OF DPASV TO THE DETERMINATION OF Hg(II) AT A FLOW-THROUGH GOLD ELECTRODE

A. Stripping Methods in Flow-Injection Analysis

The scope of analytical methods which now may be classified under the heading of FIA, has increased dramatically during the past five years (27,28). No longer is FIA restricted to only the simplest analytical schemes. Reviews of FIA which have appeared in the literature (28,33,186) demonstrate the wide variety of detection systems which have been found amenable to flow systems.

Potentiometric detectors, e.g., pH and ion-selective electrodes, are the most commonly used EC detectors in FIA. However, the inclusion of chemical separations within the scheme of FIA, especially low-pressure chromatography, holds much promise for future advances in the application of amperometric and voltammetric detectors. Such applications would seem to be obvious extensions of the use of EC detectors in the more general catagory of liquid chromatography as reviewed by Kissinger (36).

Reviews of FIA (27,28,33) and the use of EC detectors in FIA (31,187), written prior to late 1979, cite few examples of methods utilizing stripping analysis. More recently, the excellent review by Toth, et al. (188), gave somewhat more thorough coverage to the subject of flow-through stripping. Still, in all, fewer than 10 papers are cited as examples of stripping analysis in FIA. Many, if not all,

of the stripping analyses which are presently being performed in large-volume cells, e.g., with RDEs, RRDEs, etc., should be easily adapted to FIA. It is anticipated that in the next 5-10 years, research in this area will experience steady growth.

The fundamental requirement for any type of stripping analysis is that the species of interest from the bulk solution be accumulated at the surface of the indicating electrode. The rate at which the preconcentration is effected depends by varying degrees on the rate of convective mass transport of the species to the surface of the electrode; recall the V_f^{∞} term in Equation II-8. Hence, for a stripping method applied within the scheme of FIA, an increase in $V_{f,dep}$ must result in an increased rate of deposition during the residence time of the sample plug at the indicating electrode. Unfortunately the increase in the rate of deposition is more than off-set, when V_s is constant, by the decrease in the residence time which, ignoring dispersion, is inversely proportional to $V_{f,dep}$. Equation II-9 predicts and Figure III-10 demonstrates the diminution of the quantity of metal deposited from a constant, injected volume as $V_{f,dep}$ increases.

The lower the concentration of the species of interest, the longer must be the time allowed for accumulation of a detectable quantity of metal. However the trade-off required for longer T_{dep} by a decrease in $V_{f,dep}$ at constant V_s, does not permit operation of the flow system at maximum sensitivity. Alternatively increasing the length of the sample loop to lengthen T_{dep}, at constant $V_{f,dep}$, soon becomes impractical. Clearly, the independent selection of both T_{dep} and $V_{f,dep}$ is

a highly desirable feature of a flow-injection analyzer to be used for stripping analysis.

The data presented in this section illustrate the performance of a flow system and the FTD detector for the determination of Hg(II) by DPASV.

B. Description of Experimental Parameters

1. Flow system

A diagram of the flow system which was chosen to permit the independent selection of T_{dep} and $V_{f,dep}$ is shown in Figure IV-1. The peristaltic pump (C) and pulse dampener (E,F) were the same as described in Section II.B.4, Figure II-4. The FTD detector (H) was described in Section III.B.1.b. The sample injector (G) was a Cheminert, pneumatic injection valve from Laboratory Data Control which was converted to a simple switching valve. This modification allowed passage through the detector of either the supporting electrolyte or the solution containing the sample. The inconvenience of unmanageable lengths of tubing, i.e., sample loops, necessary for longer T_{dep} was thus avoided. For example, a 10 min deposition period at a flow rate of 1.0 mL min^{-1} requires a sample volume of 10 mL. More than 15 m of the Teflon tubing (~1 mm i.d.) would be required as a sample loop for this rather moderate volume. The length of tubing between the switching valve and the FTD detector was kept to a minimum (<5 cm).

Figure IV-1. Diagram of flow-injection analyzer for DPASV of Hg using the FTD detector

A - reservoir for supporting electrolyte

B - flask containing the sample in solution

C - peristaltic pump

D - slide-valve for complete blockage of flow stream

E - inverted glass T-tubes

F - adjustable needle valves

G - pnuematic switching valve

H - FTD detector

I - potentiostat

J - recorder

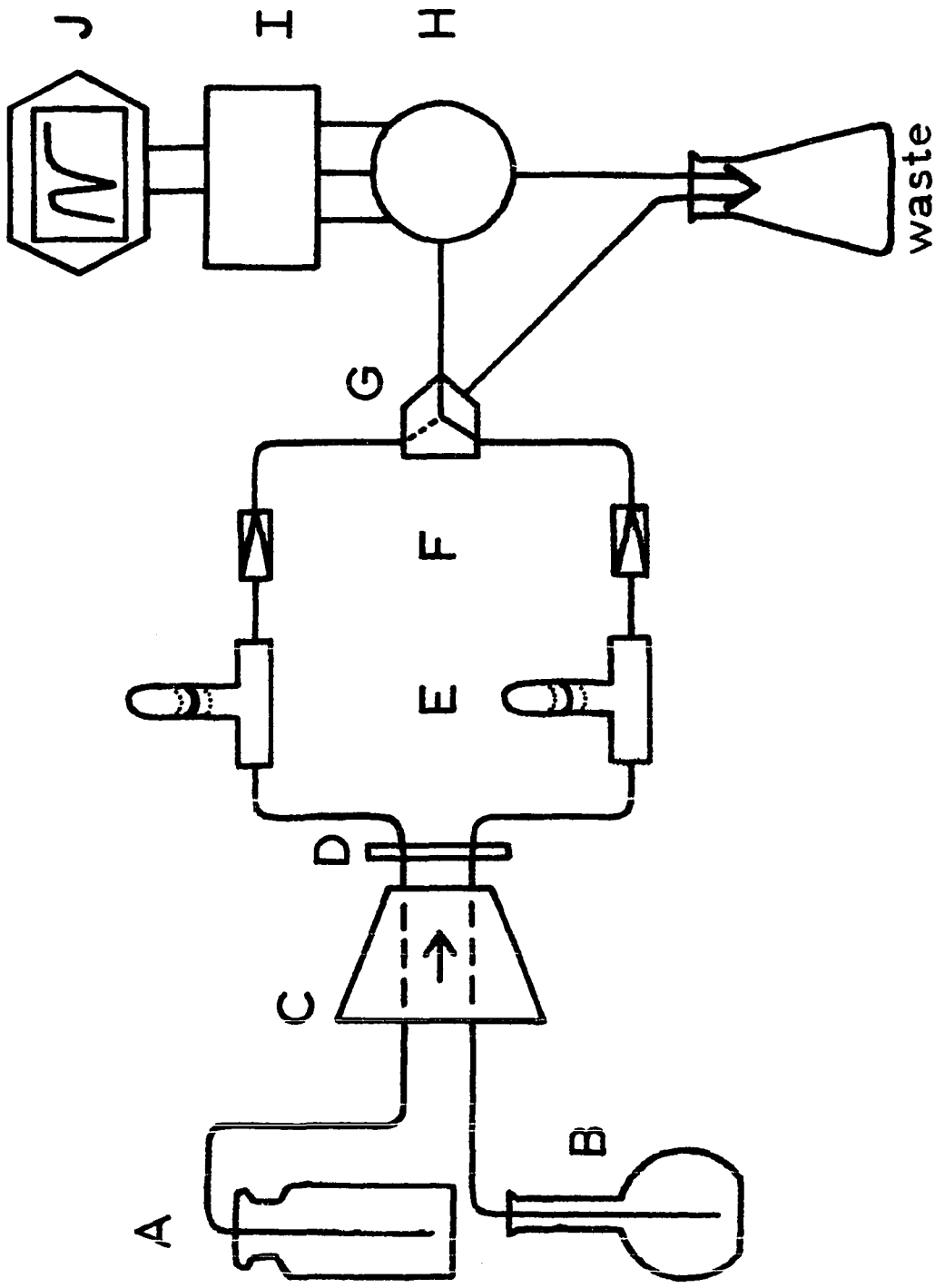
J
H
H
waste
G
F
E
D
C
B
A

The operational procedure used to prepare the flow system for each day's experimental work was as follows:

1. The manifold tubes were put in place on the pump head and the pressure pads were closed onto the manifold tubes. Valve D in Figure IV-1 was opened and the flow system was rinsed with supporting electrolyte for at least 10 min. The maximum flow rate of 1.16 mL min^{-1} was used at all times.

2. The reference electrode was placed in position in the FTD detector (see Figure III-3) and the miniature disk-electrode was positioned to constrict the flow stream at the orifice of the nozzle. The position which registered ~3 psi of back pressure in the pulse dampener was used and the distance, d, between the disk electrode and the orifice was estimated to be 0.07 mm (~3/16 turn from fully closed position). The pulse dampener in the channel containing the supporting electrolyte was used as a check of the positioning of the miniature disk between each injection.

3. The miniature, Au-disk electrode was pretreated by scanning the potential of the electrode between 0.15 and 1.65 V (vs. SCE) until the residual I-E curve was reproducible. At the beginning of each day this procedure required perhaps 10-15 min.

4. When a new sample solution was drawn into the flow system, the sample channel was rinsed for at least two minutes with the new solution. By adjusting the needle valve the pulse dampener was rinsed, and the switching valve was rinsed by making several short injections.

Finally, the needle valve was adjusted to cause ~15 psi to be registered in the pulse dampener.

5. The potential of the electrode was established at E_{dep} and the injection begun by activating the switching valve. At the conclusion of T_{dep} the switching valve was deactivated and solution flow was continued for 30 s to rinse the remainder of the sample solution through the tubing between the switching valve and the detector. The actual time required for this was ~10 s but the additional 20 s was allowed to insure that the sample solution had been completely rinsed from the vicinity of the Au electrode. The pump was then stopped and another 15 s was allowed for the establishment of quiescent conditions. The PAR 174A was then set to the DIFFERENTIAL-PULSE mode and the stripping scan was commenced 60 s after the conclusion of T_{dep}. At the conclusion of the stripping scan, solution flow was resumed. The PAR 174A was returned to the DIRECT-CURRENT mode and the potential of the electrode was scanned between 0.15 and 1.65 V until being established again at E_{dep}.

6. At the conclusion of each day's experimental work, the flow system was rinsed with TDW for at least 10 min. The reference electrode was removed from the FTD detector and replaced by a small plug so that TDW would not drain from the detector. Valve D was closed so that the flow system remained filled with TDW when the manifold tubes were removed from the drum head of the pump.

2. Instrumentation

Potential control and current measurement were made with the Model 174A Polarographic Analyzer which was described in Section III.B.2. The potential of the Au electrode was monitored only when necessary with the Model PDM 35 digital multimeter as also described in Section III.B.2. After initially locating the position of E_{dep} on the potential axis of the X-Y recorder, the pen position of the recorder was used to establish E_{dep} ± 0.03 V for all subsequent depositions that day.

The X-Y recorder used was the Model Omnigraphic 2000. The Heath-Schlumberger Strip Chart Recorder, Model SR-255 A/B, was used to record the data for evaluation of the reproducibility of the injection system.

3. Chemicals and solutions

The preparation of the supporting electrolyte (1.0 $\underline{M}$ H_2SO_4) and the solutions of Hg(II) was as described in Section II.B.5. Loss of Hg(II) due to adsorption onto the walls of the volumetric glassware (see e.g., 189-191) was minimized by preparing the dilute solutions immediately prior to the determination.

C. Results and Discussion

1. Calibration

a. Normalization of the stripping peak for T_{dep} It has been shown in Section II.C that, as the quantity of Hg accumulated at

underpotential increases, up to four unresolved stripping peaks are observed as the deposit is removed from the electrode. For very small quantities of Hg(UPD) a single stripping peak is obtained. It follows from these observations that T_{dep} must decrease as $C^{b}_{Hg(II)}$ increases to maintain conditions such that a single peak is obtained during the stripping scan. Hence, to obtain the widest dynamic range, the flow system must be one in which T_{dep} can be determined at the discretion of the operator. To portray the dynamic range of DPASV for the determination of Hg(II), a calibration curve was prepared by plotting the area of the stripping peak, ΔQ_{strip}, normalized for T_{dep}, as a function of the concentration of Hg(II) in 1.0 $\underline{M}$ H_2SO_4.

The calibration curve obtained is shown in Figure IV-2, and the data are summarized in Table IV-1. Some of the scatter of the data may be attributed to: uncertainty in the integration of peak areas obtained at different instrumental sensitivities; uncertainty in T_{dep}; and nonreproducibility due to performing the set of experiments over the period of two days.

The uncertainty in T_{dep} occurred because these data were obtained prior to final modification of the flow system to the form shown in Figure IV-1. Although the initial flow system permitted the selection of T_{dep} independent of $V_{f,dep}$, the flow streams were manually and individually switched. Delay times, such as indicated in Step 5 of the procedure outlined above in Part B.1, could not be highly reproduced. Nonetheless, even when $T_{dep} < 1$ min, the linearity of the data was not

Figure IV-2. Calibration Curve for Hg(II)

Deposition:

$V_{f,dep}$ - 1.16 mL min^{-1}

E_{dep} - 0.45 V vs. SCE

d - 0.07 mm

r_D - 1.50 mm

T_{dep} - 30.0 min; 3.0 min; 0.3 min

○ ● △

Stripping:

$V_{f,strip}$ - 0 mL min^{-1}

E - 50 mV

Ø - 5 mV s^{-1}

T_c - 0.5 s

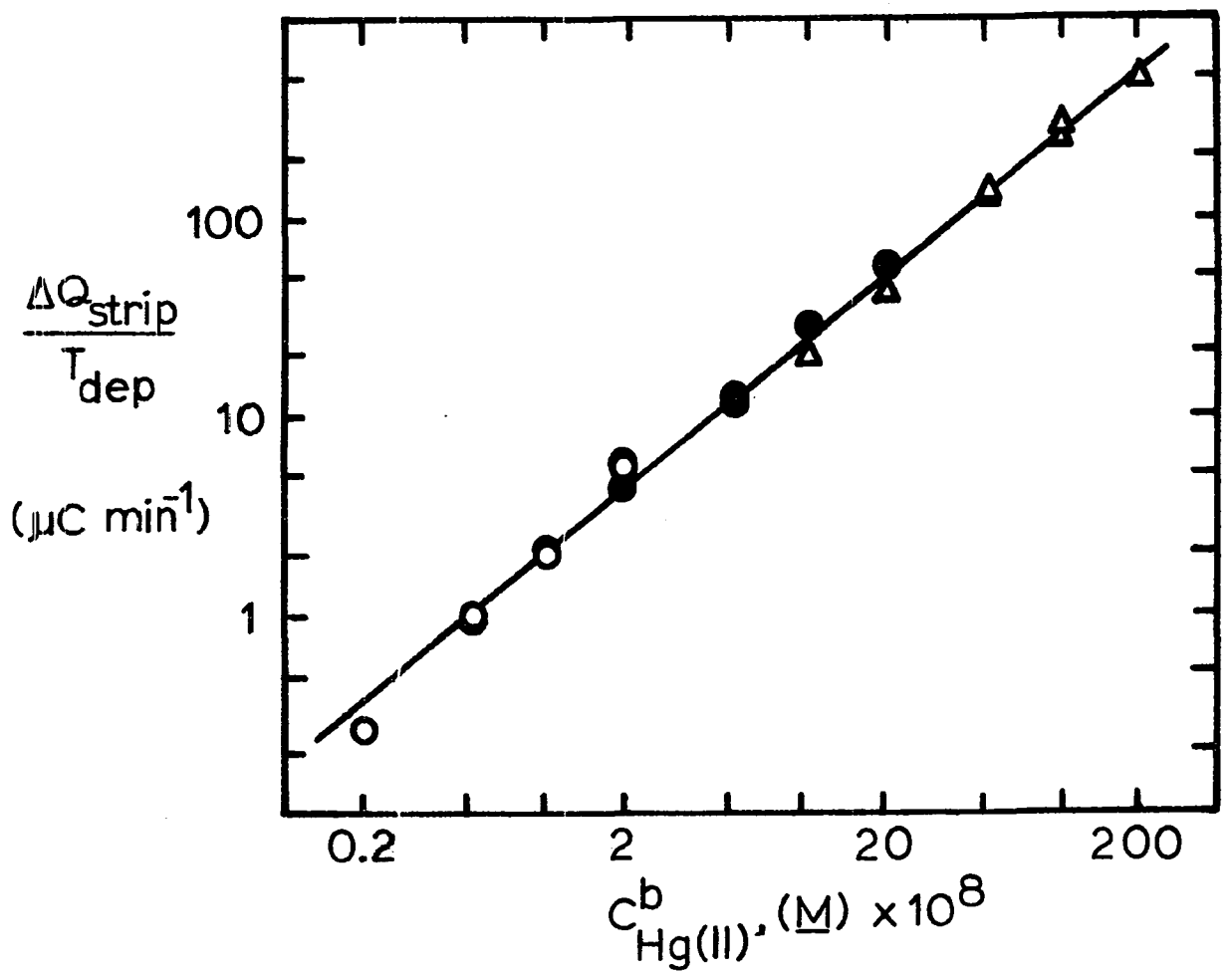
100
10
1
$\frac{\Delta Q_{strip}}{T_{dep}}$
(μC min⁻¹)
0.2
2
20
200
$C^{b}_{Hg(II)}$, (M) x 10⁸

Table IV-1. Data for Calibration Curve[a]

$C^{b}_{Hg(II)}$ ($\underline{M}$) x 10^{8}	T_{dep} (min)	ΔQ_{strip} (μC)	$\frac{\Delta Q_{strip}}{T_{dep}}$ (μC min^{-1})
0.206	30.0	7.98	0.27
0.515	30.0	28.9	0.96
	30.0	29.8	0.99
1.03	30.0	61.4	2.05
	3.0	6.36	2.12
2.06	30.0	165	5.51
	30.0	180	6.00
	3.0	13.1	4.38
5.15	3.0	37.9	12.6
	3.0	36.4	12.1
10.3	3.0	80.7	26.9
	0.3	5.91	19.7
20.6	3.0	166	55.4
	0.3	12.2	40.7
51.5	0.3	38.6	129
	0.3	37.3	124
103	0.3	84.2	281
	0.3	78.7	262
206	0.3	146	485

[a]Other parameters as given in Figure IV-3.

unreasonable. Inspection of the data in Table IV-1 also reveals that the working range for a given value of T_{dep} is approximately one order of magnitude in concentration of Hg(II).

It should also be noted from Figure IV-2 that the data were obtained prior to modification of the PAR 174A to provide $T_c = 2t_p$. Furthermore, the time period of 30 min required to obtain an appreciable signal at a level of $\leq 10^{-8}$ M Hg(II) ($\leq$2 ppb) was considered to defeat the purpose of a FIA method.

Later, the PAR 174A was modified as described in Section II.B.2, and the optimum conditions found for DPASV were used. The result was a slight extension of the dynamic range to lower concentrations, but a dramatic reduction in T_{dep}. A calibration curve for the detection of 1.03×10^{-9} to 2.06×10^{-8} M Hg(II) (0.20 to 4.1 ppb) with $T_{dep} = 5.0$ min is shown in Figure IV-3 and the data are given in Table IV-2.

b. Reproducibility The performance of the flow system was evaluated with respect to the detection of Hg(II) at a concentration of 1.03×10^{-8} M (2.0 ppb). Eight successive experiments were performed using a deposition time of 3.0 min and a flow rate of 1.16 mL min^{-1}. The results are summarized in Table IV-3. The deviation from the mean represents a relative precision of 1.9%. These results indicate that determinations of Hg(II) at levels $\geq$2 ppb may be made on a routine basis using convenient conditions of $V_{f,dep}$ and T_{dep}. Sample throughput for such determinations is approximately 10 samples hr^{-1} or more, including deposition, stripping scan, and introduction of a new sample. Regardless of the concentration of Hg(II) the entire instrumental sequence limits the through-put to a maximum of ~20 samples hr^{-1} for even the experienced operator (author).

Figure IV-3. Calibration Curve for Hg(II) - optimum conditions

Deposition:

$V_{f,dep}$ - 1.16 mL min^{-1}

T_{dep} - 5.0 min

E_{dep} - 0.45 V vs. SCE

d - 0.07 mm

r_D - 1.50 mm

Stripping:

$V_{f,strip}$ - 0 mL min^{-1}

ΔE - 100 mV

$\emptyset$ - 20 mV s^{-1}

T_c - 0.114 s

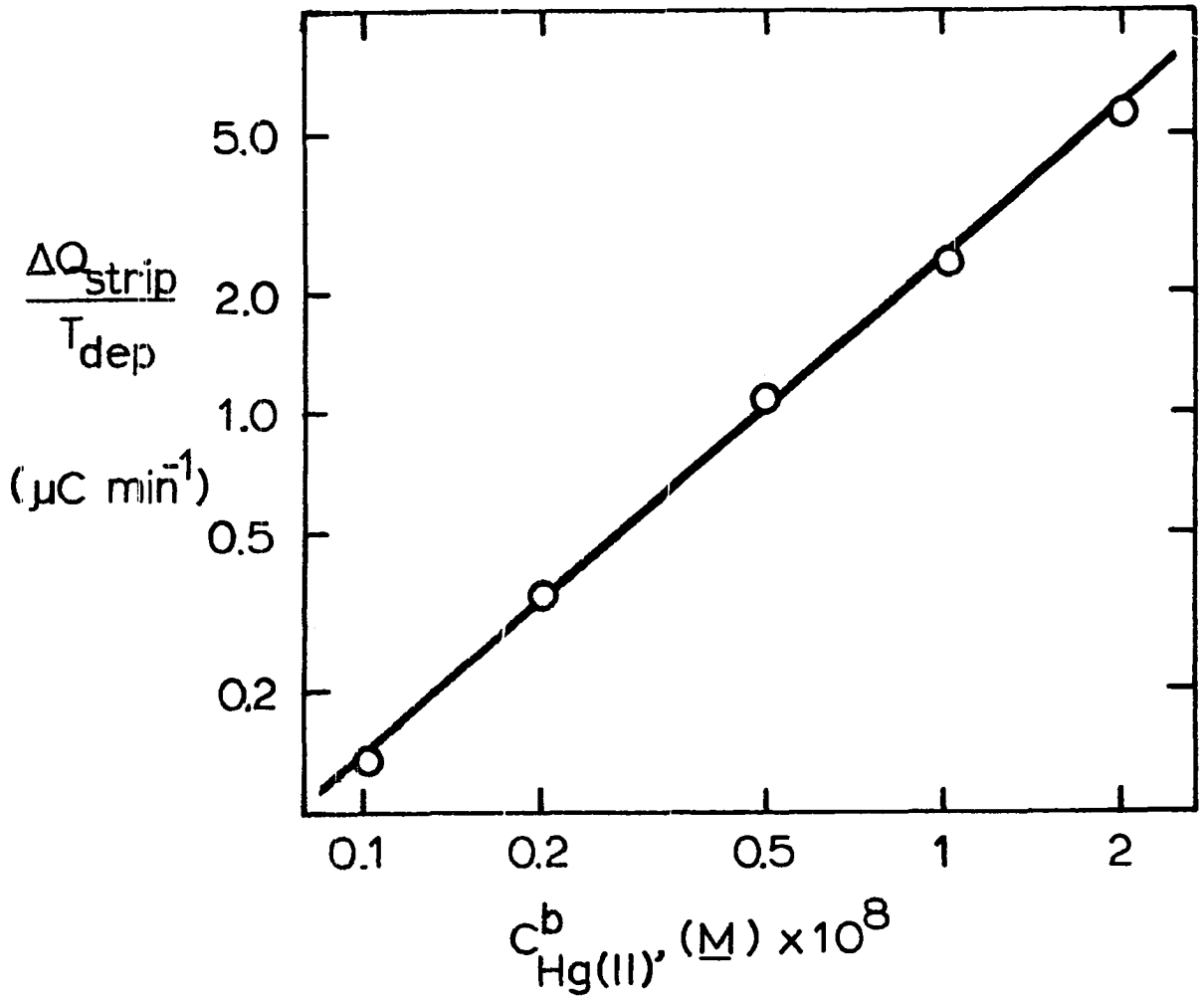
5.0
2.0
1.0
0.5
0.2
$\frac{\Delta Q_{strip}}{T_{dep}}$
(μC min^{-1})
0.1
0.2
0.5
1
2
$C^{b}_{Hg(II)}$, (M) x10^{8}

Table IV-2. Data for Calibration Curve - optimum conditions[a]

$C^{b}_{Hg(II)}$ (M) x 10^{8}	T_{dep} (min)	ΔQ_{strip} (μC)	$\frac{\Delta Q_{strip}}{T_{dep}}$ (μC min^{-1})
0.103	5.0	0.68	0.14
0.206	5.0	1.75	0.35
0.515	5.0	5.61	1.12
1.03	5.0	13.2	2.64
2.06	5.0	27.9	5.59

[a]Other parameters as given in Figure IV-3.

c. Detection limit for aqueous solutions Figure IV-4 shows the data obtained with T_{dep} = 5.0 min for concentrations of Hg(II) in 1.0 M H_2SO_4 ranging from 0.20 to 1.0 ppb. Peak A corresponds to an injected qauntity of 0.72 ng Hg, i.e., 3.6 x 10^{-12} mole. The unmarked curve is the response obtained after a 5.0-min deposition from the supporting electrolyte alone, and represents a blank of approximately 5 x 10^{-10} M Hg(II) which is considered the practical limit of detection.

The deformation of the shape of the peaks at the lowest concentrations is attributed to the effect of ΔE noted earlier in Section III.C.1.f. This observation led to the conclusion that a 100-mV modulation amplitude may not be the optimum for determinations of Hg(II) made near the detection limit.

Table IV-3. Reproducibility at the 2 ppb level[a]

$C^{b}_{Hg(II)}$ (M) x 10^{8}	T_{dep} (min)	Q_{strip} (μC)	Mean, Std. Dev., s (μC)
1.03	3.0	14.5	
		14.3	
		14.6	14.6
		14.2	0.28
		14.7	
		14.8	
		15.0	

[a]Conditions:

Deposition:

$V_{f,dep}$ - 1.16 mL min^{-1}

E_{dep} - 0.45 V vs. SCE

d - 0.07 mm

r_D - 1.72 mm

Stripping:

$V_{f,strip}$ - 0 mL min^{-1}

ΔE - 100 mV

$\emptyset$ - 20 mV s^{-1}

T_c - 0.114 s

Figure IV-4. Detection of Hg(II) in 1.0 M H_2SO_4 by DPASV using the FTD detector

Deposition:

$V_{f,dep}$ - 1.16 mL min^{-1}

T_{dep} - 5.0 min

E_{dep} - 0.45 V vs. SCE

d - 0.07 mm

r_D - 1.72 mm

Stripping:

$V_{f,strip}$ - 0 mL min^{-1}

ΔE - 100 mV

$\emptyset$ - 20 mV s^{-1}

T_c - 0.114 s

A - 1.03×10^{-9} M Hg(II)

B - 2.06×10^{-9} M Hg(II)

C - 5.15×10^{-9} M Hg(II)

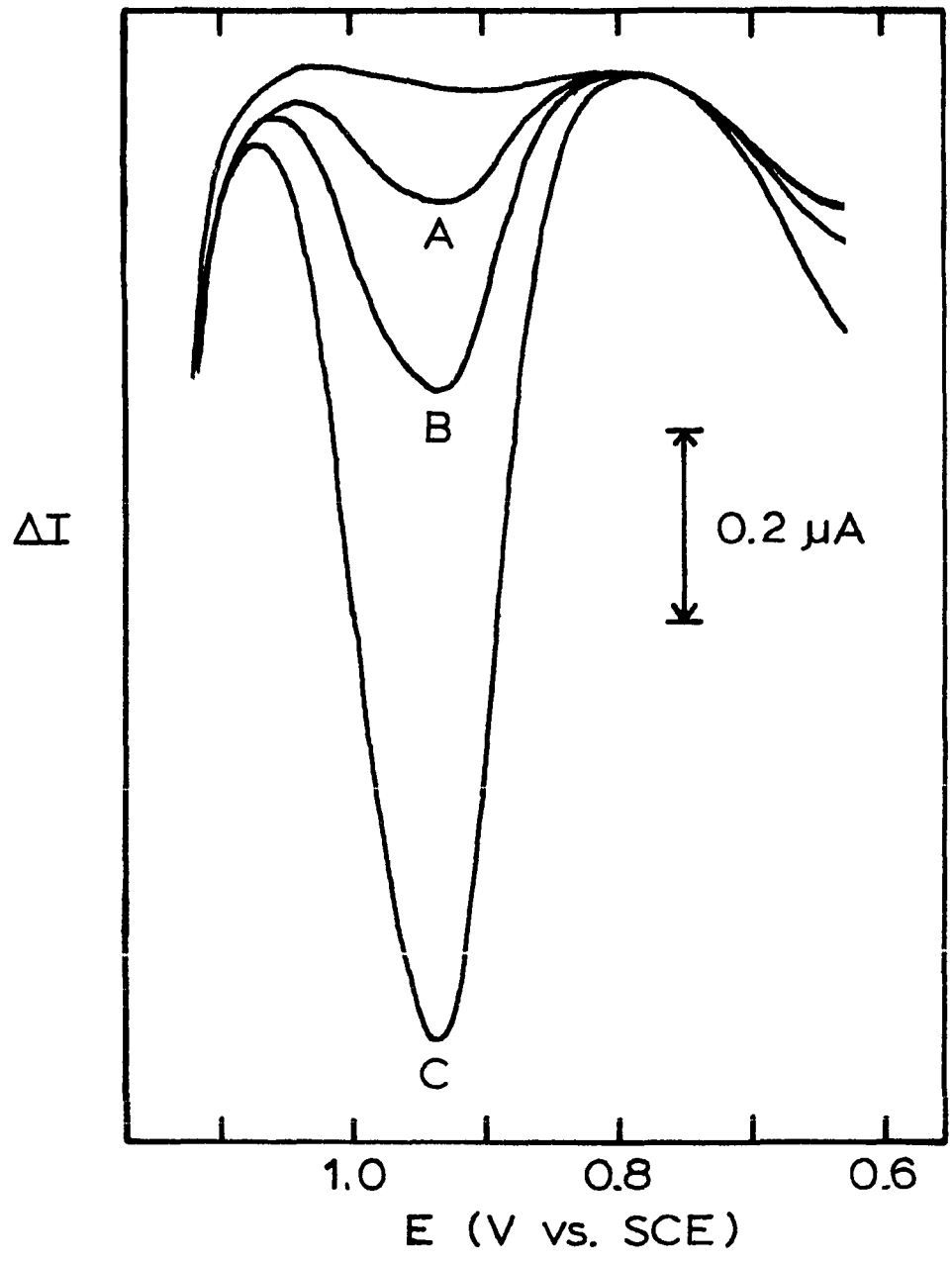
ΔI
A
B
C
0.2 μA
1.0
0.8
0.6
E (V vs. SCE)

D. Summary

In this section a flow-injection analyzer was described in which both T_{dep} and $V_{f,dep}$ may be independently selected by the operator. Calibration curves were shown which demonstrated the linear dynamic range of DPASV for the determination of Hg(II) from 1.0×10^{-9} to 2.0×10^{-6} M (0.20 to 400 ppb). Reproducibility at the 2 ppb-Hg(II) level was less than 2% relative using a deposition time of 3.0 min. The limit of detection for aqueous solutions was determined by the blank in 1.0 M H_2SO_4 and corresponded to 5×10^{-10} M Hg(II).

"Got an idea for an experiment? Try it. If it works the first time, then you're lucky. If it doesn't, then you're doing research!"

John Hauck, 1977

V. THE ANALYSIS OF SAMPLES

A. Introduction

It is necessary in the development of any analytical method to identify those chemical species which will present an interference to the quantitative determination of the species of interest. R. E. Allen (34), working about seven years ago in the laboratory of Professor Dennis C. Johnson at Iowa State University, demonstrated that Ag(I), As(III), Sb(III) and Se(IV) presented a serious interference to the determination of Hg(II) by stripping voltammetry with collection (SVWC). The technique of SVWC, applied to the determination of Hg(II), involved the deposition of Hg(II) on a Au-film, glassy carbon disk of a RRDE at a potential of 0.30 V vs. SCE. Following the deposition period, the deposited Hg was stripped from the disk electrode; the Hg(II) produced was subsequently detected at the Au-film, Pt ring electrode also at a potential of 0.30 V. Allen reported that the ions identified above, were preferentially adsorbed and/or deposited on the Au film at 0.30 V, thereby inhibiting the deposition of Hg(II). He further speculated that Te(IV) would interfere in a manner similar to Se(IV), and that Cl^- could be expected to interfere also. Because Allen had used a Au-film electrode, it was of interest to investigate

what interferences these same ions might present to the determination of Hg(II) by DPASV following UPD at 0.45 V on a Au flow-through electrode.

An attempt was made then to verify the proposed method for the determination of mercury by analyzing two "real samples". The samples were obtained from the National Bureau of Standards (NBS) which has available several physiological and biological matrices which are Certified Standard Reference Materials (SRMs) for trace metals. One sample was freeze-dried urine, certified for mercury (NBS SRM 2672, Elevated Level), and the other sample was orchard leaves (NBS SRM 1571). The certificate value for mercury in the urine, and a list of selected, certified constituents in the orchard leaves are given in Table V-1.

An obvious requirement which must be met before FIA can be applied to a given determination, is that the sample must be in a liquid form. Furthermore, for the determination of metals EC methods generally require that the final liquid be aqueous, and that all remaining constituents of the sample matrix be in their simplest ionic form. To meet these requirements, wet chemical oxidations are often employed which utilize various mixtures of concentrated acids, with and without a variety of catalysts.

Allen attempted to apply SVWC to the determination of mercury in NBS SRM 1571 (orchard leaves) following oxidation of the sample in hot, concentrated HNO_3 for 30 min. He found it necessary to follow the digestion with an ion-exchange separation to isolate the Hg(II) from

Table V-1. Concentration of selected, certified constituents in the analyzed Standard Reference Materials

Sample	Constituent	Concentration
Freeze-dried urine (NBS SRM 2672) Elevated Level: reconstituted to 50.0 mL		($mg\ L^{-1}$)
	Mercury	0.294 ± 0.024
Orchard Leaves (NBS SRM 1571)		($mg\ g^{-1}$)
	Iron	300 ± 20
	Manganese	91 ± 4
	Lead	45 ± 3
	Zinc	25 ± 3
	Copper	12 ± 1
	Arsenic	10 ± 2
	Antimony	2.9 ± 0.3
	Chromium	2.6 ± 0.3
	Nickel	1.3 ± 0.2
	Molybdenum	0.3 ± 0.1
	Mercury	0.155 ± 0.015
	Cadmium	0.11 ± 0.01
	Selenium	0.08 ± 0.01

unidentified, interfering species prior to the determination by SVWC. The additional steps not only increased the amount of sample handling prior to analysis, but also introduced another interference. On the average, the results for NBS SRM 1571 reported by Allen were 80% below the certified value for Hg.

The additional steps required in Allen's method were concluded to be unnecessary in the method proposed in this research. Hence an attempt was made to analyze the SRMs without ion-exchange separation following oxidation in hot, concentrated HNO_3.

Knechtel and Fraser (192) described the use of a mixture of HNO_3 and H_2SO_4 with a small quantity of V_2O_5 as catalyst for the oxidation of biological samples prior to the determination of mercury by flameless atomic absorption. A modification of their procedure was also used for this research.

A third method of wet chemical oxidation was used which utilized a mixture of HNO_3, H_2SO_4 and $HClO_4$. The use of $HClO_4$ in mixtures with HNO_3 and/or H_2SO_4 is well-known. An informative monograph on the subject was published by G. F. Smith in 1965 (193). Although the so-called liquid fire reaction of organic compounds in mixtures of HNO_3 and $HClO_4$ is capable of the complete oxidation of most organic matter, such a mixture alone is not recommended for dissolution of samples containing Hg. Gorsuch (194) demonstrated that Hg was lost from such mixtures, presumably as a volatile, chloromercurial compound, during the evolution of $HClO_4$ fumes at the conclusion of the digestion. However, it was thought that the use of an acid mixture consisting

primarily of HNO_3 and H_2SO_4, with only a minimum of $HClO_4$ to finish the oxidation of the organic matter, would lead to complete recovery of Hg. Satisfactory results have been obtained by Hugos (195) using a mixture of these three acids, plus Cr(III) as an oxidation indicator, for the determination of Hg in fish by flameless atomic absorption.

The work described in this section pertains to: the investigation of possible interferences to the determination of Hg(II); the use of three different methods of sample dissolution; and the analysis of the Standard Reference Materials.

B. Description of Experimental Parameters

1. Miniaturized Bethge apparatus

The Bethge apparatus, used for the controlled wet-oxidation of organic matter, is well known. The apparatus permits the regulation of the oxidizing strength of the heated mixture of acids through control of the refluxing of the distilled vapors. However, the apparatus commonly used is rather bulky, and is not conducive to the use of small volumes of concentrated acids, e.g., a final volume ≤ 5 mL. A miniaturized Bethge apparatus is shown in Figure V-1 which was constructed from miscellaneous pieces of glassware located in the laboratory. For example, the portion of the apparatus used for collection of the distillate (B) was fashioned from a 20-mL volumetric pipette. The graduations were added so that the approximate volume of collected distillate could be determined. Although not shown in Figure V-1, the

Figure V-1. Miniaturized Bethge apparatus

A - water-cooled condenser

B - collector for distillate; reflux return

C - three-way stopcock

D - small, glass stopper (thermometer, optional)

E - 50-mL reaction vessel

F - heating mantle

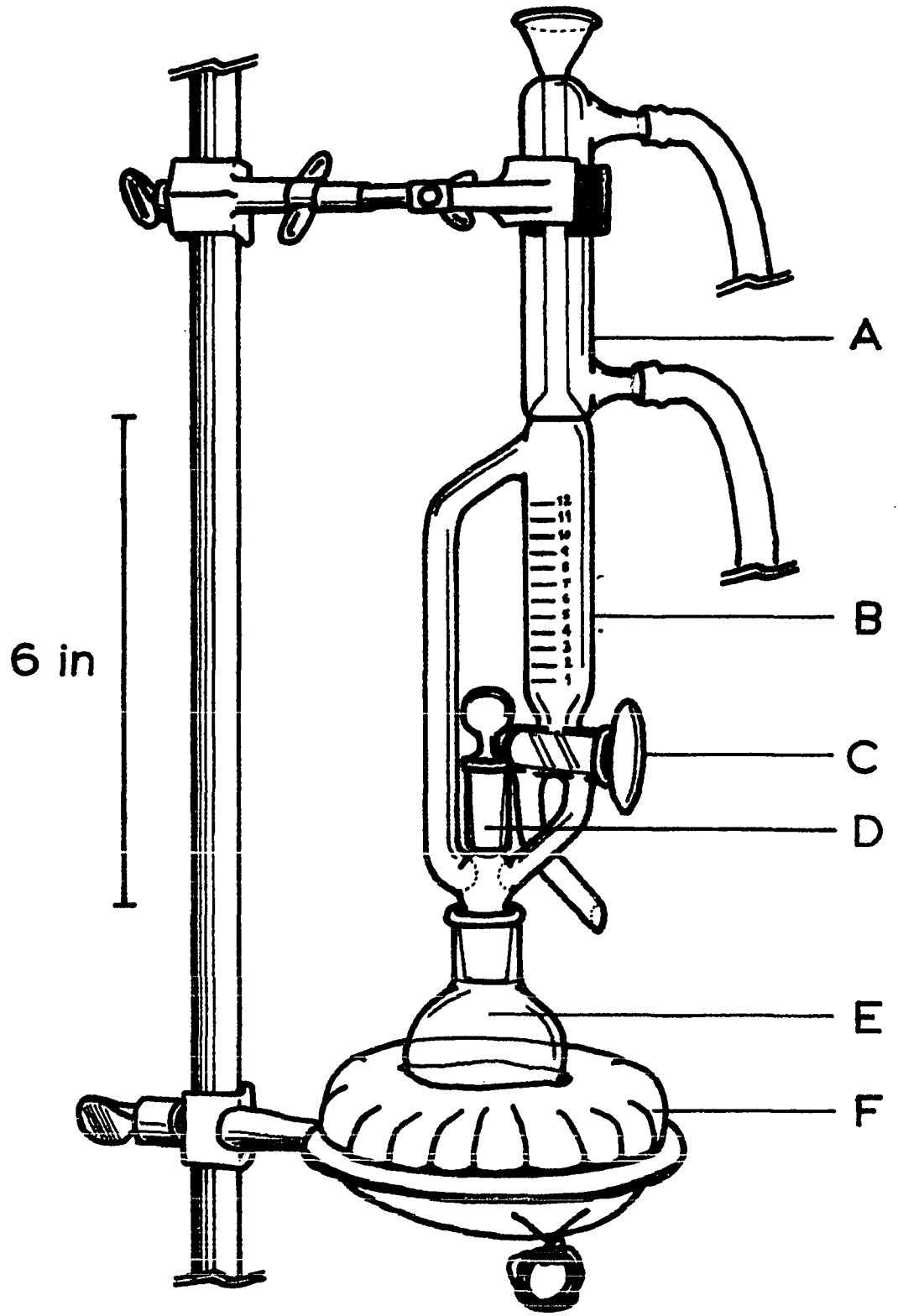
A
B
C
D
E
F
6 in

distillation arm of the apparatus was wrapped in asbestos. The reaction vessel was a 50-mL round-bottom pyrex flask from Ace Glass Co., Louisville, KT.

The reaction flask was heated with a mantle from Glascol Apparatus Co., Terre Haute, IN. Power to the mantle was supplied by a Powerstat from The Superior Electric Co., Bristol, CT. The power setting used was "120".

Early experimentation was performed with a 360^{o}C thermometer (Ace Glass Co.) in place of the small glass stopper above the reaction flask. The thermometer was used to monitor the temperature of the mixture of acids as the digestion/distillation proceeded. However, the manner in which the acid vapors condensed on the stem of the thermometer at the standard-taper joint caused an intermittant dripping of the cooled distillate into the much hotter mixture of acids. The "bumping" which was produced by the violent interaction of the cool and hot liquids often caused the bulb of the thermometer to break, especially when the temperature of the mixture of acids was above 200^{o}C. Therefore, the glass stopper was used when each digestion procedure was applied to the dissolution of a sample.

2. Digestion procedures

The quantity of each sample which was taken for digestion and analysis was as follows: a 1.00-mL aliquot of the reconstituted urine; and ~1 g (weighed accurately) of the dried orchard leaves. For the determination of the blank for each digestion procedure, a 1.00-mL aliquot of TDW was taken as the sample.

a. Procedure A: HNO_3 A 10.0-mL aliquot of concentrated HNO_3 was added to the sample which had been delivered to the reaction flask. The flask was swirled to completely mix the contents, and then connected to the Bethge Apparatus. Within 5 min after application of power to the mantle, the digest was boiling with the evolution of the characteristic, reddish-brown fumes of NO_2. After the digest had boiled under total reflux for 30 min, the stopcock was closed until approximately 9.5 mL of distillate had been collected. The collected fraction was then discarded, and the mantle was removed from the reaction flask. After the digest had cooled for 10 min, 1.0 M H_2SO_4 was used to rinse the inner walls of the Bethge apparatus and the rinses were collected in the reaction flask. The contents of the reaction flask were then quantitatively transferred to a 100-mL volumetric flask. Final dilution to volume was made with 1.0 M H_2SO_4 only after the solution had cooled to room temperature.

b. Procedure B: HNO_3, H_2SO_4, V_2O_5 A 10.0-mL aliquot of concentrated HNO_3 was added to the sample in the reaction flask. The flask was swirled to completely mix the contents, and then a 5.0-mL aliquot of concentrated H_2SO_4 was added. The flask was swirled again; ~20 mg V_2O_5 was added to the contents of the flask; and the flask was swirled a third time. The mixture was boiled under total reflux for 30 min after which the stopcock was closed. When 5 mL of distillate had been collected (~5 min), the distillate was discarded, and the condition of total reflux was restored for 5 min. The stopcock was closed a second time until another 5 mL of distillate had been collected

(15-20 min). This fraction was also discarded, and the mantle was removed from the reaction flask. After the digest had cooled for 10 min, TDW was used to rinse the inner walls of the Bethge apparatus and the rinses were collected in the reaction flask. It was found necessary to reheat the digest to boiling after the addition of the first few milliliters of TDW to the digest; the explanation for this action will be given in Part C.2 below. After cooling a second time the apparatus was rinsed with TDW and the digest was quantitatively transferred to a 100-mL volumetric flask. Final dilution to volume was made with TDW when the solution had cooled to room temperature.

c. Procedure C: HNO_3, H_2SO_4 $HClO_4$ The indicated volumes of the concentrated acids were added sequentially in the order: 10.0 mL HNO_3, 1.0 mL $HClO_4$, 5.0 mL H_2SO_4. After addition of the $HClO_4$, the reaction flask was swirled to completely mix the contents. The H_2SO_4 was then added and the flask was swirled again to mix the contents. The mixture was boiled under total reflux for 30 min, and the stopcock was closed for collection of the distillate. The distillate was collected and discarded in volumes of 4 mL, each collection period being followed by 5 min under total reflux, until the copious, white fumes of H_2SO_4 were observed within the Bethge apparatus. The mantle was then removed, and the digest was allowed to cool for 10 min. A volume of 5 mL of TDW was used to rinse the inner walls of the apparatus, and was collected in the reaction flask. The digest was then reheated to boiling. After cooling again for 10 min, the inner walls of the apparatus were rinsed a

second time with TDW and the digest was quantitatively transferred to a 100-mL volumetric flask. As before, final dilution to volume with TDW occurred only after the solution had cooled to room temperature.

3. Flow system and instrumentation

The flow system (see Figure IV-1) and operational procedure were as described in Section IV.B.1. The FTD detector was as described in Section III.B.1.b; the radius of the Au disk was 1.72 mm. Potential control and current measurement were made with the PAR 174A Polarographic Analyzer which was modified as described in Section III.B.2. The deposition potential was 0.45 V vs. SCE. The optimum values of T_c and Ø were used (see Table III-5); ΔE was either 50 or 100 mV; and T_{dep} was never longer than 5.0 min. The data were taken on the Model Omnigraphic 2000 X-Y recorder.

4. Interference study

Experiments were performed to determine whether or not the ions Ag(I), As(III), Sb(III), Se(IV), Te(IV) or Cl^- would interfere with the determination of Hg(II) by DPASV, following UPD at 0.45 V on a Au flow-through electrode. To test the interference of each ion, the stripping peak obtained for a 2-min deposition from a solution (1.0 M H_2SO_4) containing 1.0×10^{-7} M Hg(II) was compared to the peak obtained under identical conditions for a solution containing the same concentration of Hg(II) and one of the following: 1.0×10^{-5} M As(III), Sb(III), Se(IV), or Te(IV); 1.0×10^{-5} M, 1.0×10^{-3} M or 1.0×10^{-1} M Cl^-; 1.0×10^{-7} M or 1.0×10^{-6} M Ag(I).

5. Chemicals and solutions

The preparation of the supporting electrolyte, and of the standard solutions of Hg(II), was as described in Section II.B.5. Stock solutions containing various ions (1.0×10^{-3} M) were prepared as listed in Table V-2. The V_2O_5 used in Digestion Procedure B, was from Matheson, Coleman and Bell, Norwood, OH. All acids were Analytical Reagent Grade.

The NBS SRM 1571 (orchard leaves) was dated April 10, 1979, and was dried and stored according to the instructions included on the certificate. The NBS SRM 2672 (urine) was not dated, but was not reconstituted until the samples were analyzed during May, 1980. Following the instructions included on the certificate, the urine was reconstituted by addition of a 50.0-mL aliquot of TDW to the contents of the vial. The reconstituted urine was then refrigerated at ~4°C between analyses.

The diluted digest, following dissolution of the sample, was treated in the following manner: Four 10.0-mL aliquots of the diluted digest were drawn off into 10.0-mL volumetric flasks by filling each flask to the mark. This was done because a residue of silica remained after dissolution of the orchard leaves, and the transfer of particulate matter to the flow system was not considered desirable. Standard additions of 20, 50 and 100 μL of a solution containing 5.15×10^{-6} M Hg(II) in 1.0 M H_2SO_4 were made to three of the aliquots prior to the determination. The data were evaluated by preparing a standard

Table V-2. Ions investigated as possible interferences

Ion	Compound tested	Comments
Ag(I)	$AgNO_3$	1,6
As(III)	As_2O_3	2,7
Sb(III)	Sb	3,8
Se(IV)	Se	4,9
Te(IV)	Te	5,9
Cl^-	NaCl	2,6

Comments:
(1) Fisher Scientific
(2) Baker Analyzed
(3) Matheson, Coleman, and Bell
(4) Abbott Laboratories
(5) Johnson Matthey Chemicals, Ltd.
(6) Dissolved in 2.0 M HNO_3
(7) Dissolved in a minimum of 8 M NaOH and acidified to 2 M HNO_3
(8) Dissolved in 15 mL 8 M NaOH, acidified with 150 mL concentrated HCl, and diluted to 250 mL with 2.0 M HNO_3
(9) Dissolved in hot, concentrated HNO_3 and diluted to 2.0 M HNO_3

additions plot of ΔQ_{strip} vs. the concentration of Hg(II) (ng mL^{-1}) in each aliquot after the standard addition accounting for dilution.

The standard additions were made using ACCU-Fill 90 Micropets (20 and 100 μL), or Yankee Disposable Micropets (50 μL) from the Clay Adams Division of Becton, Dickinson and Co., Parsippany, NJ. These micropipettes have an accuracy stated to be ± 0.25% of the indicated volume, which was considered to be well within the limits of precision for the experimental method, e.g., recall Table IV-3.

C. Results and Discussion

1. Investigation of interferences

The observations of Allen (34) pertaining to interferences to the determination of Hg(II) by SVWC at a Au-film RRDE, led to the investigation of Ag(I), As(III), Sb(III), Se(IV), Te(IV) and Cl^- as possible interferences to the method proposed in this research. No interference was observed for a 100-fold excess of As(III), Sb(III), Se(IV) or Te(IV). As(III) and Se(IV) were not anticipated to interfere. In 1975, Andrews and Johnson (157) demonstrated that Se(IV) was not deposited on a Au electrode at potentials more positive than 0.40 V vs. SCE; and in 1979, J. A. Lown (196) observed that As(III) was neither oxidized nor reduced on a Au electrode at potentials between approximately 0.7 and 0.2 V. Furthermore, Lown found that when As metal was deposited, a process which occurs for potentials less than 0.0 V, the deposit was completely stripped from the Au electrode at potentials more positive than 0.35 V.

The UPD of Hg(II) on the Au flow-through electrode was severely inhibited when the concentration of Cl^- was 0.10 M. The interference may have been due to the formation of a slightly dissociated, ionic complex of Hg(II) in the presence of the 10^6-fold excess of Cl^-, or to the preferential adsorption of Cl^- on the surface of the Au electrode. However, for the latter case, an anodic peak would be expected during the stripping scan as the potential of the Au electrode became more positive than that required to oxidize Au in the presence of Cl^-, i.e., ~0.75 V vs. SCE. No such peak was observed. Hence it was concluded that the interference observed for $C^b_{Cl^-}$ = 0.10 M is due to the formation of a slightly dissociated, ionic complex of Hg(II) with Cl^-. No interference was observed for $C^b_{Cl^-}$ = 1.0×10^{-3} M or 1.0×10^{-5} M.

The UPD of Ag(I) on Au has been reported by many workers; refer to Table II-1. Hence, Ag(I) was expected to present an interference to the quantitative determination of Hg(II). The observed effect of Ag(I) on the peak obtained for the stripping of Hg(UPD) is shown in Figure V-2. Peak A represents the response to 1.0×10^{-7} M Ag(I) in the absence of Hg(II), while Peak B represents the response for 1.0×10^{-7} M Hg(II) alone. When Hg(II) and Ag(I) are present in equal concentrations, Peak C is obtained. Correction of the area under Peak C for the area under Peak A yields a value which is virtually identical to the area under Peak B for Hg(II) alone. However, without prior knowledge of the shape of Peak A, accurate correction of Peak C would be most difficult if not impossible. A 10-fold excess of Ag(I) results

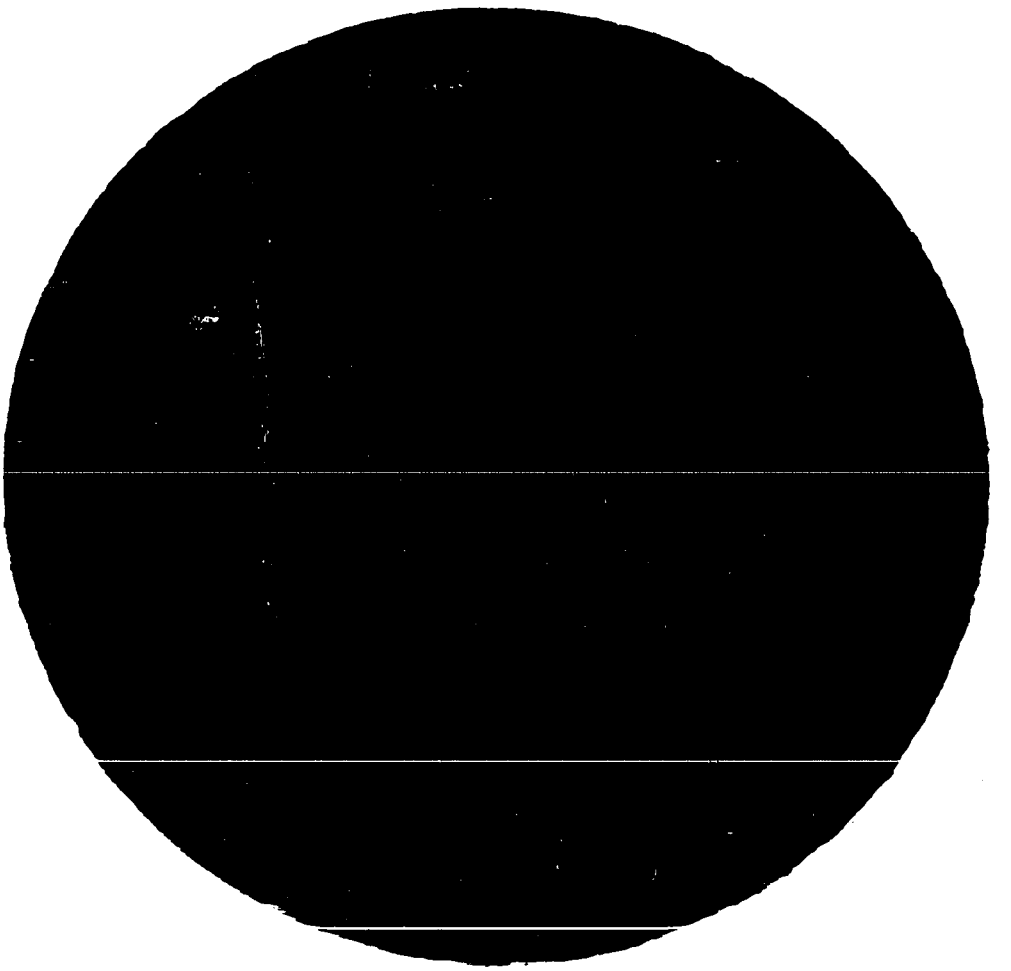

Figure V-2. Interference of Ag(I) in 1.0 M H_2SO_4

Deposition, FTD detector:

$V_{f,dep}$ - 1.16 mL min^{-1}

T_{dep} - 2.0 min

E_{dep} - 0.45 V vs. SCE

d - 0.07 mm

r_D - 1.72 mm

Stripping:

$V_{f,strip}$ - 0 mL min^{-1}

ΔE - 50 mV

$\emptyset$ - 20 mV s^{-1}

T_c - 0.114 s

A - 1.0×10^{-7} M Ag(I)

B - 1.0×10^{-7} M Hg(II)

C - 1.0×10^{-7} M Hg(II) + 1.0×10^{-7} M Ag(I)

D - 1.0×10^{-7} M Hg(II) + 1.0×10^{-6} M Ag(I)

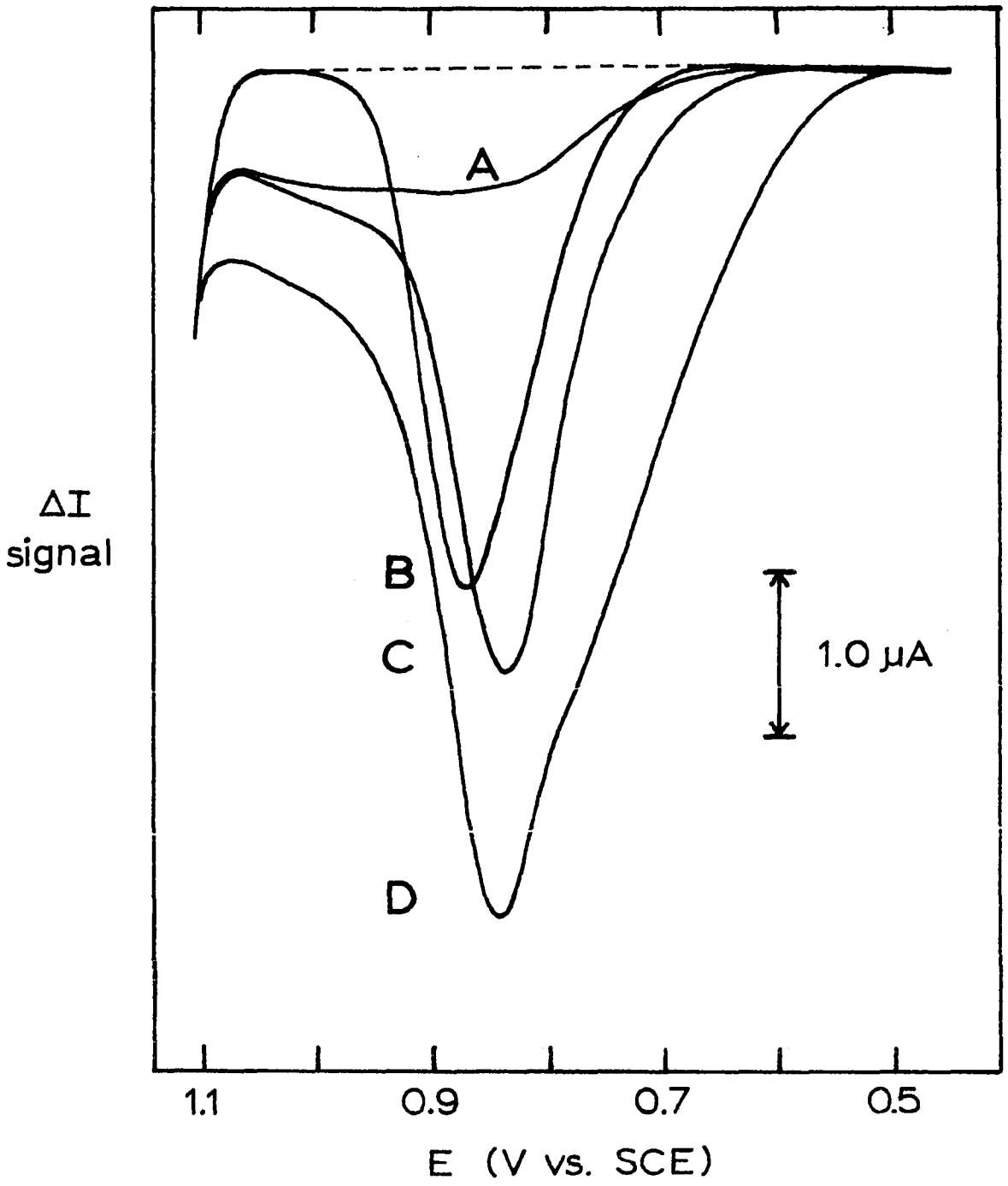
ΔI
signal
A
B
C
D
1.0 μA
1.1
0.9
0.7
0.5
E (V vs. SCE)

in a stripping peak in which the signal for Hg(UPD) is barely discernible over the broad peak (D) for the Ag.

Other cations such as Fe(III), Ce(IV) and Cr(VI) were not tested as they are simply reduced to lower oxidation stales, but not deposited at the Au electrode at 0.45 V vs. SCE. Allen (34) had demonstrated that Fe(III) did not interfere with the determination of Hg(II) by SVWC. Pt(IV) was not tested as it is known to be very easily deposited on Au, but very difficult to remove once deposited. Platinum is not expected to be present in the majority of samples for which a determination of Hg may be desired. Other anions such as Br^-, I^-, S^{2-} were not investigated, but might be expected to interfere in a manner similar to Cl^-.

It was concluded that the use of UPD on a Au electrode for the selective separation and collection of Hg(II), followed by DPASV, was practical for the quantitative determination of Hg(II) in acidic media. The only major interference found was Ag(I) when present at concentrations equal to, or greater than the concentration of Hg(II). The certificate for NBS SRM 1571 (orchard leaves) did not list Ag as a constituent of the sample, and it was anticipated that Ag would be absent in NBS SRM 2672 (freeze-dried urine) as well.

2. Digestion procedures and sample analyses

The results of the analysis of the Standard Reference Materials are given in Table V-3, which appears near the conclusion of this section. The determinations were made following dissolution of the sample

according to the procedure indicated, and the conditions of T_{dep} and ΔE were as noted in Table V-3.

The low result for the determination of Hg in the urine, following dissolution by Procedure A, is consistent with the negative error obtained by Allen (34) after dissolution of samples in HNO_3 alone. It was thought that HNO_3 alone may not have completed the oxidation of the sample; hence, complete conversion of all forms of mercury to Hg(II) may not have been accomplished.

This hypothesis was subsequently verified when a sample of orchard leaves was oxidized in a mixture of 10.0 mL HNO_3 and 5.0 mL H_2SO_4. After the initial, 30-min period of boiling under total reflux, a clear digest was obtained. However, after approximately 9 mL of distillate had been collected, the digest began to foam and eventually turned black; and smoky, brown fumes filled the Bethge apparatus. This observation is typical of the charring of residual organic species which can occur in hot, concentrated H_2SO_4. Hence, it was concluded that HNO_3 alone was not sufficient for the complete oxidation of samples for the determination of Hg(II) by DPASV from a Au electrode.

The blank for the modification of the Knechtel and Fraser procedure (192), i.e., Procedure B, was studied prior to the dissolution of samples in the mixture of HNO_3, H_2SO_4 and V_2O_5. During the initial, 30-min period of boiling under total reflux, some fumes of NO_2 were observable within the apparatus. Later, as the distillate was collected it was observed that the first 7 mL were very yellow in color, presumably saturated with NO_2. The next 2 mL were relatively colorless

and did not mix with the yellow fraction within the period of time allowed for collection. The final volume of collected distillate was again yellow in color, but did not mix with the colorless layer below. Throughout the digestion period, the digest remained transparent, but the color of the digest went from light yellow to a dark orange due to the presence of V(V). The latter color is reminiscent of $Cr_2O_7^{2-}$ in H_2SO_4. After discarding the collected fractions, the initial addition of TDW to the cooled digest caused the color to change to a light green. After diluting to volume, the blank was determined by the method of standard additions outlined above in Part B.5. Representative data are shown in Figure V-3.

The species giving rise to Peak A in Figure V-3 was concluded not to be Hg(UPD) due to the potential of ΔI_p and the asymmetry of the peak shape. Repetitive determinations of the blank revealed that the degree of interference was not reproducible. Much time was spent in attempts to identify the species which was interfering. Finally, it was discovered that the interference was virtually eliminated if the digest was reheated to boiling after the addition of the first few milliliters of TDW. Again the digest turned a light green when the water was added, but as the mixture boiled the color changed to a light yellow. If the stopcock was closed and a volume of distillate collected equal to the added volume of TDW, the color of the digest reverted to dark orange. When the digest had again cooled, further additions of TDW did not result in a change in color, but simply a fading of the original color as the final 20-fold dilution was made.

Figure V-3. Initial blank for mixture of HNO_3, H_2SO_4 and V_2O_5

Deposition, FTD Detector:

$V_{f,dep}$ - 1.16 mL min^{-1}

T_{dep} - 5.0 min

E_{dep} - 0.45 V vs. SCE

d - 0.07 mm

r_D - 1.72 mm

Stripping:

$V_{f,strip}$ - 0 mL min^{-1}

ΔE - 100 mV

$\emptyset$ - 20 mV s^{-1}

T_c - 0.114 s

Standard additions of 5.15×10^{-6} M Hg(II):

A - blank

B - blank + 20 µL standard addition

C - blank + 50 µL standard addition

D - blank + 100 µL standard addition

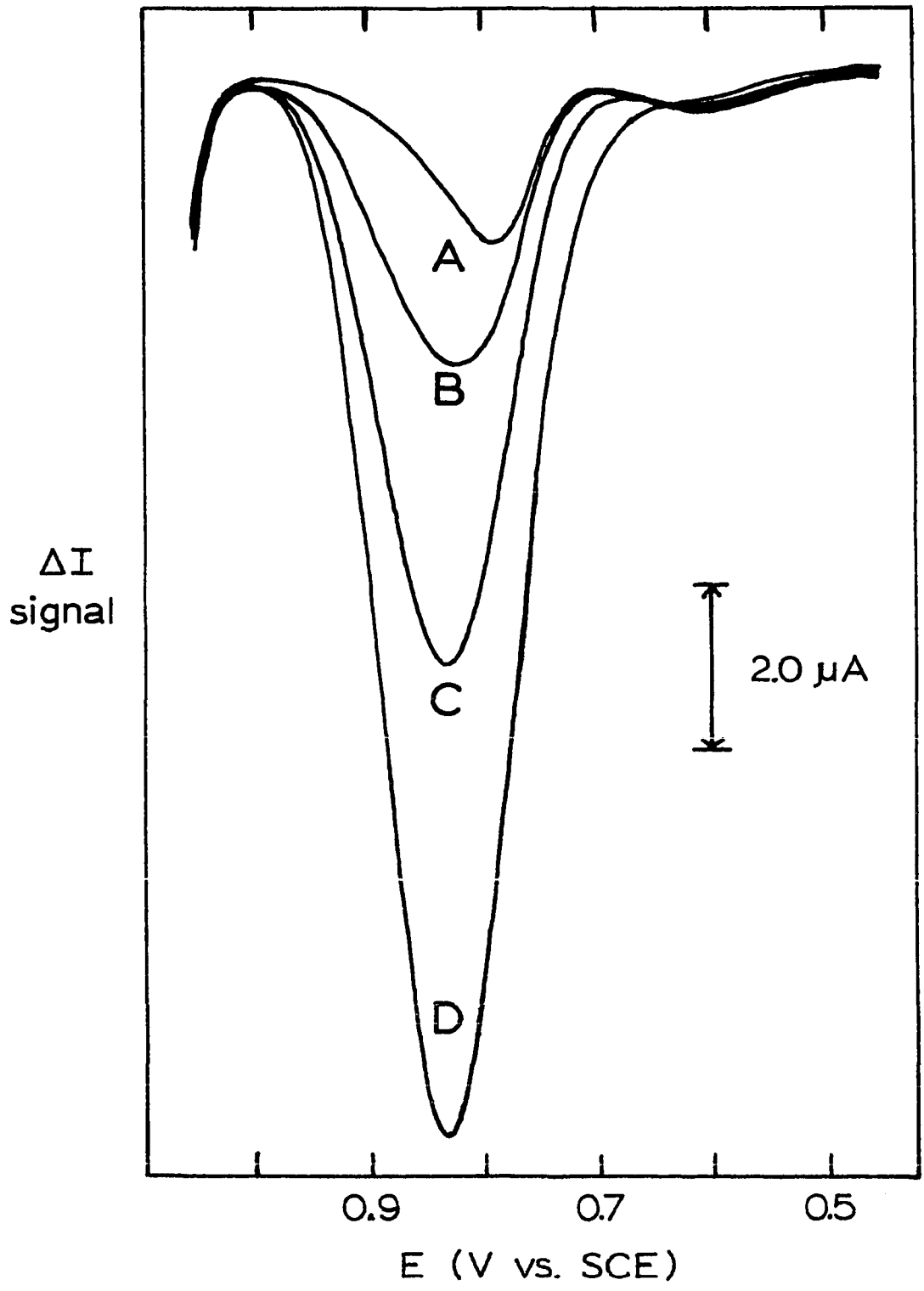
ΔI
signal
A
B
C
D
2.0 μA
0.9
0.7
0.5
E (V vs. SCE)

It was concluded that the initial interference, which had been observed, was due to a volatile species, probably NO_2, which was not volatilized from the final digest of concentrated H_2SO_4, but was removed by boiling a somewhat more dilute solution of the final digest.

Two samples of urine were digested using Procedure B. Representative data are shown in Figure V-4, and the results are summarized in Table V-3. Note that the blank is insignificant with respect to the signal for the sample in Figure V-4, and that the peak shapes are those which are expected for the stripping of Hg(UPD) alone.

Again, the results were low, but the recovery of Hg by Procedure B was better by about a factor of two than that obtained by digestion with HNO_3 alone. Because a considerable period of time had passed since the urine had been reconstituted, it was thought likely that some mercury might have been lost from the reconstituted urine by an unknown mechanism. The certificate did not specify the length of time for which the urine could be considered stable.

Subsequent to the analysis of the urine, an attempt was made to oxidize a sample of the orchard leaves using Procedure B. The acids and V_2O_5 were added to the sample, and approximately 10 min were given for the oxidation to begin prior to the application of heat. After the initial, 30-min period of boiling under total reflux the stopcock was closed, and 5 mL of distillate was collected and then discarded. The color of the digest turned light green as the distillate was collected. This color remained unchanged after more than one hour of continued boiling. Finally the stopcock was closed and collection of

Figure V-4. Analysis of NBS SRM 2672 (freeze dried urine)

Deposition, FTD detector:

$V_{f,dep}$ - 1.16 mL min^{-1}

E_{dep} - 0.45 V vs. SCE

d - 0.07 mm

r_D - 1.72 mm

Stripping:

$V_{f,strip}$ - 0 mL min^{-1}

Ø - 20 mV s^{-1}

T_c - 0.114 s

Standard additions of 5.15×10^{-6} M Hg(II):

1) T_{dep} - 4.0 min

ΔE - 50 mV

2) T_{dep} - 2.0 min

ΔE - 100 mV

A - blank

B - sample

C - sample + 20 μL standard addition

D - sample + 50 μL standard addition

E - sample + 100 μL standard addition

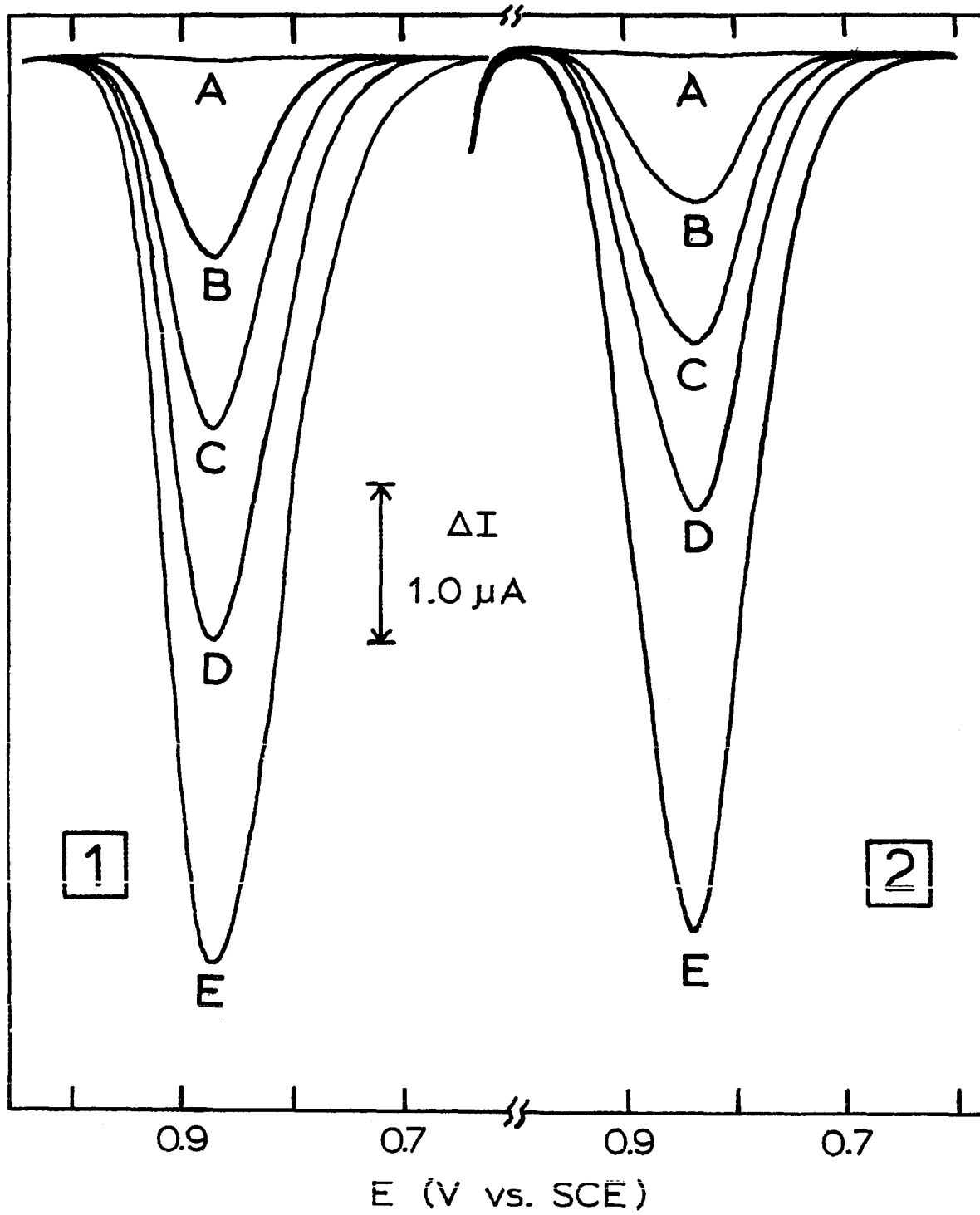
A
B
C
D
E
ΔI
1.0 μA
1
2
0.9
0.7
0.9
0.7
E (V vs. SCE)

distillate begun again. Before an additional 5 mL of distillate could be collected, the digest began to foam and char as in the case of the dissolution in a mixture of HNO_3 and H_2SO_4 without the addition of V_2O_5.

It was concluded that a mixture of HNO_3, H_2SO_4 and V_2O_5 was not satisfactory for the complete destruction of organic matter which is necessary for the quantitative recovery of Hg(II) as determined by DPASV at a Au flow-through electrode. This conclusion might also be used to explain the negative error obtained for the analysis of the urine. Nonetheless, because the stability of the reconstituted urine was questionable, the decision was made to use the sample of orchard leaves in all subsequent evaluations of digestion procedures.

The third mixture of concentrated acids, used in an attempt to oxidize the sample of orchard leaves, consisted of HNO_3, H_2SO_4 and $HClO_4$ (Procedure C). No appreciable foaming of the sample was observed if the contents of the reaction flask were well-mixed before the addition of H_2SO_4. The distillate was collected and discarded until the fumes of H_2SO_4 were observed within the Bethge apparatus. No charring of the sample occurred. A small quantity of white, undissolved silica was the only residue. A portion of this residual silica was transferred inadvertently to the 100-mL volumetric flask with each rinse of the reaction vessel.

A deposition time of 4.0 min and a modulation amplitude of 50 mV were used for two determinations of Hg(II) in each of the four aliquots taken for analysis. The standard additions plot of the data is shown in Figure V-5, and the results are summarized in Table V-3.

Figure V-5. Standard additions plot for the determination of Hg in the orchard leaves after digestion with a mixture of HNO_3, H_2SO_4 and $HClO_4$

Determination I

Aliquot	Hg added (ng mL^{-1} after addition)	ΔQ_{strip} (μC)
1	0	3.49
2	2.06	9.60
3	5.17	19.3
4	10.3	32.9

Determination II

Aliquot	Hg added (ng mL^{-1} after addition)	ΔQ_{strip} (μC)
1	0	3.36
2	2.06	9.65
3	5.17	20.2
4	10.3	33.7

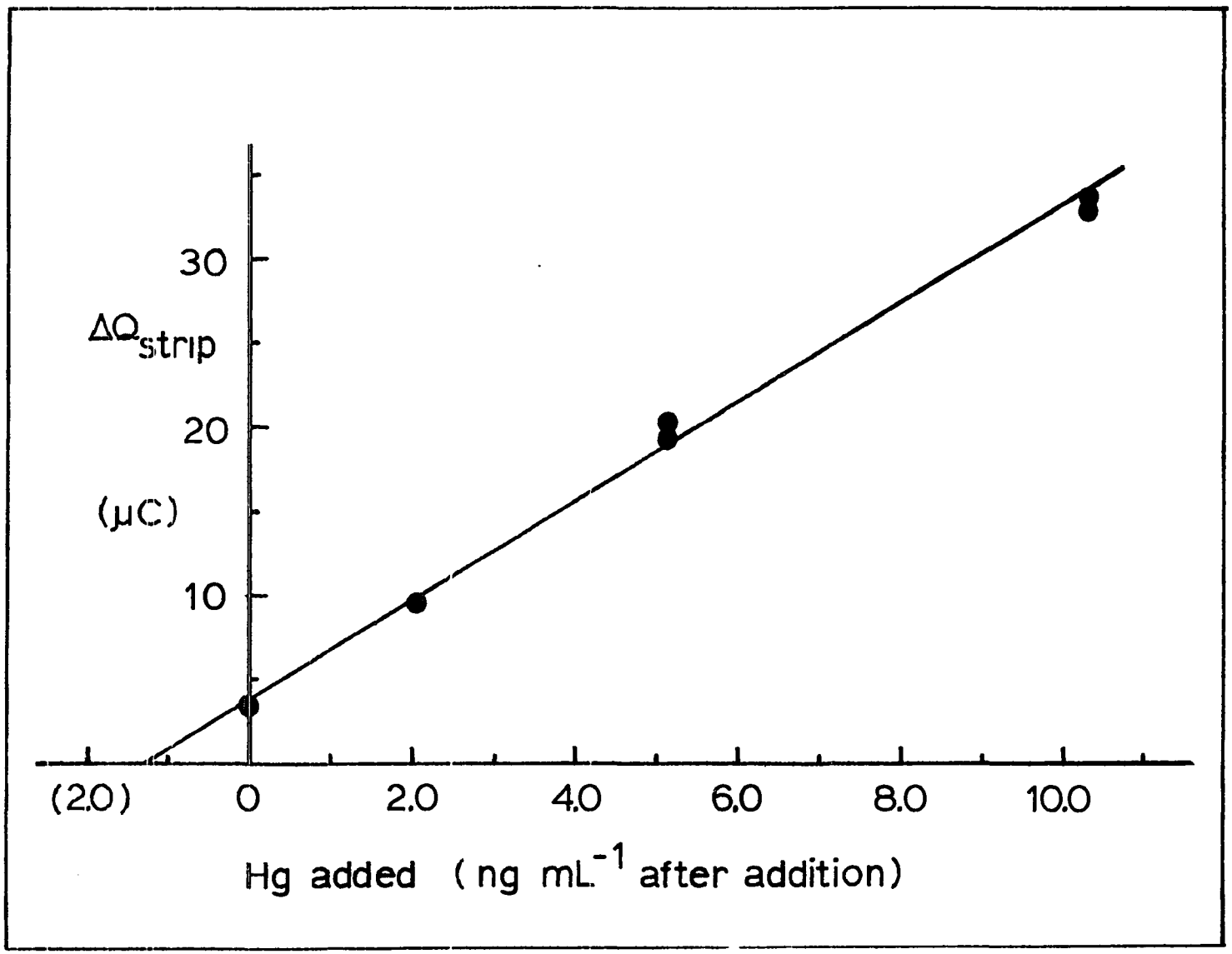
30
ΔQ_{strip}
20
(μC)
10
(2.0)
0
2.0
4.0
6.0
8.0
10.0
Hg added (ng mL.$^{-1}$ after addition)

Table V-3. Results for the analysis of the NBS Standard Reference Materials

NBS SRM	Quantity taken	Digestion procedure	T_{dep} ΔE	Hg expected	Hg found	Error
2672	1.00 mL	Procedure A: HNO_3	4.0 min 100 mV	0.294 mg L^{-1}	0.097 mg L^{-1}	-67%
2672	1.00 mL	Procedure B: HNO_3, H_2SO_4, V_2O_5	4.0 min 50 mV	0.294 mg L^{-1}	0.202 mg L^{-1}	-31%
			2.0 min 100 mV	0.294 mg L^{-1}	0.190 mg L^{-1}	-35%
2672	1.00 mL	Procedure B: HNO_3, H_2SO_4, V_2O_5	4.0 min 50 mV	0.294 mg L^{-1}	0.229 mg L^{-1}	-22%
			2.0 min 100 mV	0.294 mg L^{-1}	0.188 mg L^{-1}	-36%
1571	1.0450 g	Procedure C: HNO_3, H_2SO_4, $HClO_4$	4.0 min 50 mV	0.155 g g^{-1}	0.130 g g^{-1}	-16%

Unfortunately, the result calculated for Hg was again significantly below the certified value. However, Procedure C resulted in the best recovery of Hg, as Hg(II), of the three procedures attempted. In this instance, it was concluded that the error stemmed from the formation of the volatile, chloromercurial compound, as proposed by Gorsuch (194), during the final stages of the dissolution as the remaining $HClO_4$ was distilled from the H_2SO_4.

The determinations of Hg in the orchard leaves were further complicated by the presence of finely divided and suspended particles of silica which were carried over from the diluted digest to each aliquot. These particles tended to clog the needle valve of the pulse dampener; and precise control of flow rate during the deposition was virtually impossible without constant attention and minor adjustments of the needle valve.

D. Summary and Conclusions

Interferences to the determination of Hg(II) in acidic media were investigated. The species studied included Ag(I), As(III), Sb(III), Se(IV), Te(IV) and Cl^-. Of these species only Ag(I) was observed to interfere at concentrations equal to, or up to 100X greater than the concentration of Hg(II), which was 1.0×10^{-7} M in 1.0 M H_2SO_4. The interference presented by Cl^- at a concentration of 0.10 M was concluded to be due to the formation of a slightly dissociated, ionic complex of Hg(II) with Cl^-.

Because Ag was not present in the NBS Standard Reference Materials which were to be analyzed, no interferences from this metal were expected. Another interference resulted from a volatile species, presumably NO_2, which remained in the final digest of concentrated acid and produced an asymmetrical peak in the vicinity of the stripping peak for Hg(UPD). The interference was virtually eliminated by the addition of a small volume of water to the cooled digest, which was then reheated to boiling. Following this procedure, the blank signal for the mixture of acids used for sample dissolution was insignificant with respect to the signal obtained when the sample was digested.

Three different dissolution procedures were used in an attempt to analyze the Standard Reference Materials: 1) HNO_3 alone (Procedure A); 2) HNO_3 and H_2SO_4 plus a small amount of V_2O_5 as catalyst (Procedure B); and 3) HNO_3, H_2SO_4 plus a small volume of $HClO_4$ (Procedure C). The first two procedures yielded low results for the determination of Hg in NBS SRM 2672 (freeze-dried urine). It was concluded that neither Procedure A nor Procedure B resulted in complete oxidation of the organic matter in the sample. The low results were attributed to the incomplete conversion of all forms of Hg to Hg(II), i.e., some mercury remained complexed with residual organic species.

Procedure C resulted in the complete oxidation of a sample of NBS SRM 1571 (orchard leaves) except for a white residue of silica which remained. However, results were also low, and it was postulated that some Hg had been lost by volatilization of a chloromercurial

compound which formed during the final stages of the dissolution as the $HClO_4$ was distilled from the H_2SO_4. A major drawback to the determination of Hg in the orchard leaves was the presence of finely divided particles of silica which remained suspended in solution. These particles tended to clog the pulse dampener of the flow system during each determination.

The data obtained for the analysis of the NBS Standard Reference Materials, although giving low results, did not indicate interference from any other constituents in the sample. Hence, the selectivity of the proposed method, utilizing the UPD of Hg(II) on a Au electrode followed by DPASV, is concluded to be verified. Despite the difficulties encountered during the analysis of the NBS samples, it is thought that the sensitivity, selectivity, short deposition periods, and precision of the proposed method make the use of the UPD of Hg(II) on a Au electrode, followed by DPASV, significant for the determination of Hg(II). For example, the method could be applied with relative ease to the determination of Hg in reagent grade acids and certain other inorganic chemicals. However, before the method can be used routinely for the analysis of physiological and biological samples, the problem of complete oxidation of all organic matter in the sample without loss of Hg must be solved. Furthermore, for samples with a high content of silica, special handling-procedures will be required to minimize the quantity of suspended particles which is transferred to the aliquots from which the determination is made.

VI. SUMMARY

The electrochemical investigations which have been made and the conclusions which have been drawn with respect to the development of a flow-injection, electroanalytical method for the quantitative determination of Hg(II) in acidic media have been described. The method utilizes the deposition of Hg(II) at underpotential on a Au electrode followed by Differential Pulse Anodic Stripping Voltammetry (DPASV). The linear dynamic range of calibration for the method was shown to be over three orders of magnitude in concentration of Hg(II) with a detection limit in 1.0 $\underline{M}$ H_2SO_4 of approximately 5×10^{-10} $\underline{M}$ Hg(II) using a deposition time of 5.0 min. Reproducibility at a concentration of 1.0×10^{-8} $\underline{M}$ Hg(II) was less than 2% relative using a deposition time of 3.0 min.

The underpotential deposition (UPD) of Hg(II) on Au was investigated using rotating electrodes and flow-through detectors. It was found that the UPD process occurs, for potentials more negative than 0.9 V vs. SCE, at a rate which is limited by the rate of mass transport of Hg(II) to the surface of the electrode only when the surface coverage of the deposit is very small, i.e., much less than the equivalent of a monolayer. Furthermore, it was shown that the reduction process occurs with n_{app} = 1.60 equivalents $mole^{-1}$ at all potentials within the UPD region, i.e., $0.9 \geq E \geq 0.4$ V.

The oxidation of Hg deposited at underpotential was demonstrated to produce up to four unresolved stripping peaks. However, for very

small quantities of deposited Hg a single, symmetrical stripping peak was obtained at ~0.9 V.

Maintaining the conditions of UPD such that a single, symmetrical stripping peak was obtained, the experimental variables of DPASV, using the PAR 174A Polarographic Analyzer, were studied and optimized within the scheme of Flow-Injection Analysis. Studied were the effects of flow rate during the stripping scan; modulation amplitude; rate of potential scan; cycle period of pulses; flow rate during deposition when the injected, sample volume was constant; and the time of deposition. Further, a comparison was made of the results obtained by applying the DPASV potential waveform in a "reverse" fashion to the results obtained by DPASV applied in the conventional manner.

Ag(I), As(III), Sb(III), Se(IV), Te(IV) and Cl^- were studied as possible interferences to the proposed method. Of these species only Ag(I) was found to cause a significant interference.

The method was shown to be highly selective for Hg(II) with the exception of Ag(I). However, Ag was not present in the samples which were analyzed, and an ion exchange separation was concluded to be unnecessary prior to the determination of Hg as Hg(II) in the dissolved sample.

Three methods of sample dissolution were used in an attempt to analyze two NBS Standard Reference Materials. All three dissolution procedures led to low results due to one or both of the following reasons: incomplete destruction of all organic matter of the sample

matrix; or/and loss of Hg due to volatilization. Because a satisfactory method of sample dissolution was not found, accurate determination of Hg in neither of the NBS Standard Reference Materials (NBS SRM 1571 orchard leaves, and NBS SRM 2672 freeze-dried urine) was possible.

VII. SUGGESTIONS FOR FUTURE WORK

The review by Kissinger (36) has, for the past four years, been a primary source of reference on the subject of flow-through electrochemical detectors. Just recently another comprehensive, and excellent, review was published by Rucki (197). However, to the knowledge of this author the fundamental response of detectors of the design of the FTD detector, described in this work, has not been fully investigated. Certainly, the solution to the equation for mass transport to the indicating electrode will not be easily solved. However, certain parameters should lend themselves to evaluation. These include the effects on I_{lim} of the diameter of the nozzle; the distance from the indicating electrode to the orifice of the nozzle; the radius of the indicating electrode; and flow rate.

Coulometric detection should be applied to the evaluation of n_{app} for other metals which are deposited at underpotential on Au or Pt.

A unique feature of the FTD detector, which deserves attention in the future, is that the indicating electrode lends itself to applications other than those requiring solution flow. For example, there is a rapidly expanding area of research in the field of EC fuel cells based upon reactions catalyzed by submonolayer deposits of metals (adatoms) on metallic substrates. Using the miniature disk electrode as an RDE, fundamental EC studies of the deposition of the catalysts could be performed. Following this the same electrode could be inserted in an instrument for characterization of the submonolayer

deposit by various techniques of surface analysis. Finally, the same electrode could be used in the FTD detector for the rapid evaluation of reactions which are catalyzed by the particular adatom on the given metallic substrate.

Finally, it is obvious that not all possible methods of sample dissolution were attempted in this research. The prospect of the proposed detection system as a highly specific method for Hg should continue to spur the search for a dissolution procedure which will result in complete destruction of all organic matter with full recovery of Hg as Hg(II).

VIII. BIBLIOGRAPHY

1. Goldwater, L. J. "Mercury: A History of Quicksilver"; York Press: Baltimore, MD, 1972.

2. Jones, J. R. "Mercury Pollution Control"; Noyes Data Corporation: Park Ridge, NJ, 1971.

3. Trakhtenberg, I. M. "Chronic Effects of Mercury on Organisms" (Engl. Transl.); DHEW Publication No. (NIH) 74-473, 1974; Heath Publishers: Kiev, USSR, 1969.

4. "The Chemistry of Mercury"; McAuliffe, C. A., Ed.; The Macmillan Press, Ltd.: London, 1977.

5. "An Assessment of Mercury in the Environment"; Panel on Mercury of the Coordinating Committee for Scientific and Technical Assessments of Environmental Pollutants, Environmental Studies Board, Commission on Natural Resources, National Research Council; National Academy of Sciences: Washington, D.C., 1978.

6. "Mercury and the Environment: Studies of Mercury Use, Emission, Biological Impact and Control"; Organisation (sic) for Economic Co-operation and Development (OECD): Paris, 1974.

7. D'Itri, F. M. "The Environmental Mercury Problem"; CRC Press: Cleveland, OH, 1972.

8. Montague, K.; Montague, P. "Mercury"; Sierra Club: New York, 1971.

9. "Analytical Aspects of Mercury and Other heavy Metals in the Environment"; Frei, R. W.; Hutzinger, O., Eds.; Gordon and Breach Science Publishers: London, 1975.

10. "Mercury in the Western Environment"; Proceedings of a Workshop, Portland, OR, Feb. 1971; Buhler, D. R., Ed.; Continuing Education Publications: Corvallis, OR, 1973.

11. "Mercury, Mercurials and Mercaptans"; Miller, M. W.; Clarkson, T. W., Eds.; Charles C Thomas, Publisher: Springfield, IL, 1973.

12. Farrar, W. V.; Williams, A. R. In "The Chemistry of Mercury"; McAuliffe, C. A., Ed.; The Macmillan Press, Ltd.: London, 1977, Part 1.

13. Browning, E. "Toxicity of Industrial Metals", 2nd ed.; Butterworths: London, 1969, Chapter 24.

14. Saha, J. G.; McKinlay, K. S. In "Analytical Aspects of Mercury and Other Heavy Metals in the Environment"; Frei, R. W.; Hutzinger, O., Eds.; Gordon and Breach Science Publishers: London, 1975, Chapter 1.

15. Ruska, J. Z. angew. Chem. 1926, 39, 790.

16. Cheinisse, L. Presse med. 1922, 30, 356; Chem. Abstr. 1923, 17, 434.

17. Stock, A. Z. angew. Chem. 1926, 39, 461.

18. Stock, A. Z. angew. Chem. 1926, 39, 984.

19. Stock, A.; Cucuel, F. Angew. Chem. 1934, 47, 641.

20. Stock, A.; Cucuel, F. Angew. Chem. 1934, 47, 801.

21. Stock, A. Z. physik. Chem. 1941, A189, 63.

22. Ruzicka, J.; Hansen, E. H. Anal. Chim. Acta 1975, 78, 17.

23. Stewart, K. K.; Beecher, G. R.; Hare, P. E. Anal. Biochem. 1976, 70, 167.

24. Anal. Chim. Acta 1980, Vol. 114.

25. Skeggs, L. T. Am. J. Clin. Pathol. 1957, 28, 311.

26. Snyder, L. R.; Levine, J.; Stoy, R.; Conetta, A. Anal. Chem. 1976, 48, 942A.

27. Ruzicka, J.; Hansen, E. H. Anal. Chim. Acta 1978, 99, 37.

28. Ruzicka, J.; Hansen, E. H. Anal. Chim. Acta 1980, 114, 19.

29. Reijn, J. M.; van der Linden, W. E.; Poppe, H. Anal. Chim. Acta 1980, 114, 105.

30. Mindegaard, J. Anal. Chim. Acta 1979, 104, 185.

31. Pungor, E.; Feher, Z.; Nagy, G.; Toth, K.; Horvai, G.; Gratzl, M. Anal. Chim. Acta 1979, 109, 1.

32. Snyder, L. R. Anal. Chim. Acta 1980, 114, 3.

33. Betteridge, D. Anal. Chem. 1978, 50, 832A.

34. Allen, R. E. Ph.D. Dissertation, Iowa State University, Ames, IA, 1974.

35. Uthe, J. F.; Armstrong, F. A. J. In "Analytical Aspects of Mercury and Other Heavy Metals in the Environment"; Frei, R. W.; Hutzinger, O., Eds.; Gordon and Breach Science Publishers; London, 1975, Chapter 2.

36. Kissinger, P. T. Anal. Chem. 1977, 49, 447A.

37. Allen, P. L.; Hickling, A. Anal. Chim. Acta 1954, 11, 467.

38. Astley, D. J.; Harrison, J. A.; Thirsk, H. R. J. Electroanal. Chem. 1968, 19, 325.

39. Beckers, M. Bull. classe sci., Acad. roy. Belg. 1958, 44, 661; Chem. Abstr. 1959, 53, 9760.

40. Bewick, A.; Thomas, B. J. Electroanal. Chem. Interfacial Electrochem. 1977, 85, 329.

41. Bixler, J. W.; Bruckenstein, S. Anal. Chem. 1965, 37, 791.

42. Bowles, B. J. Electrochim. Acta 1965, 10, 717.

43. Bowles, B. J. Electrochim. Acta 1965, 10, 731.

44. Bowles, B. J. Electrochim. Acta 1970, 15, 589.

45. Bowles, B. J. Electrochim. Acta 1970, 15, 737.

46. Bowles, B. J. Nature 1966, 212, 1456.

47. Bowles, B. J. Cranshaw, T. E. Phys. Lett. 1965, 17, 258.

48. Brainia, Kh. Z.; Zakharchuk, N. G.; Synkova. D. P.; Yudelevich, I. G. J. Electroanal. Chim. Interfacial Electrochem. 1972, 35, 165.

49. Breiter, M. W. J. Electrochem. Soc. 1967, 114, 1125.

50. Breiter, M. W. Trans. Faraday Soc. 1969, 65, 2197.

51. Brubaker, R. L. Ph.D. Dissertation, Princeton University, Princeton, NJ, 1966.

52. Bruckenstein, S. Gov. Rep. Announce. Index (U.S.) 1979, 79, 96; Chem. Abstr. 1979, 91, 99140j.

53. Bruckenstein, S.; Hassan, M. Z. Anal. Chem. 1971, 43, 928.

54. Byrne, J. T.; Rogers, L. B. J. Electrochem. Soc. 1951, 98, 457.

55. Byrne, J. T.; Rogers, L. B.; Griess, J. C., Jr. J. Electrochem. Soc. 1951, 98, 452.

56. Cadle, S. H. Ph.D. Dissertation, State University of New York at Buffalo, Buffalo, NY, 1972.

57. Cadle, S. H.; Bruckenstein, S. Anal. Chem. 1971, 43, 932.

58. Cadle, S. H.; Bruckenstein, S. Anal. Chem. 1971, 43, 1858.

59. Cadle, S. H.; Bruckenstein, S. Anal. Chem. 1972, 44, 1993.

60. Coche, A. Compt. rend. 1947, 225, 936.

61. Coche, A. J. Chim. Phys. 1951, 48, 135.

62. Cox, J. A. Ph.D. Dissertation, University of Illinois, Urbana, IL, 1967.

63. Dannon, J.; Haissinsky, M. J. Chim. Phys. 1950, 47, 953.

64. Dannon, J.; Haissinsky, M. J. Chim. Phys. 1952, 49, C123.

65. Degeiso, R. C.; Rogers, L. B. J. Electrochem. Soc. 1959, 106, 433.

66. Erdey-Gruz, T.; Wick, H. Z. Physik. Chem. 1932, A162, 63.

67. Gerischer, H.; Kolb, D. M.; Przasnyski, M. Surf. Sci. 1974, 43, 662.

68. Gilman, S. J. Electrochem. Soc. 1971, 118, 1953.

69. Griess, J. C.,; Byrne, J. T.; Rogers, L. B. J. Electrochem. Soc. 1951, 98, 447.

70. Haenny, C.; Mivelaz, P. Helv. Chim. Acta 1948, 31, 633.

71. Haissinsky, M. J. Chim. Phys. 1933, 30, 27.

72. Haissinsky, M. J. Chim. Phys. 1935, 32, 116.

73. Haissinsky, M.; Coche, A. J. Chem. Soc. 1949, S397.

74. Hassan, M. Z. Ph.D. Dissertation, University of Minnesota, Minneapolis, MN, 1973.

75. Hassan, M. Z.; Untereker, D. F.; Bruckenstein, S. J. Electroanal. Chem. Interfacial Electrochem. 1973, 42, 161.

76. Heumann, Th.; Forch, K. Metall 1960, 14, 691.

77. Hevesy, G. Phil. Mag. 1912, 23(S.6), 628.

78. Hevesy, G.; Paneth, F. Monatsh. 1915, 36, 45.

79. Hiebert, A. G. Ph.D. Dissertation, University of Illinois, Urbana, IL, 1967.

80. James, S. D. Electrochim. Acta 1967, 12, 939.

81. Joliot, F. J. Chim. Phys. 1930, 27, 119.

82. Kolb, D. M.; Gerischer, H. Surf. Sci. 1975, 51, 323.

83. Kolb, D. M.; Przasnyski, M.; Gerischer, H. J. Electroanal. Chem. Interfacial Electrochem. 1974, 54, 25.

84. Lorenz, W. J.; Moumtzes, I.; Schmidt, E. J. Electroanal. Chem. 1971, 33, 121.

85. Mansurov, G. N.; Balashova, N. A. Elektrokhim. 1966, 2, 1358.

86. Mansurov. G. N.; Balashova, N. A.; Kazarinov, V. E. Electrokhim. 1968, 4, 641.

87. Marsh, F. L. Ph.D. Dissertation, University of Minnesota, Minneapolis, MN, 1965.

88. Mayer, C.; Juettner, K.; Lorenz, W. J. J. Appl. Electrochem. 1979, 9, 161.

89. McIntyre, J. D. E.; Kolb, D. M. Symp. Faraday Soc. 1970, No. 4, 99.

90. Motoo, S. J. Electroanal. Chem. Interfacial Electrochem. 1979, 100, 771.

91. Napp, D. T.; Bruckenstein, S. J. Amer. Chem. Soc. 1968, 90, 6303.

92. Nicholson, M. M. Anal. Chem. 1960, 32, 1058.

93. Nicholson, M. M. J. Amer. Chem. Soc. 1957, 79, 7.

94. Nicol, M. J.; Philip, H. I. J. Electroanal. Chem. Interfacial Electrochem. 1976, 70, 233.

95. Nisbet, A. R.; Bard, A. J. J. Electroanal. Chem. 1963, 6, 332.

96. Perone, S. P. Anal. Chem. 1963, 35, 2091.

97. Propst, R. C. J. Electroanal. Chem. 1968, 16, 319.

98. Riedhammer, T. M. Ph.D. Dissertation, State University of New York at Buffalo, Buffalo, NY, 1977.

99. Riedhammer, T. M.; Melnicki, L. S.; Bruckenstein, S. Z. Phys. Chem. (Wiesbaden) 1978, 111, 177.

100. Robbins, G. D.; Enke, C. G. J. Electroanal. Chem. 1969, 23, 343.

101. Rogers, L. B. Rec. Chem. Progr. 1955, 16, 197.

102. Rogers, L. B.; Krause, D. P.; Griess, J. C., Jr. J. Electrochem. Soc. 1949, 95, 33.

103. Rogers, L. B.; Stehney, A. F. J. Electrochem. Soc. 1949, 95, 25.

104. Sandoz, D. P.; Peekma, R. M.; Freund, H.; Morrison, C. F., Jr. J. Electroanal. Chem. 1970, 24, 165.

105. Schmidt, E.; Gygax, H. R. Helv. Chim. Acta 1965, 48, 1178.

106. Schmidt, E.; Gygax, H. R. Helv. Chim. Acta 1965, 48, 1584.

107. Schmidt, E.; Gygax, H. R. J. Electroanal. Chem. 1966, 12, 300.

108. Schmidt, E.; Gygax, H. R. J. Electroanal. Chem. 1967, 13, 378.

109. Schmidt, E.; Gygax, H. R. J. Electroanal. Chem. 1967, 14, 126.

110. Schmidt, E.; Lorenz, W. J. Ber. Bunsenges. Phys. Chem. 1971, 75, 71.

111. Schmidt, E.; Wuetrich, N. J. Electroanal. Chem. 1972, 34, 377.

112. Schultz, J. W. Ber. Bunsenges. Phys. Chem. 1970, 74, 705.

113. Sharp, W. Ph.D. Dissertation, University of Ottawa, Ottawa, Canada, 1976.

114. Sherwood, W. G. Ph.D. Dissertation, State University of New York at Buffalo, Buffalo, NY, 1978.

115. Sherwood, W. G.; Bruckenstein, S. J. Electrochem. Soc. 1978, 125, 1098.

116. Sherwood, W. G.; Untereker, D. F.; Bruckenstein, S. J. Electrochem. Soc. 1970, 117, 626.

117. Stucki, S. J. Electroanal. Chem. Interfacial Electrochem. 1977, 78, 31.

118. Takamura, T.; Takamura, K.; Nippe, W.; Yeager, E. J. Electrochem. Soc. 1970, 117, 626.

119. Tindall, G. W. Ph.D. Dissertation, University of Minnesota, Minneapolis, MN, 1969.

120. Tindall, G. W.; Bruckenstein, S. Anal. Chem. 1968, 40, 1051.

121. Tindall, G. W.; Bruckenstein, S. Anal. Chem. 1968, 40, 1637.

122. Tindall, G. W.; Bruckenstein, S. Electrochim. Acta 1971, 16, 245.

123. Untereker, D. F. Ph.D. Dissertation, State University of New York at Buffalo, Buffalo, NY, 1973.

124. Untereker, D. F.; Bruckenstein, S. Anal. Chem. 1972, 44, 1009.

125. Untereker, D. F.; Sherwood, W. G.; Bruckenstein, S. J. Electrochem. Soc. 1978, 125, 380.

126. Vassos, B. J.; Mark, H. B., Jr. J. Electroanal. Chem. 1967, 13, 1.

127. Vicente, V. A. Ph.D. Dissertation, State University of New York at Buffalo, Buffalo, NY, 1973.

128. Vicente, V. A.; Bruckenstein, S. Anal. Chem. 1972, 44, 297.

129. Vicente, V. A.; Bruckenstein, S. Anal. Chem. 1973, 45, 2036.

130. Vijh, A. K. Surf. Sci. 1974, 46, 282.

131. Vihj, A. K. Surf. Sci. 1975, 47, 709.

132. Wang, M. Ph.D. Dissertation, Michigan State University, East Lansing, MI, 1978.

133. Watanabe, W.; Motoo, S. J. Electroanal. Chem. 1975, 60, 259.

134. Watanabe, W.; Motoo, S. J. Electroanal. Chem. 1975, 60, 267.

135. Watanabe, W.; Motoo, S. J. Electroanal. Chem. 1975, 60, 275.

136. Watanabe, W.; Motoo, S. J. Electroanal. Chem. 1976, 69, 429.

137. Winterhager, H.; Schlosser, W. Metall 1960, 14, 1.

138. Winterhager, H.; Schlosser, W. Metall 1960, 14, 396.

139. Zakumbaeva, G. D.; Toktabaeva, F. M.; Solol'skii, D. V. Elektrokhim. 1970, 6, 777.

140. Conway, B. E.; Angerstein-Kozlowska, H.; Sharp, W. B. A. Z. Phys. Chem. (Frankfurt au Main) 1975, 98, 61.

141. Trasatti, S. Z. Phys. Chem. (Frankfurt au Main) 1975, 98, 74.

142. Kolb, D. M. In "Advances in Electrochemistry and Electrochemical Engineering", Gerischer, H.; Tobias, C. W., Eds.; John Wiley & Sons: New York; Volume 11, Chapter 2.

143. Literature available from Pine Instrument Co., Grove City, PA.

144. Maitoza, P. Ph.D. Dissertation, Iowa State University, Ames, IA, 1980, Section IV.

145. Schwartz, A. "Calculus and Analytical Geometry", 2nd ed.; Holt, Rinehart and Winston: New York, 1967, pp. 372-373.

146. Morris, V. L. M.S. Thesis, Iowa State University, Ames, IA, 1976.

147. Koile, R. C. Ph.D. Dissertation, Iowa State University, Ames, IA 1979.

148. Allen, R. E.; Johnson, D. C. Talanta 1973, 20, 799.

149. Johnson, D. C. Chemistry Dept., Iowa State University, Ames, IA, March 1979; private communication.

150. Pleskov, Yu. V.; Filinovskii, V. Yu. "The Rotating Disc Electrode" (Engl. Transl.); Consultants Bureau: New York, 1976; Nauka Press: Moscow, 1972.

151. Koch, W. F.; Hoyle, W. C.; Diehl, H. Talanta 1975, 22, 717.

152. Johnson, D. C. "Introduction to Electrochemical Methods of Analysis"; University Bookstore: Ames, IA, 1976.

153. Levich, V. G. "Physiochemical Hydrodynamics"; Prentice-Hall: Englewood Cliffs, NJ, 1962.

154. Meschi, P. L. Chemistry Dept., Iowa State University, Ames, IA, March, 1980; private communication.

155. Andrews, R. W.; Larochelle, J. H.; Johnson, D. C. Anal. Chem. 1976, 48, 212.

156. Cadle, S. H.; Bruckenstein, S. Anal. Chem. 1974, 46, 16.

157. Andrews, R. W.; Johnson, D. C. Anal. Chem. 1975, 47, 294.

158. Johnson, D. C.; Larochelle, J. Talanta 1973, 959.

159. Taylor, L. R.; Johnson, D. C. Anal. Chem. 1974, 46, 262.

160. Larochelle, J. H.; Johnson D. C. Anal. Chem. 1978, 50, 240.

161. Larochelle, J. H. Ph.D. Dissertation, Iowa State University, Ames, IA, 1977.

162. Heyrovsky, J. Chem. Listy 1922, 16, 256.

163. Barker, G. C.; Jenkins, I. L. Analyst 1952, 77, 685.

164. Barker, G. C. Anal. Chim. Acta 1958, 18, 118.

165. Christian, G. D. J. Electroanal. Chem. Interfacial Electrochem. 1969, 23, 1.

166. Flato, J. B. Anal. Chem. 1972, 44(11), 75A.

167. Siegerman, H.; O'Dom, G. Amer. Lab. 1972, 4(6), 59.

168. Lund, W.; Onshus, D. Anal. Chim. Acta 1976, 86, 109.

169. Copeland, T. R. Ph.D. Dissertation, Colorado State University, Fort Collins, CO, 1973.

170. Copeland, T. R., Christie, J. H.; Osteryoung; R. A.; Skogerboe, R. K. Anal. Chem. 1973, 45, 2171.

171. Turner, J. A.; Eisner, U.; Osteryoung, R. A. Anal. Chim. Acta 1977, 90, 25.

172. Nurnberg, H. W.; Valenta, P.; Mart, L.; Raspor, B.; Sipos, L. Z. Anal. Chem. 1976, 282, 357.

173. Nurnberg, H. W. Electrochim. Acta 1977, 22, 935.

174. Nurnberg, H. W. Proc. Anal. Div. Chem. Soc. 1978, 15, 275.

175. Valenta, P.; Mart. L.; Reutzel, H. J. Electroanal. Chem. Interfacial Electrochem. 1977, 82, 327.

176. De Angelis, T. P.; Heineman, W. R. Anal. Chem. 1976, 48, 2262.

177. De Angelis, T. P.; Bond, R. E.; Brooks, E. E.; Heineman, W. R. Anal. Chem. 1977, 49, 1792.

178. Sipos, L.; Valenta, P.; Nurnberg, H. W.; Branica, M. J. Electroanal. Chem. Interfacial Electrochem. 1977, 77, 263.

179. Sipos, L.; Golimowski, J.; Valenta, P.; Nurnber, H. W. Z. Anal. Chem. 1979, 298, 1.

180. Kritsotakis, K.; Laskowski, N.; Tobschall, H. J. Intern. J. Environ. Anal. Chem. 1979, 6, 203.

181. Fleet, B.; Little, C. F. J. Chromatogr. Sci. 1974, 12, 747.

182. Sherwood, G. A., Jr. Ph.D. Dissertation, Iowa State University, Ames, IA, 1979, Section III.B.3 and III.C.1.

183. Chassis Wiring Diagram, Model 174A Polarographic Analyzer, Operating and Service Manual, EG&G Princeton Applied Research, Princeton, NJ, 1976, p. VIII-13.

184. Parry, E. P.; Osteryoung, R. A. Anal. Chem. 1965, 13, 1634.

185. Evenson, E.; Lindstrom, T. R., Johnson, D. C. Chemistry Dept., Iowa State University, Ames, IA; unpublished data.

186. Ruzicka, J.; Hansen, E. H. Chemtech 1979, 9(12), 765.

187. Alexander, P. W. Proc. R. Aust. Chem. Inst. 1976, 43, 358.

188. Toth, K.; Nagy, G.; Feher, Z.; Horvai, G.; Pungor, E. Anal. Chim. Acta 1980, 114, 45.

189. Mahan, K. I.; Mahan, S. E., Anal. Chem. 1977, 49, 662.

190. Heiden, R. W.; Aikens, D. A., Anal. Chem. 1977, 49, 670.

191. Mart, L. Z. Anal. Chem. 1979, 296, 350.

192. Knechtel, J. R.; Fraser, J. L. Anal. Chem. 1979, 51, 315.

193. Smith, G. F. "The Wet Chemical Oxidation of Organic Compositions Employing Perchloric Acid"; The G. Frederick Smith Chemical Co., Inc.: Columbus, OH, 1965.

194. Gorsuch, T. T. Analyst 1959, 84, 135.

195. Hugos, H. J. Laboratory Information Bulletin No. 2279; U. S. Food and Drug Administration: Detroit, MI, March, 1979.

196. Lown, J. A. Ph.D. Dissertation, Iowa State University, Ames, IA, 1979.

197. Rucki, R. J. Talanta 1980, 27, 147.

IX. ACKNOWLEDGEMENTS

First, and foremost I wish to express my thanks to God for His steadfast direction in my life. When at times my research seemed to be in chaos, He strengthened me in spirit and gave me a sense of purpose to continue. And now I have seen the conclusion of another, major episode in the story of my life in which He has brought me to a fuller understanding of a portion of His magnificent creation.

Second, my respect for, and admiration of, my major professor, Dr. Dennis C. Johnson, is beyond words. The example of scientific integrity and academic excellence which he provides for all of his graduate students will remain with me always. Many, many thanks to you Denny!

To the members of our research group at Iowa State University, both past and present, I am in many ways indebted. Though I mean to slight no one, I am particularly mindful of the aid of Drs. Glenn A. Sherwood, Jr. (DuPont, Wilmington, DE), Ross C. Koile (Dow Chemical, Midland, MI), and Paul Maitoza (General Electric, Waterford, NY); and Mr. Kenneth W. Pratt. During the past five years, their interaction with me was both stimulating to my research effort and helpful in my personal growth.

The financial support of the Department of Chemistry at Iowa State University by way of many quarters as an appointed Teaching Assistant; of grant CHE 76-17826 from the National Science Foundation; and of the Sciences and Humanities Research Institute of Iowa State University is gratefully acknowledged.

Much credit is given to Mr. Eldon E. Ness and Mr. George W. Steininger of the Chemistry Shop at Iowa State University for their nothing-less-than amazing skill with machine tools. I'm sure that they hope to never see another "mini-disk-electrode". I can only express a hearty "Thank You!" for their patience and expertise.

What can be said about parents like the ones that I have? They have taught me the most important things that I know. The thing which I am remembering now is that dad said, "Can't never did anything, boy!" I will ever be thankful to them for their love and never-ending support, both prayerful and financial, throughout the past nine years of college and graduate education.

I see that I failed to acknowledge another colleague who has been influential in my graduate education. Thanks goes to Mr. John W. Furry for his friendship, and example as a young scientist, and...for writing a longer dissertation than this one!

Finally, without a doubt this dissertation would not have been completed without the support of my wife, Candy. Typing final copy for your husband is not recommended in the book "How to make your marriage last", yet Candy not only typed the final copy, but also the several rough drafts which preceded the final copy. Her patience and understanding throughout this most trying period has only increased my love for her. And so to her I say...

After college you said, "I do."
Then you went to work to put me through.
And now, tis done, the end is in view.
The final period is placed just for you.